M-Pos238

ACTION POTENTIAL VOLTAGE CLAMP OF Na-Ca EXCHANGE CURRENT: AGE-DEPENDENT CHANGES IN RABBIT VENTRICLE.

((**P.S. Haddock**, M. Artman and W.A. Coetzee)) Departments of Pediatrics, Physiology and Neuroscience, NYU Medical Center, New York, NY 10016.

Previous studies, in which identical voltage clamp waveforms were used in different age groups, suggest enhanced Na-Ca exchange current (I_{NaCa}) in the newborn compared with the adult. However, the increase in action potential duration (APD) which occurs postnatally, may promote Ca^{2+} influx via the Na-Ca exchanger and thus compensate for the postnatal decline in Na-Ca exchange expression in the mature heart. To examine this possibility, we measured I_{NaCa} in rabbit myocytes from different age groups, with age-appropriate action potentials (AP) as command waveforms. APs were recorded at 34°C using the perforated-patch technique from ventricular myocytes isolated from the hearts of newborn (1-8 day) and adult rabbits. APD_{90} increased from 160±15 (1 day old;n=25) to 268±22ms in adults (n=25,p<0.05;see figure). Despite the shorter AP, outward I_{NaCa} was high at birth and fell significantly during the post-natal period (1 day: 0.4±0.06, adult : 0.04±0.01 pC/pF; n=15-20, p<0.05, see figure). Similarly, Ca^{2+} extrusion via inward I_{NaCa} also declined after birth (1 day: -0.3±0.02, adult: -0.08±0.02 pC/pF; n= 12-20, p<0.05,see figure).I_{NaCa} elicited contraction in 1-11 day old myocytes (1 day: 4.8±0.58% resting length), but was unable to evoke contraction in adults. We conclude that, despite a relatively short APD_{90}, I_{NaCa} is greater in the newborn, and declines postnatally, even though APD_{90} lengthens.

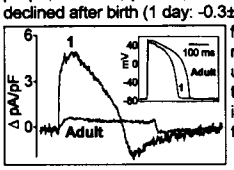

M-Pos239

EXPRESSION OF CALCIUM TRANSPORT PROTEINS DURING ISCHEMIA AND REPERFUSION IN RABBIT HEARTS IN VIVO.

((**Malcolm M. Bersohn** and Cecil R. Carmack)) Veterans Affairs Medical Center and University of California, Los Angeles, CA 90073

We investigated the effects of coronary occlusion and reperfusion in the open-chest rabbit on the expression of the sarcolemmal sodium-calcium exchanger (NCX1), the sarcoplasmic reticulum Ca-ATPase (SERCA2) and calcium release channel (CRC), along with heat-shock protein (HSP70). A large branch of the circumflex artery was occluded for 30 minutes, 60 minutes, or 60 minutes followed by 30 minutes reperfusion. Tissue from the ischemic zone was compared to control tissue from the same heart. We quantitated mRNA levels in Northern blots of total RNA, and all data were normalized for GAPDH mRNA levels in each extract. Results are expressed as the fraction of the control value for the same heart (Mean ± SE, n=6-7).

	30 min ischemia	60 min ischemia	60 isch. 30 reperfuse
NCX1	91 ± 12%	50 ± 11%	88 ± 12%
SERCA2		48 ± 10%	72 ± 13%
CRC		58 ± 14%	88 ± 11%
HSP70	112 ± 12%	170 ± 37%	809 ± 316%

One hour of ischemia causes a significant reduction in the expression of 3 major Ca transport proteins while HSP70 expression increases moderately. Thirty minutes of reperfusion leads to recovery of Ca transporter mRNA levels while HSP70 levels are greatly increased, suggesting a regulated transcriptional response to the stress of ischemia and reperfusion.

MEMBRANE STRUCTURES

M-Pos240

TRANSIENT CONFINEMENT OF GPI-ANCHORED PROTEINS BY GLYCOLIPID MEMBRANE DOMAINS.

((**E.D. Sheets** and K. Jacobson)) Departments of Chemistry and Cell Biology & Anatomy, University of North Carolina, Chapel Hill NC 27599.

Movements of membrane components can be followed with nanometer precision by using the microscopy-based technique of single particle tracking (SPT). The trajectories from 6.6 s observation periods are classified into four modes of transport—fast random diffusion, slow random diffusion, confined diffusion and a fraction of molecules that are stationary on this time scale. The latter three categories exhibit highly anomalous diffusion, whereas the rapidly diffusing class undergoes normal Brownian motion. We used SPT to assay the movements of Thy-1, a glycosylphosphatidylinositol (GPI) anchored protein, on the surfaces of C3H fibroblasts and found that 37% of Thy-1 undergo confined diffusion to regions ~315 nm in diameter. Longer observations showed that Thy-1 is confined for ~8 s durations and that no Thy-1 molecules remain completely stationary, suggesting that molecules can switch between modes of transport. Because results of recent biochemical analyses of detergent inextractable cell lysates suggested that GPI-anchored proteins are associated with glycosphingolipid (GSL) domains, we assayed the movements of GM1, a representative GSL. We find that GM1 behaves similarly to Thy-1; that is, 35% of GM1 undergo confined diffusion to ~400 nm diameter domains. However, only 16% of fluorescein phosphatidylethanolamine (which had been incorporated into the plasma membrane) experience confined diffusion, suggesting that phospholipids may be excluded from domains containing GPI-anchored proteins and GSLs. The effects of cholesterol- or glycosphingolipid-depletion on the movements of Thy-1 and GM1 were also assayed by SPT. These results intimate that the lipid milieu plays a dominant role in restricting the movements of GPI-anchored proteins. Supported by NIH grant 41402.

M-Pos241

HOW ADAPTATION TO DIFFERENT NITROGEN SOURCES CHANGES THE POLYPEPTIDE COMPOSITION OF THE *SYNECHOCOCCUS* PCC 7942 CYTOPLASMIC MEMBRANE.

((**M. Zinovieva**, C. Fresneau and B. Arrio)) University Paris-XI, LBM URA 1116 CNRS, Orsay 91405, FRANCE.

Changes in nitrogen sources have been shown to modify the cytoplasmic membrane protein composition. Several years ago, a NO_3^--dependent 47 kDa polypeptide was described in *Synechococcus* cytoplasmic membrane. By use of SDS-PAGE polypeptide analysis we found that another 126 kDa polypeptide existed in the cytoplasmic membrane of *Synechococcus* PCC 7942 cells grown in the presence of NO_3^-. The presence of NH_4^+ led to the disappearance of this protein. The amount of 126 kDa polypeptide was inversely related to the NO_3^- concentration. Transfer of NH_4^+-grown cells to a medium containing NO_3^-, as the sole nitrogen source, induced the appearance of both polypeptides. Up to 12 hours, increase in polypeptides was similar at $NaNO_3$ concentration of 2 mM and 175 mM, which are the extreme concentrations for these cells. Later, the 2 mM $NaNO_3$ concentration resulted in higher levels of the polypeptides. Similar effects were observed for 2 mM and 15 mM of $NaNO_2$. The modifications in protein composition were independent of Na^+. The change in the protein composition exerted an influence on the number of electrostatic charges at the membrane surface resulting in electrophoretic mobility variations, as measured by laser Doppler electrophoresis. The study of the cytoplasmic membrane electrophoretic mobility in the absence and in the presence of various salts showed the binding of NO_3^-. It was more pronounced in the membranes from the cells grown at low NO_3^-. The data obtained suggest that composition of surrounding medium may regulate the affinity of transport system(s) to nitrate.

M-Pos242

DOCOSAHEXAENOIC ACID (DHA)-INDUCED EXFOLIATED VESICLES ARISE FROM DISTINCT PLASMA MEMBRANE DOMAINS.

((**E. Eugene Williams**, William Stillwell and Laura J. Jenski)) Dept. of Biology, Indiana University-Purdue University at Indianapolis, Indianapolis IN 46202

Cell membranes are organized into poorly understood patchworks of lipid and protein known as membrane domains. We isolated and analyzed membrane vesicles shed from the surface of a murine leukemia cell line (T27A) in order to determine whether these structures represent random regions of the plasma membrane or instead are derived from distinct domains which could be used to assess domain structure and composition. From the fluorescence depolarization of diphenylhexatriene-derived membrane probes, we found the released vesicles (EVs) were significantly more ordered than the parent plasma membrane (PM), indicating distinct, and thus non-random, compositions. When cells were cultured in medium enriched with DHA, a membrane component known to induce domain formation in artificial membranes, the PM was unaffected while EV order was significantly reduced. EVs from DHA-cultured cells contained 5 times more DHA than the PM fraction and than EV and PM from untreated cells. Eighty percent of the shed DHA was found in the form of a single molecular species, *sn*-1 steroyl, *sn*-2 DHA-phosphatidylethanolamine (PE). EVs were also found to contain elevated levels of cholesterol. These combined results were unexpected since cholesterol interacts unfavorably with both DHA and PE. The incompatibility of the observed membrane components suggest there may be two or more separate populations of EVs. We conclude that EVs from this cell line represent membrane domains, and that T27A cells regulate membrane DHA content and structure by forming and then shedding these domains.

M-Pos243

DIFFUSION AND ITS RESTRICTION IN AXONS AND DENDRITES OF DEVELOPING HIPPOCAMPAL NEURONS

((**A. Pralle**, E.-L. Florin, C. Dotti and J.K.H. Hörber)) *Cell Biophysics, European Molecular Biology Laboratory, D-69117 Heidelberg, Germany*

Mature neurons exhibit highly specialized plasma membrane areas, including an axonal and a somatodendritic surface. So far it is not clearly understood how this polarisation is established and maintained. A current hypothesis is that site-directed insertion of membrane proteins establishes the membrane polarisation. To maintain the distinct membrane area the diffusion of the constituents must be restricted.

We investigate the variations of the diffusion of membrane components in different functional areas. Experiments are performed on cells throughout the various developmental stages of neuronal cells to study the changes of diffusion during the establishment of the polarisation. Using single-particle tracking methods we analyse the free diffusion of lipids in the axonal and somato-dendritic plasma membrane to determine the flow of membrane along the growing axon and to locallize areas of reduced or blocked diffusion. Additionally experiments with an optical trap are performed to investigate the nature of the obstacles to diffusion.

M-Pos244

DEFINING LIPID AND PROTEIN DOMAINS IN INTACT CELL MEMBRANES BY IMAGING FLUORESCENCE ENERGY TRANSFER. ((**A.K. Kenworthy** and M. Edidin)) Dept. of Biology, Johns Hopkins University, 3400 N. Charles St, Baltimore, MD 21218.

Membrane microdomains containing clustered lipid-anchored proteins, glycosphingolipids, and cholesterol have been implicated in events ranging from membrane trafficking to signal transduction. Such clusters have been isolated from detergent extracts of cell membranes. However, electron microscopy shows no clustering of lipid-anchored proteins occurs unless they are crosslinked by secondary antibodies. Hence, the existence of such domains in natural membranes is disputed. To better understand the organization of glycosylphosphatidylinositol (GPI)-anchored proteins at the cell surface, we are using digital microscopy to map the molecular associations of these molecules *in situ* by combining immunofluorescence microscopy and quantiative fluorescence resonance energy transfer measurements. We detect energy transfer between molecules of the GPI-anchored protein 5' nucleotidase (5' NT) at the apical membrane of transfected Madin Darby Canine Kidney (MDCK) cells. The extent of energy transfer scales with the surface density of the acceptor-labeled antibody against 5' NT. To determine whether the magnitude of energy transfer is consistent with a random or clustered distribution of 5' NT, we independently estimated the absolute surface densities of 5' NT using fluorescent bead standards. Our preliminary analysis suggests that the observed energy transfer efficiencies are within the range predicted for randomly distributed donors and acceptors. This approach provides a basis for defining conditions under which proteins and lipids associate on the molecular level in intact cell membranes.

M-Pos245

EFFECT OF HYDRATION ON THE DISTRIBUTION OF DOUBLE - BONDS IN FLUID DOPC BILAYERS. ((**K. Hristova** and S.H. White)) Department of Physiology and Biophysics, University of California Irvine, CA 92697.

The time-averaged transbilayer distribution of the double - bonds in DOPC bilayers has been determined as a function of bilayer hydration by X-ray diffraction using bromine labels. 1-oleoyl-2(9,10-dibromostearoyl) phosphatidylcholine (OBPC), whose bromines report the double bond distribution, has been shown to be isomorphous with DOPC [Wiener & White (1991) Biochemistry 30: 6997]. Both oriented multilayers equilibrated at relative humidities (RH) from 66 to 93% and unoriented liposomal suspensions in PVP solutions (30 to 60% PVP) were examined for 6 different OBPC concentrations in the range 0 to 50 mol%. The hydration under these conditions varies from 5.4 to 16 water molecules per lipid molecule. The transbilayer distribution of bromine in the DOPC/OBPC bilayer is described by a pair of Gaussians of 1/e half-width A_{DB} located at $z = \pm Z_{DB}$ relative to the bilayer center at all hydrations studied. For hydrations from 5.4 water molecules (66% RH) up to 9.4 water molecules per lipid (93% RH) the bromine position gradually decreases from Z_{DB} = 7.97±0.27Å to Z_{DB} = 6.59±0.15Å, while A_{DB} increases from 4.62±0.62Å up to 5.92±0.37Å. After the hydration shell is filled at about 12 water molecules per lipid (60% PVP), we observe a shift in Z_{DB} to about 7.3Å, suggesting that some major structural change takes place at the point of completion of the hydration shell. In the range 12 to 16 water molecules per lipid the double-bond distribution remains constant at Z_{DB} = 7.33±0.25Å and A_{DB} = 5.35±0.5Å. *Supported by NIH grants GM46823 & AI31696.*

M-Pos246

SOLID STATE MAS NMR MEASUREMENTS ON THE DOCOSAHEXAENOIC CHAIN IN BILAYERS.
((**L.L. Holte** and K. Gawrisch))
NIH/NIAAA Rockville, MD 20852

It has been hypothesized that the six methylene interrupted *cis*-double bonds found in docosahexaenoic acid (DHA) impart a unique conformation to this fatty acid, whose inclusion is critical for proper function of neural and retinal membranes. Membrane models in which the DHA chain has a helical or angle-iron like conformation have been suggested. The influence of DHA on neighbored saturated hydrocarbon chains and on membrane bulk properties is well studied. However, experimental information on conformation of the DHA chain in bilayers is almost nonexistent. We are investigating conformation and dynamics of the polyunsaturated chain in multilamellar liposomes of 18:0-22:6n-3 PC with magic-angle spinning ^{1}H- and ^{13}C NMR. Even without isotopic labeling we resolve seven ^{1}H resonances and fourteen ^{13}C resonances including nine of the twelve vinyl carbons in DHA. The measurements of proton-proton and proton-carbon dipolar interactions within DHA provide strong evidence for the occurrence of a flexibility gradient along the polyunsaturated chain with higher order at the lipid-water interface and significantly lower order in the membrane center.

M-Pos247

DETERMINATION OF VOLUMES OF COMPONENTS OF LIPID BILAYERS FROM SIMULATIONS
((**Horia Petrache**[1], Scott Feller[2] and John F. Nagle[1]))
[1]Carnegie Mellon University, Pittsburgh, PA
[2]FDA, Rockville, MD; Whitman College, Walla Walla, WA

An efficient method for obtaining volumes from simulations is developed. The method is illustrated using a recent molecular dynamics simulation (Feller et al., 1996) of L_α phase DPPC. Results are obtained for the volumes of water V_W, lipid V_L, chain methylenes V_2 and terminal methyls V_3, lipid headgroups V_H, including separate volumes for carboxylate V_{COO}, glycerol V_{gly}, phosphate V_{PO_4} and choline V_{chol} groups. The method assumes that each group has the same average volume regardless of its location in the bilayer and this assumption is then tested with the simulations. The volumes obtained using this method and the recent simulation agree satisfactorily with V_W and V_L that have been obtained directly from experimental data as well as with the volumes V_H, V_2 and V_3 that have required assumptions in addition to the experimental data. These latter results help to support and refine the assumptions that have had to be made when interpreting experimental data.

Research supported by NIH grant GM-44976-07.

PHYSICAL PROPERTIES OF BILAYERS I

M-Pos248

FROM MOLECULAR SOLUTION TO MODEL CELLS VIA SELF-ASSEMBLY. ((S. A. Walker, M. Kennedy and **J. A. Zasadzinski**)) Department of Chemical Engineering, University of California, Santa Barbara, CA. 93106

Sequential self-assembly has been exploited to progress directly from molecular solutions to multifunctional aggregates resembling simple biological cells. In nature, cells divide essential functions between a variety of membrane enclosed structures; exterior membranes regulate permeation and recognition, while interior membranes encapsulate solutes and perform specific chemical and physical processes. We have produced a model cell, or "vesosome," by progressive self-assembly of molecules and molecular aggregates. Vesosomes are made by encapsulating tethered vesicle aggregates with an outer membrane. 50-100 nm vesicles are formed either spontaneously from charged surfactant mixtures or by high pressure extrusion of multilamellar liposomes. Vesicles are "cross-linked" by incorporating a biotin-conjugated surfactant (the ligand) into the vesicle bilayer and adding streptavidin (the receptor) to the dispersion. The vesicles then self-assemble into multi-micron sized aggregates containing thousands of individual vesicles. The aggregate size is controlled chemically by manipulating the ionic strength of the solution (for charged surfactants) or physically by high pressure extrusion (for lipid dispersions), yielding monodisperse multivesicular aggregates. We can now divide tasks between a variety of membrane enclosures or membrane compositions within the vesosome; this multifunctional "division of labor" resembles that of biological cells.

M-Pos249

^{2}H NMR STUDIES OF THE EFFECT OF DPPC/DPPG RATIO ON BILAYER PROPERTIES IN THE PRESENCE OF Ca^{2+}. ((M. L. Kilfoil and **M. R. Morrow**)) Department of Physics and Physical Oceanography, Memorial University of Newfoundland, St. John's, NF, Canada, A1B 3X7.

^{2}H NMR has been used to study how bilayer lipid chain order and deuteron transverse relaxation times depend on the relative abundances of chain perdeuterated dipalmitoyphosphatidylcholine (DPPC-d_{62}) and dipalmitoylphosphatidylglycerol (DPPG-d_{62}) in the presence of 5 mM Ca^{2+} in the aqueous phase. De-Paked spectra indicate that DPPC-d_{62} and DPPG-d_{62} chains are virtually indistinguishable up to DPPG-d_{62} concentrations of 50 mol% which suggests that 5 mM Ca^{2+} does not induce significant phase separation for these bilayer compositions. The DPPC-d_{62}/DPPG-d_{62} ratio does alter the bilayer main transition temperature and the temperature dependence of deuteron transverse relaxation, particularly in the gel phase. Liquid crystalline phase transverse relaxations times display a sensitivity to hydration protocol that depends on sample composition and the presence of Ca^{2+}. This may provide some insight into the way in which vesicle morphology is affected by composition of the bilayer and the aqueous medium and may have relevance to the understanding of some aspects of pulmonary surfactant function. (Supported by NSERC Canada.)

M-Pos250

INFLUENCE OF THE INTRINSIC MEMBRANE PROTEIN BACTERIORHODOPSIN ON THE GEL PHASE DOMAIN TOPOLOGY IN TWO-COMPONENT PHASE-SEPARATED BILAYERS. ((**Vincent Schram** and Thomas E. Thompson)) Department of Biochemistry, University of Virginia, Charlottesville, VA, 22908.

We have investigated the effect of the intrinsic membrane protein bacteriorhodopsin of *Halobacterium halobium* on the lateral organization of the lipid phase structure in the coexistence region of an equimolar mixture of dimyristoylphosphatidylcholine and distearoylphosphatidylcholine. The Fluorescence Recovery After Photobleaching (FRAP) technique was used to monitor the diffusion of a lipid analog (NBD-DMPE) and of fluorescein-labeled bacteriorhodopsin (Fl-BR). Both probes give essentially identical results: in presence of bacteriorhodopsin, 1) the mobile fractions display a shift of the percolation threshold toward lower temperatures (larger gel-phase area fractions), independent of the protein concentration, from 43°C (without bacteriorhodopsin) to 39°C and 41°C for NBD-DMPE and Fl-BR, respectively, and, 2) the gel phase domains are much less efficient in restricting diffusion than they are in absence of the protein. These observations suggest that bacteriorhodopsin induces the formation of much larger and/or more centrosymetric gel phase domains than those formed in its absence. Based on hydrophobic matching arguments, we suspect that a small amount of the protein accumulates at the gel/fluid phase boundary. The agreement with previous observations of the effect of the transmembrane peptide pOmpA of *Escherichia coli* investigated in the same lipid system (Sankaram et al, 1994, *Biophys. J.* 66: 1959-1968) suggests that rather non specific lipid/protein interactions are involved. This work was supported by NIH grants GM-14628 and GM-23573.

M-Pos251

A FLUORESCENCE QUENCHING STUDY OF PERCOLATION IN TWO-PHASE LIPID BILAYERS CONTAINING BACTERIORHODOPSIN.

((**Barbora Piknová**[1], Derek Marsh[2] and Thomas E. Thompson[1])) [1]Biochemistry Department, University of Virginia, Charlottesville, VA 22908, [2]Max Planck Institut für biophysikalische Chemie, D-37077 Göttingen, Germany

Bacteriorhodopsin (BR) was incorporated into the DMPC/DSPC lipid bilayers. The phase diagram for BR/PC mixtures was established by DSC. ΔH_{trans} data show that a small portion of lipids is sequestered by BR and does not participate in the lipid phase transition. The phase transition undergone by the remaining lipid is not significantly influenced by BR. However, fluorescence quenching and ESR data show that the percolation properties and domain topology of lipid bilayer are strongly affected by the protein. Contrary to our previous fluorescence data for pure lipid mixtures (Piknová et al., 1996, Biophys. J., *71*, 892 - 897), the fluorescence quenching in the two-phase coexistence region is similar to that observed in the all-fluid-phase system regardless of the actual fluid phase fraction. The percolation threshold value determined by ESR is shifted in the presence of BR to a lower fluid phase fraction than in its absence. Fluorescence quenching and ESR data together with the results of simulations (Piknová et al. 1996, Biophys. J., *71*, 892 - 987) strongly suggest that the fluid phase lipid domains are substantially larger in the presence of BR than in its absence. A similar effect of pOmpA peptide on the fluid lipid domain connectivity in binary lipid mixtures was reported previously (Sankaram et al. 1994, Biophys. J, *66*, 1959 - 1968).
This work was supported by NIH grants GM-14628 and GM-23573.

M-Pos252

PHASE BEHAVIOR OF FLUORINATED PHOSPHOGLYCERIDES - CAN A SINGLE FLUORINE ATOM INDUCE INTERDIGITATION? ((Nancy Lazaro-Llanos*, Donald J. Hirsh†, Jacob Schaefer†, and **Jack Blazyk***)) *Department of Chemistry, College of Osteopathic Medicine, Ohio University, Athens, OH 45701, and †Department of Chemistry , Washington University, St. Louis, MO 63130.

We synthesized 16-monofluoropalmitic acid from 16-hydroxypalmitic acid using diaminosulfurtrifluoride. The fluorinated fatty acid then was added to the sn-2 position of lysophosphatidylcholine to form 1-palmitoyl-2-(16-fluoropalmitoyl)-phosphatidylcholine (FDPPC). FDPPC was then transesterified with glycerol to produce 1-palmitoyl-2-(16-fluoropalmitoyl)-phosphatidylglycerol (FDPPG). The T_m of both FDPPC and FDPPG occurs at ~50°C, nearly 10° higher than their nonfluorinated counterparts, as judged by both differential scanning calorimetry and FTIR spectroscopy. No pretransition is observed in the fluorinated lipids. Mixtures of fluorinated and nonfluorinated lipids show a single T_m intermediate between the two lipids, suggesting ideal mixing and the absence of phase separation. This is further corroborated by FTIR experiments to monitor the C-D and C-H stretching frequencies in mixtures of d_{62}-DPPC (acyl chain perdeuterated DPPC) and FDPPG. Solid-state NMR experiments employing rotational echo double resonance (REDOR) reveal that significant dipolar coupling occurs in FDPPC and FDPPG between the fluorine atom on on the tail of the lipid and both phosphorus in the polar head group and the carbonyl carbon in the ester linkage. The relatively short distance between fluorine and the polar head group could be explained if the lipid bilayer is interdigitated below T_m. Through X-ray diffraction experiments in collaboration with Dr. Thomas J. McIntosh at Duke University Medical Center, we intend to determine if, in fact, these lipids form interdigitated bilayers and to provide an explanation for the markedly elevated T_m observed in these fluorinated lipids.

M-Pos253

MEMBRANE MODELS AND THEIR RELATION TO MEMBRANE STABILITY IN ELECTRIC FIELDS. ((**V.L. Dorman**, M.B. Partenskii and P.C. Jordan)) Dept. of Chemistry, Brandeis University, Waltham, MA 02254.

We study the "smectic bilayer model" (SBLM: Huang, *Biophys J.*, **50**, 1061 [1986]) and analyze membrane stability under applied voltages. The electro-elastic problem is solved for perturbed membrane surfaces in contact with electrolyte. We compute the dependence of the free energy on wave vector (**k**) and amplitude (Δ_k) and consider a range of boundary conditions. In the familiar "elastic slab model" (ESM: Crowley, *Biophys. J.*, **13**, 711 [1973]), a limiting case of the SBLM, instability is not **k** dependent and is preceded by large membrane electrostriction. In the SBLM the critical voltage for instability, $V_{cr}(\mathbf{k})$, is **k**-sensitive. For $|V| < V_{cr}(0)$, the ESM is always stable but the SBLM may be unstable. In the SBLM the minimum critical voltage, V_{cr}^{min}, for instability when $\mathbf{k} \neq 0$ depends on a membrane's elastic moduli and surface tension. V_{cr}^{min} is less than in the ESM and there is limited electrostriction. The instabilities cause membrane rupture or transition to a second, non-uniform state. Models treating large surface perturbations are discussed and yield estimates of the potential V_0 for transition to the non-uniform state; V_0 is less than V_{cr}^{min}. We study the behavior of the frequency dependent admittance, $Z(\omega,V)$. Its intense low frequency dispersion due to critical mode softening signals the approach to V_{cr}; the system's behavior becomes highly nonlinear. Implications for the design of biosensors are discussed.

M-Pos254

EFFECTS OF CHOLESTEROL AND LYSOLIPIDS ON PHOSPHOLIPID MEMBRANE CURVATURE AND BENDING ELASTICITY. (**Z. Chen**, N. Fuller and R. P. Rand) Biological Sciences, Brock University, St. Catharines, Canada.

Membrane curvature and curvature energy are expected to affect lipid/protein interactions and membrane fusion. We have used X-ray diffraction and osmotic stress to measure structural dimensions, spontaneous curvature and bending moduli of the monolayers of the reverse hexagonal (HII) phase. Phospholipids, dioleoylphosphatidylethanolamine/ choline (DOPE/C), with added cholesterol or lyso-oleoylPC have been examined. The elastic deformation of these mixed-lipid monolayers usually can be described as bending around a pivotal surface that remains constant in area; a surface that divides the molecular volume at a position close to the polar/hydrocarbon interface. Cholesterol decreases the radius of spontaneous curvature, Ro, of pure DOPE monolayers, and increases the bending modulus very slightly, both parameters defined for the pivotal surface. Cholesterol causes large decreases in the radius of spontaneous curvature of DOPC compared to DOPE monolayers. Given its large effect on area compressibility in bilayers, it is surprising that cholesterol has no greater an effect on the bending modulus of these phospholipid monolayers than does diacylglycerol (Biophys. J. November '96). Lyso-oleoylPC strongly increases Ro for DOPE, and we have measured the apparent negative curvature of pure lyso-oleoylPC.

M-Pos255

INTERACTION OF THE SURFACE OF BIOMEMBRANE WITH SOLVENTS INDUCES INTERDIGITATED GEL STRUCTURES IN DPPC-MLV ((**K. Kinoshita**, and Masahito Yamazaki)) Dept.of Physics, Fac.of Science, Shizuoka University, Shizuoka, 422, Japan.

In order to elucidate a mechanism of the phase transition between bilayer structure and interdigitated gel ($L_\beta I$)structure of phospholipid vesicles, we have investigated effects of several water-soluble organic solvents which also have high solubility of alkane, on the structure and phase behavior of multilamellar vesicle of dipalmitoylphosphatidylcholine (DPPC-MLV).

Main transition temperature of DPPC-MLV decreased with an increase in acetonitrile concentration from 0% to 6.0 % (v/v), and increased above 6.0 %(v/v). X-ray diffraction data indicated that a phase transition from L_β' to $L_\beta I$ phase in DPPC- MLV occurred at 5.0 %(v/v) and DPPC-MLV were completely in $L_\beta I$ phase above 6.0 %(v/v) acetonitrile at 20 °C. Results of the excimer method (1) supported the above results; ratio of excimer to monomer fluorescence intensity (*E/M*) of pyrene-PC in DPPC-MLV rapidly decreased at 5.1 %(v/v) and *E/M* became very low above 6.0 %(v/v) acetonitrile. By the excimer method, we have found that other organic solvents (acetone, propionaldehyde and tetrahydrofurane) induced a phase transition from L_β' to $L_\beta I$ phase in DPPC-MLV. Threshold concentrations of acetone, ethanol, propionaldehyde, and tetrahydrofurane for this phase transition at 20 °C were 9.4 %(v/v), 5.5% (w/v), 3.5 %(w/v), and 3.7 %(w/v), respectively. Substitution of H_2O by D_2O increased their threshold concentrations of all the organic solvents.

A mechanism of these phase transitions and the effect of the substitution of H_2O by D_2O is proposed and discussed; an interaction energy between the surface segments of DPPC-MLV and solvents, may be important.

(1) M.Yamazaki et.al., BBA, 1106, 94-98, 1992; Biophys.J., 66,729-733,1994

M-Pos256

PROPERTIES OF TWO-COMPONENT AQUEOUS BILAYERS COMPOSED OF HIGH MOLECULAR WEIGHT MIXED-CHAIN-LENGTH PHOSPHATIDYLCHOLINES. ((J.T. Mason, R. Gupta, M.M. Batenjany*, and T.J. O'Leary)) Department of Cellular Pathology, AFIP, Washington DC 20306, and *Biomira USA Inc., 1002 Eastpark Blvd., Cranbury, NY 08512.

A series of high molecular weight mixed-chain-length phosphatidylcholines (PCs) have been prepared with the *sn*-1 acyl chain of the PC about twice the length of the *sn*-2 acyl chain. Aqueous bilayers composed of such PCs adopt a mixed-interdigitated packing arrangement in the bilayer gel phase. Two-component aqueous bilayers composed of 1-stearoyl-2-decanoyl-PC (C18C10PC) in combination with C20C12PC, C22C13PC, or C24C14PC were studied by differential scanning calorimetry (DSC) and Raman spectroscopy. The phase diagram, derived from DSC data, for bilayers composed of C18C10PC + C20C12PC indicate that these two PCs mix nearly ideally in both the gel and liquid-crystalline bilayer phases. The phase diagrams for the two-component bilayers C18C10PC + C22C13PC and C18C10PC + C24C14PC were of the eutectic type indicating lateral separation of two immiscible gel phases over most of the compositional range, but complete miscibility of the PCs in the liquid-crystalline bilayer phase. Raman spectroscopy measurements performed in the C-H stretching mode region of the two binary mixtures suggest that the PCs in both immiscible gel phases adopt a mixed-interdigitated packing arrangement. The DSC results obtained with the C18C10PC + C24C14PC two-component mixtures indicate that the incorporation of up to 10mol% C24C14PC in the bilayer yields a gel to liquid-crystalline phase transition profile virtually identical to that of pure C18C10PC. This result is interpreted to support a model in which the mixed-interdigitated gel phase is organized into planar domains interconnected by thin regions of boundary lipid in order to conform to the spherical geometry of the liposome. At concentrations below 10mol%, the C24C14PC molecules are suggested to be sequestered into these boundary regions due to their gel phase immiscibility with C18C10PC. Under these conditions the C24C14PC component will not contribute significantly to the overall phase transition of the two-component bilayer due to the poorly cooperative nature of the phase transition arising from the boundary lipid.

M-Pos257

NOVEL MECHANISM FOR THE MAIN TRANSITION OF PHOSPHOLIPID BILAYERS

((Arimatti Jutila and Paavo K. J. Kinnunen)) Department of Medical Chemistry, Institute of Biomedicine, P.O. Box 8, FIN-00014 University of Helsinki, Finland.

One of the pertinent current questions regarding biomembrane function concerns the mechanisms causing two dimensional ordering of their components. Dynamic lateral heterogeneity due to co-existing fluctuating gel and liquid crystalline domains accompanies the main transition of phospholipids and may explain increased ion permeability and augmented susceptibility of bilayers to hydrolysis by phospholipase A_2 near the transition temperature T_m. Lateral heterogeneity in large unilamellar bilayer vesicles of dimyristoylphosphatidylcholine (DMPC) *below* T_m is revealed by the transient peak at $T^* \approx 22$ °C in excimer formation by the pyrene-labelled phospholipid probe, PyrPC (1-palmitoyl-2-pyrenedecanoyl-PC). Using three different fluorescence quenchers partitioning preferentially into either the (i) phase boundary, (ii) gel phase, or (iii) fluid phase we could demonstrate PyrPC to favor at T^* localization into the interface between 'fluid' domains in the bulk gel phase. However, our data are incompatible with the coexistence of such domains at T_m. Accordingly, the identity of the fluctuating entities underlying the heat capacity maximum at T_m must be reconsidered. One possibility could be a 'pseudocrystalline' superlattice of fluid ('excited') and gel ('ground') state lipids existing in the vicinity of T_m, analogously to the hexatic phase.

M-Pos258

Cholesterol-Induced Lipid Microdomains in Docosahexaenoic Acid-containing Mixed Phosphospholipid Membranes. ((**A.C. Dumaual**, W. Stillwell, and L.J. Jenski)) Department of Biology, Indiana University-Purdue University at Indianapolis, Indianapolis, IN 46202-5132.

Here we test the hypothesis that the omega-3 fatty acid, docosahexaenoic acid (DHA), induces lipid microdomain formation in cholesterol-rich membranes. Phospholipid bilayers and monolayers composed of 18:0, 18:1 PC/18:0, 22:6 PC with differing amounts of cholesterol are used as models for biological membranes. 18:0, 18:1 PC represents a "typical" membrane phospholipid while 18:0, 22:6 PC contains DHA, the longest and most unsaturated fatty acid found in nature. Previous experiments have shown that cholesterol interacts poorly with DHA-containing phospholipids compared to most unsaturated phospholipids including 18:0, 18:1 PC. Three biophysical techniques are employed with mixed phospholipid bilayers to demonstrate cholesterol-induced lateral phase separation: fluorescence resonance energy transfer (FRET), fluorescence spectroscopy using the probe pyrene, and differential scanning calorimetry (DSC). Lateral phase separation is also demonstrated in monolayers made from the same phospholipid/cholesterol mixtures by area-pressure isotherms on a Langmuir-Blodgett trough. Finally, we present visual evidence of lipid microdomains in these same monolayers by digital imaging microscopy using probes containing a fluorescent moiety of either NBD or Rhodamine. These findings demonstrate in model membrane systems DHA's ability to induce membrane structural alterations, forming lipid microdomains. We propose a similar role for DHA in biological membranes.

M-Pos259

WATER DIFFUSION IN A MODEL MEMBRANE MEASURED BY PULSED FIELD GRADIENT - SPIN ECHO NMR ((**Stephen R. Wassall**)) Department of Physics, IUPUI, Indianapolis, IN 46202-3273.

The reduction in reorientational motion of water molecules near the surface of phospholipid membranes is well documented. In contrast, characterization of the restriction to translational movement has remained poorly defined and sometimes controversial. A pulsed field gradient - spin echo (PFGSE) ^1H NMR study of water diffusion in the lamellar phase of egg phosphatidylcholine (egg PC) - water aligned between glass slides addresses this issue. The approach is non invasive and utilization of samples in which all lipid lamellae possess a single alignment resolves ambiguities associated with the anisotropy of water diffusion relative to the bilayer. Measurements made as a function of orientation categorically establish that water diffusion is much faster parallel than perpendicular to lamellae. The diffusion coefficients $D_{\parallel}$ parallel to the bilayer are on the order of 10^{-10} m^2s^{-1}, which is approximately a factor of 10 slower than in pure water. This is due to water binding and steric restrictions to translational motion within the water layer. The dependence upon water concentration is monotonic, convincingly refuting previous reports of a sudden drop in water diffusion at specific water content. Crucial to the conclusion is the study of an aligned system.

M-Pos260

^2H NMR STUDIES OF UNSATURATION IN LIPID BILAYERS. ((**Stephen R. Wassall**, M. Alan McCabe and John M. Prescott)) Department of Physics, Indiana University-Purdue University Indianapolis, Indianapolis, IN 46202-3273.

The health benefits associated with dietary ω3 PUFA (polyunsaturated fatty acid) and the high concentration of ω3 PUFA in certain membranes provide the motivation for our work on unsaturated lipid bilayers. Solid state ^2H NMR of positional isomers of polyunsaturated and monounsaturated phospholipids has unequivocally established that the molecular properties of membranes are tremendously affected by the location of unsaturation, which must be included in attempts to explain the unique biological role of ω3 PUFA (1). Specifically, lineshape analyses of ^2H NMR spectra for [$^2H_{31}$]16:0-18:3PC (1-[$^2H_{31}$]palmitoyl-2-*cis*-*cis*-*cis*-octadecatrienoylphosphatidylcholine) bilayers in which the double bonds were at the 6, 9, 12 or 9, 12, 15 positions and for [$^2H_{31}$]16:0-18:1PC (1-[$^2H_{31}$]palmitoyl-2-*cis*-octadecenoylphosphatidylcholine) bilayers in which the double bond was at the 6, 9, 12 or 15 position demonstrate that location of unsaturation is a determinant of phase behaviour and membrane order. An important key to understanding the differences seen is to ascertain the conformation of double bonds. Determination of the molecular order parameter in potassium [9,10-$^2H_2$]oleate bilayers serves as our model for subsequent studies of phospholipids.

1. McCabe, M. A., Griffith, G. L., Ehringer, W. D., Stillwell, W. and Wassall, S. R. (1994) *Biochemistry 33*, 7203-7210.

M-Pos261

RUPTURE OF LIPID MEMBRANES ((Marcus Lindemann and Mathias Winterhalter)) Dept. of Biophysical Chemistry, Biozentrum, University of Basel, Switzerland

We applied short electric field pulses across lipid bilayers. One pulse charges the membrane and gives raise to electric forces. Above a critical threshold voltage rupture of the membrane is induced and a fast discharge of the membrane across the defect is observed. An analysis of the time course of the voltage gives information on the energy barrier of the membrane against rupture and allows conclusion on the kinetics of the defect widening. Our set-up allows to follow the kinetics from the ns to s range. We observed that in planar lipid membranes held under tension the defects spread very fast with about 0.1–0.3 m/s. Creating a polymer network by polymerizing actin onto the lipid membrane causes a qualitative change in the rupture kinetics [1]. The rupture process is now determined by the membrane viscosity and not anymore by the inertia of the lipid. We show evidences for membrane fluctuations and the resealing of ion conducting defects.

[1] M. Lindemann, M. Steinmetz, and M. Winterhalter, *Prog. Coll. Polymer Sci.* (1997), in press.

M-Pos262

PARTITIONING BEHAVIOR OF MEMBRANE COMPONENTS BETWEEN GEL AND FLUID PHASES OF MODEL MEMBRANES. (Charles H. Spink) Chemistry Department, SUNY-Cortland, Cortland, Ny 13045.

Evidence has been accumulating that membranes often are mixtures of gel and fluid domains of phospholipid. It thus is important to know membrane lipid components will partition between the phases. This paper is a summary of data for the partition coefficients and thermodynamic properties for the transfer of membrane solutes between gel and fluid phases of model membranes. The experimental data come from measurements of partitioning by fluorescence and differential scanning calorimetry. Using simple phospholipids as models for membranes, the free energies, enthalpies and entropies of transfer between gel and fluid phase are evaluated. Membrane solutes are chosen which allow the effects of structural variation on partitioning behavior to be sorted out. The effects of variation in head group, length of aliphatic chains in lipid solutes, degree of unsaturation in the chain, and the effects of cholesterol are presented. Interpretation of the thermodynamics of the transfer process suggests that steric mismatch is a key factor in determining the partitioning behavior.

M-Pos263

PHASE PREFERENCES OF PHOSPHOLIPIDS IN POLYMORPHISM BY MASS NMR

((L. Moran, N. Janes)) Thomas Jefferson University, Philadelphia, PA 19107

The curvature stress imparted by membrane consitituents is often evaluated from the changes in the $L_\alpha \rightarrow H_{II}$ transition of mixtures. Implicit is that the difference in the entropy of mixing or lipid phase preferences is small. We developed a method whereby the ^{31}P MASS NMR sidebands are used to evaluate phospholipid phase preferences. Mixtures containing PC:DOPE:Cholesterol (chol), PC:DOPE: tetradecane (td), and PMe:POPE:diolein were examined. The DOPC/DOPE ratio in each phase was constant in the chol and td mixtures. By contrast, the DMPC/DOPE ratio in the chol mixture varied throughout the transition with a preference of DMPC for the planar bilayer and DOPE for the curved H_{II}, as anticipated from their molecular shape and polymorphic tendencies in isolation. This "demixing" coincided with an increased transition width. Yet, no dramatic phase preferences were observed in any system examined, suggesting that the contribution of the entropy of mixing to changes in the transition midpoint is generally small. Larger effects on the transition width are expected due to changes in stress.

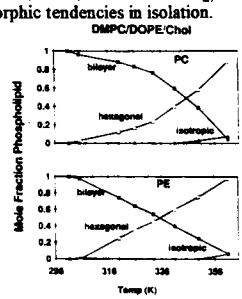

Figure: Phospholipid populations of the L_α, H_{II}, and isotropic phases throughout the thermotropic $L_\alpha \rightarrow H_{II}$ transition of DMPC:DOPE:Chol-(21:34:45). The midpoint temperature of the PC fraction in the mixture is elevated compared to the PE fraction, thereby demonstrating an enrichment of PC in the planar bilayer structure relative to PE, and the converse for H_{II}.

M-Pos264

CHOLESTEROL REGULAR DISTRIBUTION AND ITS EFFECT ON SOLUTE PARTITIONING IN LIPID MEMBRANES. ((**Mei Mei Wang** and Parkson Lee-Gau Chong)) Dept. of Biochemistry, Temple Univ. Sch. of Med., Philadelphia, PA 19140.

In previous studies, we used fluorescence intensity dips, fluorescence polarization peaks, fluorescence lifetime dips, and quenching rate constant peaks as evidence that dehydroergosterol (DHE) and cholesterol molecules can be regularly distributed into lipid membranes. In the present study, we have used steady-state fluorescence measurements to determine the fractional sterol concentration dependence of partition coefficients of nystatin (a fluorescent polyene antifungal drug) and Prodan (6-propionyl-2-(dimethylamino) naphthalene, a synthetic fluorescence probe) in the liquid-crystalline state of cholesterol/DMPC (L-α–dimyristoylphosphatidylcholine) bilayers. It is found that the partition coefficients of both nystatin and Prodan reach a local minima at 20, 22, and 25 mol% cholesterol. These concentrations match well with the critical sterol mole fractions predicted by the hexagonal and the centered rectangular superlattice model. In addition, the intensity and lifetime of nystatin fluorescence exhibit local minima at 20, 22, and 25 mol% cholesterol. These fluorescence minima can be understood in terms of the changes of solute partitioning with the extent of cholesterol regular distribution in the membrane. These results strongly support our previously proposed model that membrane free volume reaches a local minimum at critical sterol mole fractions because it is known that solute partitioning is affected by membrane surface density (or membrane free volume in the water-membrane interfacial region). This study provides the first direct evidence that solute partitioning can be affected by the extent of sterol regular distribution in membranes. (Supported by AHA and ONR)

M-Pos265

QUANTITATIVE ANALYSIS OF Gd3+ BINDING TO LIPOSOMES, PLANAR BILAYERS AND LIPID MONOLAYERS. ((Yu.A.Ermakov, A.Z. Averbakh*, V.L.Shapovalov* and S.I. Sukharev**)) Inst. of Electrochemistry and *Chem.Physics RAS, Moscow, Russia, and **Laboratory of Molecular Biology,University of Wisconsin, Madison, WI 53706.

In the present work we further explore the hypothesis that the blocking effects of Gd3+ on mechanosensory transduction are mediated by high-affinity binding of these ions to the lipid component of receptory membranes, thereby changing physical properties of the bilayer which are critical for gating of mechanosensitive ion channels. The magnitude of adsorption of these ions was assessed by their effects on the boundary, surface and Volta potentials measured with planar bilayers, liposomes and lipid monolayers, respectively. Due to the extremely high affinity of the ions for negatively charged lipid surfaces the mass balance condition for both the lipid and binding ion was used for the analysis of adsorption isotherms. The 'corrected' isotherms for the Gd3+/phosphatidylserine pair obtained by microelectrophoretic measurements of surface potential were well fitted according to the Gouy-Chapman-Stern theory with the association constant of 50000 M-1. A comparison of data obtained by different techniques showed that binding of Gd3+ to phosphatidylserine membranes strongly and specifically affects the dipole component of the boundary potential. The pressure-area curves obtained on monolayers made of DMPC/DMPS mixtures indicated dramatic changes in mechanical properties in the presence of Gd3+. Our data, although obtained in model systems, are consistent with the above hypothesis.

M-Pos266

CHOLESTEROL REGULAR DISTRIBUTION AND ITS EFFECT ON THE HYDROLYTIC ACTIVITY OF SECRETED PHOSPHOLIPASE A2
((**Fang Liu** and Parkson Lee-Gau Chong)) Dept. of Biochemistry, Temple University School of Medicine, Philadelphia, PA 19140

Sterol concentration dependencies of steady-state anisotropy of diphenylhexatriene (DPH) and dehydroegosterol (DHE) fluorescence have been examined in DPH/cholesterol/DMPC, DHE/cholesterol/DMPC, and DHE/cholesterol/DPPC lipid bilayers at T>Tm. The anisotropy reaches a local maximum when the total sterol content in the bilayer reaches the critical sterol mole fraction predicted by the hexagonal and the centered rectangular superlattice model (1,2). The anisotropy results supported our previously proposed model (1) that the membrane free volume (or membrane defect) reaches a local minimum at critical mole fractions for sterols being regularly distributed into superlattices. We have also examined the effect of cholesterol mole fraction in DMPC bilayers on the hydrolytic activity of *crotalus durissus terrificus* venom phospholipase A2. The hydrolytic activity has been determined by the method of Richieri et al (3) at 37 °C. It is found that the initial hydrolytic activity of secreted phospholipase A2 reaches a local minimum at 20, 22.2 and 25 mol% cholesterol. These concentrations are the critical sterol mole fractions predicted for sterol regular distribution in diacylphosphatidylcholines (1,2). This result indicates that cholesterol regular distribution can modulate the hydrolytic activity of phospholipase A2. It appears that the hydrolytic activity reaches a local minimum when the membrane free volume (or membrane defect) reaches a local minimum. This phenomenum will be discussed in terms of the molecular action of the phospholipase A2 on lipid bilayers. (Supported by AHA).

1. Chong. (1994) Proc. Natl.Acad.Sci.USA 91: 10069-10073. 2. Virtanen et al. (1995) Biochemistry 34: 11568-11581. 3. Richieri et al. (1992) J.Biol.Chem. 267: 23495-23501.

M-Pos267

ENERGY OF DISSOCIATION BETWEEN THE LIPID BILAYER AND THE MEMBRANE SKELETON IN RED BLOOD CELLS

((**William C. Hwang** and Richard E. Waugh))

Department of Biochemistry and Biophysics, School of Medicine and Dentistry, University of Rochester, NY 14642

The energy of association (dissociation) between the lipid bilayer and the membrane skeleton can be studied by formation of a small strand of membrane material (tether) from the red cell. The tethering force depends on the velocity of tether formation in a complex way, but the elastic component of association energy can be estimated either by measuring the energy of dissociation at different, constant tether growth rates and then extrapolating to zero tether growth rate, or by measuring the energy of dissociation from force relaxation at constant tether length. Both approaches yield a value of dissociation energy of 0.06 mJ/m^2 in normal red cells. Preliminary measurements of tether formation from reticulocytes appear to indicate that the work of dissociation is smaller in these cells than in mature red cells. However, when the antibodies against transferrin receptor were used to form the adhesive contacts with reticulocytes, the force to separate the cell from the bead was more than ten times larger than when a non-specific adhesive contact was formed. These results demonstrate the importance of the nature of the molecular bonds and differences in membrane structure in determing how cells dissociate from adhesive contacts. (Supported by NIH grant nos. HL 18208 and HL 31524.)

M-Pos268

LOW PERMEABILITY OF LIPOSOMAL MEMBRANES COMPOSED OF ARCHAEBACTERIAL TETRAETHER LIPIDS. ((**H. Komatsu** and P. L.-G. Chong)) Dept. of Biochemistry, Temple Univ. Sch. of Med., Philadelphia, PA 19140.

The polar lipid extract (PLFE) of the membrane of the thermophilic archaebacterium *Sulfolobus acidocaldarius* is composed of bipolar fractions, including glycerol dialkyl glycerol tetraether and glycerol dialkyl nonitol tetraether. Membrane permeabilities of large unilamellar vesicles composed of PLFE were studied by monitoring releases of a fluorescent dye, 5,6-carboxyfluorescein (CF), from the inner aqueous phase of the liposome. The permeability was examined in the temperature range 25 - 75 °C, and the results were compared with those of dipalmitoyl phosphatidylcholine (DPPC), egg yolk phosphatidylcholine (eggPC), eggPC/cholesterol (7/3 in molar ratio), and diphytanoyl phosphatidylcholine (DPhyPC) liposomes. The release of CF is conveniently detected through the fluorescent increase due to a relief of self-quenching of the CF present at a high concentration inside the liposomes. In comparison with liquid-crystalline eggPC, eggPC/cholesterol and DPPC membranes, the PLFE membrane is of the lowest permeability among them. Even at high temperatures (65 - 75 °C) where *S. acidocaldarius* lives, the PLFE membrane was remarkably stable, with a permeability similar to that in the DPPC membrane in the gel phase. The liposomal membrane composed of DPhyPC, which is similar to PLFE in respect of having two long phytanyl chains, was very leaky, and the membrane stability of DPhyPC was the lowest among the membranes examined. This indicates that the low permeability in the PLFE membrane could be ascribed to other unique structural features of PLFE such as (i) bonding of the alkyl chains to glycerol through ether linkages, (ii) replacement of one of glycerol molecules by nonitol, (iii) galactose and/or glucose at one head group and *myo*-inositol phosphate at the other side, (iv) cyclopentane rings in the alkyl chains, and (v) negative charges at the measured pH of 7.5. (Supported by NSF)

M-Pos269

LIPID PACKING IN ARCHAEBACTERIAL TETRAETHER LIPOSOMES. ((**Ayanna Okolo Laney** and Parkson Lee-Gau Chong)) Dept. of Biochemistry, Temple University School of Medicine, Phila., PA 19140

Polar lipid fraction E (PLFE) is the major polar lipid fraction in thermoacidophilic archaebacterium *Sulfolobus Acidocaldaruis*. PLFE includes both dibiphytanyldiglycerol-tetraether and glyceroldialkynonitol tetraether. These lipids are characterized by their double glycerol backbone and C40 hydrocarbon chains with branched methyl groups and cyclopentane rings(1). In the present study, we characterize membrane packing in the membrane-water interfacial region in PLFE liposomes by measuring generalized polarization (GP) of 6-dodecanoyl-2-dimethylaminonaphthalene (Laurdan) fluorescence as a function of temperature (15-65 °C) and pH (7.4 and 3.0). Based on previous studies (2), and our studies on Laurdan's derivative (Prodan (3)), Laurdan is an excellent indicator of membrane-water interfacial region of membrane packing. At pH 7.4, the GP values are found to decrease linearly with increasing temperature. This trend indicates that the packing of the membrane-water interfacial region in the PLFE liposomes becomes loose as temperature increases. The linearity is consistent with the DSC results previously obtained by Dr. Eddie Chang at Naval Research Laboratory who showed that PLFE liposomes lack a distinct phase transition. At pH 3.0, the GP values also decrease with increasing temperature. However, at a given temperature, the GP value of Laurdan at pH 3.0 is always higher than the GP value at pH 7.4. The difference of the GP values at these two pHs may be understood in terms of tighter packing in the interfacial region at lower pHs due to less negatively charged phosphate in the polar head groups. (Supported by NSF)

1. Kates, M. (1991) Biochem. Soc. Symp. 58: 51-72 2. Parasassi et al. (1991) Biophys. J. 60: 179-189. 3. Chong et al. (1991) Biochemistry 30: 9485-9491.

M-Pos270

THE EXPLORATION OF LIPID DOMAIN FORMATION USING CLASSICAL AND IMAGING VIBRATIONAL SPECTROSCOPIC METHODS ((**Linda H. Kidder**, E. Neil Lewis, C. Huang* and Ira W. Levin)) Laboratory of Chemical Physics, NIDDK, National Institutes of Health, Bethesda MD 20892-0510. *Dept. of Biochemistry, University of Virginia School of Medicine, Charlottesville VA 22908.

The structural and dynamic properties of lipids provide information relating to their aggregation and packing properties. Vibrational spectroscopic methods have proven to be a non-invasive and sensitive probe for examining molecular reorganizations of biological materials. In general, infrared and Raman spectroscopies are applied to samples that are considered to be homogeneous over the field of view. However, recent Raman spectroscopic studies of multilamellar lipid dispersions of 1-palmitoyl-2-oleoylphosphatidylcholine [POPC] suggest the formation of domains. By synthesizing *cis*-double bond positional isomers of POPC with a deuterated sn-1 chain and hydrogenated sn-2 chain, conformational and packing characteristics of the two chains have been determined. By monitoring the inter- and intra- chain interactions as a function of temperature and chain position, the introduction of lateral heterogeneities is indicated. The addition of an imaging component to FT-IR spectroscopy can clarify heterogeneities of sample composition, molecular orientation and chain conformation. We report on microscopic domain formation in a phosphatidylcholine lipid assembly composed of di-saturated chain lipids and di-multiply unsaturated chain lipids as determined by an FT-IR spectroscopic imaging technique.

M-Pos271

SPECTROSCOPY & MICROSCOPY OF AQUEOUS LIPID MONOLAYERS WITH APPLICATIONS TO PULMONARY SURFACTANT: IR AND FLUORESCENCE STUDIES. ((J. Wilkin, Zhao Ping and R.A. Dluhy)) Department of Chemistry, University of Georgia, Athens, GA 30602; ((S. Weinbach and R. Notter)) Department of Pediatrics, University of Rochester Medical School, Rochester, NY 14642; ((M. Lösche)) Institute of Experimental Physics, University of Leipzig, Leipzig, Germany

Current research in this laboratory uses a combined spectroscopic-imaging approach to study biophysical membrane model monolayers. This approach employs IR spectroscopy to obtain conformational information and fluorescence microscopy to visualize monolayer domains. These methods have been applied to the quantitative determination of domain formation in single and binary mixtures of lipid-peptide mixtures used as models of mammalian pulmonary surfactant. Using polarized external reflectance IR spectroscopy of single component lipid monolayers, we have identified individual C-H stretching bands resulting from both gel and liquid domains; these bands qualitatively track the formation of gel domains upon compression as seen in epi-fluorescence microscopy. Both IR spectroscopy and fluorescence microscopy were used to study domain formation in binary mixtures of lipids in the presence and absence of the SP-B and SP-C surfactant peptides. Fluorescence microscopy was also used to study the individual phase behavior of a phosphocholine plasmalogen lipid which has been recently observed to occur at high levels (5 mole %) in surfactant.

M-Pos272

TWO-PHOTON FLUORESCENCE MICROSCOPY OF LAURDAN GP DOMAINS IN MULTILAMELLAR PHOSPHOLIPID VESICLES USING POLARIZED LASER EXCITATION. ((Enrico Gratton, Moshe Levi, Weiming Yu and **Tiziana Parasassi**)) LFD, U of Illinois at Urbana-Champaign, IL; U of Texas Southwestern Med Ctr and DVAMC, Dallas, TX; and CNR, Roma, Itay.

Two-photon microscopy images of multilamellar phospholipid vesicles labeled with LAURDAN show coexisting regions of different generalized polarization (GP) values. The LAURDAN GP function measures the relative water content of the membrane. We have used polarized laser excitation which selectively excites high GP domains. The histogram of the GP values in vesicles of gel, of liquid-crystalline and of equimolar mixture of the two phases is distributed. The GP distribution in the gel phase vesicles is relatively narrow, while in the liquid-crystalline phase and in the mixture of the two phases is broad. Analysis of the images lead to the conclusion that the coexisting regions of different GP values have dimensions smaller than the microscope resolution (about 200 nm). The vesicles composed of an equimolar mixture of gel and liquid-crystalline phase show coexisting domains but the "rigid" domains have lower average GP than the pure gel phase and the "fluid" domains have higher average GP than the pure liquid-crystalline phase. Cholesterol strongly modify the domains morphology. In gel phase vesicles, in the presence of 30 mol% cholesterol the average GP is higher and the GP distribution shows the appearance of a small component at low GP. In the presence of cholesterol, the mixture of the two coexisting phases still shows disjoined regions with different GP values, and the histogram of the GP is narrower than in the absence of cholesterol. The two-photon microscope images are discussed considering the molecular orientation of the lipid bilayer in the microscope section relative to the excitation polarization. (Supported by grants from NIH, VA and CNR).

M-Pos273

ALTERED MEMBRANE LOCALIZATION AND BEHAVIOR OF HALOGENATED CYCLOBUTANES THAT VIOLATE THE MEYER-OVERTON HYPOTHESIS. ((**C. L. North** and D. S. Cafiso)) Department of Chemistry, University of Virginia, Charlottesville, VA 22901.

Although the common predictors of anesthetic activity suggest they should have similar anesthetic potencies, the halogenated cyclobutane c($CClFCClFCF_2CF_2$) is not an effective anesthetic, while c($CClFCF_2CH_2CH_2$) is an effective general anesthetic (Kobin et al., 1994, *Anesth. Analg.* **79**, 1043). Using ^2H NMR, the effect of these compounds on the acyl chain packing in $P(d_{31})OPC$ membranes was examined. Addition of the anesthetic c($CClFCF_2CH_2CH_2$) results in small increases in the segmental order for segments near the headgroup, while segments deeper in the bilayer show decreases. These results are similar to those obtained previously for halothane, isoflurane and enflurane (Baber et al, 1995, *Biochemistry*, **34**, 6533). On addition of the non-anesthetic c($CClFCClFCF_2CF_2$), the segmental order was virtually unchanged except for slightly increased order near the segments 10 to 12 of the palmitoyl chains. These results, and an analysis of ^{19}F chemical shifts, indicate that the anesthetic c($CClFCF_2CH_2CH_2$) exhibits a preference for the membrane interface, as do the other general anesthetics, whereas the non-anesthetic c($CClFCClFCF_2CF_2$) resides within the membrane hydrocarbon core. The compound c($CClFCClFCF_2CF_2$) and other non-anesthetic halocarbons have lower molecular dipole moments compared to effective anesthetic halocarbons, which may account for their altered distribution within the membrane. These data strongly suggest that localization within the membrane interface is a predictor of anesthetic potency and may mediate anesthetic activity.

M-Pos274

ELECTRIC FIELD-INDUCED REORGANIZATION OF PROTEINS AND LIPIDS IN A FLUID BILAYER MEMBRANE

((**Jay T. Groves**, Nick Ulman, and Steven G. Boxer)) Department of Chemistry, Stanford University, Stanford, CA 94305-5080.

Lipid bilayer vesicles spontaneously fuse with an appropriate hydrophilic surface to form an extended planar supported bilayer. The membrane is generally separated from the substrate by a ~10 Å film of water and retains many of the properties of free membranes including lateral fluidity. We have shown that electric fields can induce concentration gradients of charged molecules in confined regions of the membrane and that these can be quantitatively described by a simple competition between diffusion and field-induced drift[1]. More extensive studies reveal deviations from this model for highly concentrated components which provide information about intermolecular interactions in the membrane. Analyses of the field-induced reorganization of three different GPI-tethered proteins have demonstrated an abrupt transition between concentrated and dilute regions of the concentration profiles[2]. Similar studies with streptavidin linked to the membrane with a biotinylated lipid suggest the field may be used to direct formation of two-dimensional crystalline or polycrystalline domains. Current work is directed at furthering our quantitative understanding of the behavior of highly concentrated components under the influence of an electric field as a way of learning more about the organization of molecules in a bilayer membrane.

[1]Groves, J. T. and S. G. Boxer. (1995) *Biophys. J.* **69**: 1972-1979
[2]Groves, J. T., C. Wülfing, and S. G. Boxer. (1996) *Biophys. J.* **71**

M-Pos275

HOW IS THE L_α TO H_{II} PHASE TRANSITION OF PE TRIGGERED

(M. Ge and J.H. Freed), Baker Laboratory of Chemistry, Cornell University, Ithaca, New York 14853

The stress tensor components in a frustrated PE bilayer have been estimated in terms of Dill-Flory [1] and Tang's lattice models [2]. The nearly hard-core repulsions between the chain segments are dominant over the long range weak attractions, which provide a mean field to fix the density. We suggest that the lateral expansion in the chain region, arising from the chain splaying, is resisted by the strong electrostatic interactions between PE head groups. Thus, a compression in the chain region and a tension in the head group region are induced, thereby resulting in a bending moment in the monolayer. Due to the opposite senses of the bending moment in two monolayers, the bilayer becomes frustrated .The profile of the conformation of the segment was given by Dill and Flory, a profile of the two-dimensional pressure in the chain region can be evaluated by using Tang's model. With the assumed tension in the head group region, the profile of lateral components of the stress tensor can be obtained. When the bilayer is treated as a continuum medium, the longitudinal component can also be derived. The calculation shows that an L_α to H_{II} phase transition could be triggered as a result of peeling off at the center of the bilayer or breakage of the head group hydrogen bonding network.

[1] Dill-Flory, Proc. Natl. Acad. Sci. USA. (1980)77:3115-3119.[2] Tang, Statistical mechanics and its application in physical chemistry. (1979) Scientific Press.Beijing.

M-Pos276

GEL-SUPPORTED PLANAR LIPID BILAYERS

Joyce Wong, Chad Park, Markus Seitz, and Jacob Israelachvili, Department of Chemical Engineering, University of California-Santa Barbara, Santa Barbara, CA 93106.

Lipid bilayer systems have been used extensively to study the structure and function of biomembranes including recognition, adhesion and fusion. Phospholipid bilayers supported on flat solid substrates have been used to model interactions between membranes, but have several drawbacks: (i) the membrane fluidity is decreased since it is constrained by the substrate surface; and (ii) it is difficult to insert transmembrane proteins into the membrane.

Our approach is to create biomembranes supported on a polymer cushion which can swell and act as a deformable and mobile substrate, thus resembling the cytoskeletal support in actual cells. We adsorbed a highly-branched cationic polymer (polyethyleneimine, PEI) onto mica substrates, and phospholipid bilayers were formed via Langmuir-Schaefer deposition or adsorption of small unilamellar vesicles. The surface of the adsorbed polymer was imaged using atomic force microscopy in tapping mode and appeared uniform. The uniformity of the bilayer was characterized by fluorescence and reflectance interference contrast microscopic techniques. Studies with the surface forces apparatus indicate that these membranes are highly fluid since we can induce full fusion of the bilayers. This system of increased membrane fluidity will in turn allow functional reconstitution of integral membrane proteins into the membrane.

M-Pos277

EFFECT OF ACYL CHAIN ASYMMETRY ON THE THERMODYNAMIC PROPERTIES OF L-α-PHOSPHATIDYLGLYCEROL

((**Ramesh V. Durvasula** and Ching-hsien Huang)) Department of Biochemistry, University of Virginia, Charlottesville, VA 22908.

The single-crystal structure of the natural form of dimyristoylphosphatidylglycerol (1'-DMPG) shows an acyl chain configuration that is opposite to that of phosphatidylcholine (PC) (Pascher et.al., *BBA* 896:77-88, 1987). Specifically, the *sn*-1 chain of 1'-DMPG is bent at C(2) while the *sn*-2 chain is straight, whereas for DMPC, the *sn*-2 chain contains the bend and the *sn*-1 chain is straight. If this difference in acyl chain configuration in the crystal structures persists in the 1'-DMPG gel-state bilayer, then modulation of the acyl chain length asymmetry is expected to have an opposite effect on the thermodynamic parameters -- e.g. phase transition temperature (T_m) and transition enthalpy (ΔH) -- of PG when compared to PC. For example, molecular mechanics calculations indicate that C(15):C(13)PC should have a higher T_m than C(14):C(14)PC, and indeed this has been demonstrated (Li, et.al, *Biophys J*, 65:1415-28, 1993). Similar calculations done on PG indicate that C(15):C(13)PG should have a lower T_m than C(14):C(14)PG. In this work, 24 molecular species of PG with different acyl chain compositions and with M, homologous to either C(14):C(14)PG or C(16):C(16)PG were semisynthesized, and the T_m and ΔH of each PG were measured using high-resolution differential scanning calorimetry. These calorimetric and molecular mechanics calulations will be presented.

M-Pos278

RESPONSE OF PHOSPHOLIPID MEMBRANES TO LATERAL PRESSURE - EFFECT OF POLYUNSATURATED ACYL CHAINS

((**B.W. Koenig**, L.L. Holte, H. Strey[r], and K. Gawrisch)) LMBB, NIAAA, NIH and [r]LSB, DCRT, NIH, Bethesda, MD 20892

Multilamellar liposomes of either di[(14:0)-d_{27}]PC, (18:0)-d_{35}(18:1)PC, or (18:0)-d_{35}(22:6n-3)PC in the L_α phase were dehydrated by applying defined levels of osmotic stress covering the range of water activities from $a_w = 0.94$ to 1. Resulting changes in average order, length, and area of the saturated acyl chains were studied by ^2H NMR. Area per lipid molecule in the bilayer was also calculated from X-ray diffraction data. The lipid-to-water ratio in equilibrated multilamellar liposomes was determined by ^1H-magic-angle-spinning NMR. By comparison of NMR and X-ray results we were able to qualitatively differentiate the response to lateral pressure of the saturated and the polyunsaturated chains in (18:0)-d_{35}(22:6n-3)PC. Lateral area compressibility coefficients of bilayers were calculated from the data. Values of 136 ± 20 dyn/cm for di[(14:0)-d_{27}]PC, 221 ± 20 dyn/cm for (18:0)-d_{35}(18:1)PC, and 110 ± 20 dyn/cm for (18:0)-d_{35}(22:6n-3)PC were obtained. The trends observed are in good agreement with area expansion coefficients from micromechanical manipulation on large unilamellar vesicles by Evans and Needham {J. Phys. Chem. 91 (1987) 4219-4228}.

M-Pos279

PROSTAGLANDIN E-1 INDUCES A RIPPLE PHASE IN DIPALMITOYLPHOSPHATIDYLCHOLINE MULTILAMELLAR VESICLES

((**Sharon M. K. Davidson**, Sharma R. Minchey and Andrew S. Janoff)) The Liposome Company, Inc., Princeton, NJ 08540.

A ripple phase was observed at room temperature in multilamellar vesicles composed of DPPC and PGE1 (0.6 - 16.7 mol %) prepared in pH 4.5 buffer using freeze fracture electron microscopy. At lower mole ratios of PGE1, areas of ripple phase with a periodicity of ca. 13 nm coexist with areas of gel phase. At higher PGE1 ratios, the ripple phase begins to predominate, and at 16.7 mol % it is the only structure evident. In this case, the ripple periodicity is predominantly ca. 25 nm. DSC data reveal that the pretransition initially broadens and shifts to lower temperatures as the mole ratio of PGE1 increases, then disappears at higher concentrations. The main transition broadens and shifts to lower temperatures, followed by a decrease in the area of the main peak at the expense of a new peak emerging at lower temperatures. The appearance of this new endotherm (T_m=36.2 °C, $\Delta T_{1/2}$=0.4 °C) suggests that at 16.7 mol % a highly cooperative 5:1 DPPC:PGE1 complex is formed. ^{31}P NMR confirms that a gel-to-fluid lamellar phase transition is maintained. The addition of PGE1 has resulted in the formation of a specific complex that stabilizes the phospholipid lattice in a ripple configuration. ESR spectra using 12-doxyl PC reveal a significant increase in the outer hyperfine splitting ($2A_{max}$) in DPPC:PGE1 (5:1) bilayers below the T_m. These data may be explained by an extended PGE1 configuration in which the carboxyl group is located at the level of the phosphate group of the lipid and the C_{20} end of the molecule penetrates the region of the C-12 position of the phospholipids.

M-Pos280

CALORIMETRIC INVESTIGATION OF BINARY MIXTURES OF α-BROMOACYL TAXANES AND PHOSPHOCHOLINES ((**Shaukat Ali**, Eric Mayhew, Sharma Minchey and Andrew Janoff)) The Liposome Company, Inc., Princeton, NJ 08540.

High sensitivity differential scanning calorimetry (DSC) was used to study the thermotropic phase properties of binary mixtures of α-bromoacyl taxanes and saturated diC14 PC, di C16PC, and diC18PC multilamellar bilayers. The α-bromoacyl chains of the taxane were varied from C-6 to C-12 and C-16 carbons long. Calorimetric data of each of the binary mixtures of the α-bromoacyl taxanes (0-17 mol%) and the PC showed that the pretransition temperature of each of the PCs was abolished with the increasing mol% of taxane. The bilayer perturbation was chain length dependent for both the taxanes and the phospholipids. For instance, bilayers composed of short chain diC14PC in binary mixtures were more significantly perturbed compared to the long chain diC16PC or diC18PC bilayers. In most cases the incorporation of taxanes was low; short chain diC14PC bilayers incorporated ~10-15 mol% of the derivatives and were more perturbed with the long chain taxanes. In contrast, the long chain diC16PC and diC18PC bilayers incorporated ~2-5 mol% taxane. The heat of enthalpy (ΔH) of each of the binary mixtures of taxane and PC remained constant at all concentrations investigated. Taken together, the DSC data show that hydrophobic taxanes have only limited access to the association with the hydrophobic interiors of the bilayers due, in part, to the bulky size of the taxane.

PROTEIN STRUCTURE PREDICTION

M-Pos281

COMPUTATIONAL MODELING OF MEMBRANE PROTEIN STRUCTURE BASED ON INDUCED PARAMAGNETIC CHEMICAL SHIFTS: THE FIRST STEPS ((**John G. Pearson**, Thomas B. Woolf)) Dept of Physiology, School of Medicine, Johns Hopkins University, 725 N. Wolfe St., Baltimore, MD 21205 (Spon. by C. Abeygunawardana)

The determination of membrane protein structure continues to be a difficult problem. We are exploring the utility of a novel approach to the determination of a-helical transmembrane protein structure using a combination of cysteine scanning mutagenesis and computational modeling. The modeling consists of two phases. The first phase is described in this poster and consists of electronic structure calculations for the local paramagnetic tensor to describe the pseudo-contact shift. The pseudo-contact paramagnetic shift contains information about both distance and angle from the paramagnetic site. The utility of this information depends on detailed knowledge of the local tensor and a framework for using the information in refinement. We present electronic structure calculations using the deMon (Malkin, Malkina, and Salahub (1994), *JACS* **116**, 5898) code modified to predict paramagnetic tensors. Once these tensors have been determined, the second phase of refinement will consist of incorporation of these restraints into the CHARMm molecular dynamics package.

M-Pos282

COMBINING SECONDARY STRUCTURE PREDICTION WITH SELF-CORRECTING DISTANCE GEOMETRY CALCULATION: APPLICATION TO HIV-1 REV PROTEIN MODELLING ((**Hongyao Zhu**, Robert Fraczkiewicz and Werner Braun)) Department of Human Biological Chemistry and Genetics, Sealy Center for Structural Biology, University of Texas Medical Branch, Galveston, TX 77555-1157.

An automated method for protein three-dimensional structure modelling has been developed based on the combination of self-correcting distance geometry calculation with secondary structure and solvent accessibility. To make further improvement of the method, new statistics on a set of representative proteins from PDB has been made, and implemented in a translation program to generate dihedral angle and distance constraints for distance geometry calculation. Calculations with simulated data sets from known X-ray structure have been performed for several test proteins to assess the current method. Further improvements and development of the approach are addressed.

This automated method has been applied to three-dimensional structure modelling for HIV-1 Rev protein (human immunodeficiency virus type-1 Rev trans-activator). No three-dimensional structures are so far available for Rev or homologous proteins. Secondary structure is predicted using various approaches and experimental observations. Inside and outside information for individual residues comes from the prediction of a pattern recognition algorithm and from experimental data on the RNA-binding domain which recognizes the Rev responsive element, and the activation domain which acts as a cofactor-binding domain. Clusters of possible HIV-1 Rev folds are presented. Finally, these structures are refined with the energy minimization program FANTOM.

M-Pos283

PREDICTIONS OF TRANSMEMBRANE α-HELICES USING A HYDROPATHY SCALE DERIVED FROM FIRST PRINCIPLES. ((Nir Ben-Tal and Barry Honig)) Department of Biochemistry and Molecular Biophysics, Columbia University, NY 10032.

A unique hydropathy (hydrophobicity) scale, based on the free energies of transfer of the amino acids from aqueous phase to lipid bilayers, is presented. Unlike other hydropathy scales (e.g. Kyte and Doolittle) which assume that the free energies of transfer are proportional to some inherent property (an individual atom, a chemical group or an amino acid), our scale was derived using a theoretical model that accounts for the amino acids in the context of an α-helix embedded in implicit solvent. The scale will be used to predict the location of bilayer spanning helices in membrane proteins. The results will be compared to experimental data, to predictions using other hydropathy scales, and to prediction algorithms that are based on data base derived propensities. The hydropathy scale and the prediction algorithm will be analyzed, and suggestions for improvements will be made. This is a first stage in developing an energy based prediction scheme for transmembrane helices using structural information.

M-Pos284

PROPOSED STRUCTURE FOR THE NPxxY SEQUENCE MOTIF IN TRANSMEMBRANE SEGMENT 7 OF G-PROTEIN COUPLED RECEPTORS. ((**K. Kouvicka**, F. Guarnieri, J. A. Ballesteros and H. Weinstein)) Mount Sinai School of Medicine, Dept. of Physiology & Biophysics, New York, NY 10029.

Construction of the transmembrane part of the GnRH receptor followed the general methodological patterns for the modeling of G-protein coupled receptors (GPCRs) (see Ballesteros & Weinstein, Meth. Neurosci, 1995, 25:366-428). A specific inconsistency emerged between experimental data and the model of transmembrane segment (TS) 7 as an ideal α-helix structure. Thus, structural proximity constraints derived from experiments for specific residues in TS 7 cannot be simultaneously incorporated in a model consisting of helices arranged in a sequential anticlockwise manner (viewed from the extracellular side) on the rhodopsin "footprint" if TS 7 is an ideal α-helix. Residue 7.39 proposed to face TS 1 and/or 2 and residue 7.43 suggested to interact with TS 2 appear to be positioned on opposite side of TS 7 relative to residue 7.49 which was also proposed to interact with TS 2. A regular Pro-kink due to the conserved Pro7.50 did not appear sufficient to produce the structural rearrangements required for the experimentally determined interactions. However, a search of the protein structure database revealed that NP or DP sequences (conserved among GPCRs in TS 7) have characteristic properties that are significantly different from a Pro-kink. These are produced by the combination of the helix disruptive Pro residue with the H-bonding properties of the N or D. The NP or DP sequence produces a characteristic break in a helix and a flexible hinge which can accommodate a large rearrangement of the two helix parts. All these special structural properties were used to construct the TS 7 model. The conserved Tyr7.53 also appears to play a significant structural role in the TS 7 model supporting the parallel orientation of the two helix parts of TS 7 needed to cross the membrane. The modeled TS 7 structure was probed computationally with novel MC simulations (see Guarnieri & Weinstein, J. Amer. Chem. Soc. 1996, 118: 5580-5589). The resulting TS 7 appeared to be one of the lowest energy structures and can easily accommodate all experimentally set constraints for TS 7. The constructed model of the transmembrane part of the GnRH receptor incorporating this TS 7 is stable in MD simulations. *Supported by NIH grants DK-46943 and DA-00060.*

M-Pos285

^{1}H MAS NMR OF GRAMICIDIN A IN A LIQUID-CRYSTALLINE MULTILAMELLAR PHASE. ((**Christophe Farès**, James H. Davis, Frances J. Sharom)) Departments of Physics, and Chemistry and Biochemistry and the Biophysics Interdepartmental Group, University of Guelph, Guelph, Ontario, N1G 2W1 (Canada).

Using a recently-built very high speed MAS probe capable of spinning at rates of at least 20 kHz, we have shown that it is possible to obtain ^{1}H signals with line widths in the range of 25-30 Hz, an improvement of three orders of magnitude. To establish that it is possible to obtain distance restraints between nuclei, we have performed 1D nuclear Overhauser effect (NOE) experiments on gramicidin A. The build-up curves for these NOEs clearly show that one can obtain the same sort of distance restraints for peptides in membrane bilayers as are obtained in well-established solution NMR studies. This is a crucial step in demonstrating that high resolution solution NMR techniques can be applied to structure determination in membrane systems. Extending this to two dimensions, we have performed a series of 2D-NOESY experiments which establish unambiguously that gramicidin A adopts the same conformation in multilamellar dispersions as that reported in SDS micelles by Arseniev et al. [Biol. Membr. (1986) **3(5)**, 437-462]. The ^{1}H MAS NMR technique that we have developed is therefore potentially capable of determining the complete 3D structure of a membrane spanning peptide.

M-Pos286

PREDICTING PROTEIN SECONDARY STRUCTURE USING STRUCTURE-BASED MODELS OF EVOLUTIONARILY-DERIVED SITE HETEROGENEITY ((**M. J. Thompson** and R. A. Goldstein)) Biophysics Research Division and Department of Chemistry, University of Michigan, Ann Arbor, MI 48109-1055, USA

Abstract

We construct a statistical model of the heterogeneity of distributions of amino acid substitutions found in alignments of homologous proteins. This model is optimized by maximizing the mutual information between a set of profiles and the secondary structures corresponding to the alignment sites represented by the profiles. We incorporate this model into our previous method for predicting one dimensional features of protein structure. Using a set of profiles optimized over 103 training proteins, 3-state accuracies above 72% are achieved over 187 test proteins. Unlike manual "expert heuristic" methods, this approach has been demonstrated to work well over large datasets. Unlike neural network algorithms, this approach is amenable to physicochemical interpretation. Moreover, the model-optimization procedure, the formalism for predicting structural features, and our previously developed method for tertiary structure recognition all share a common Bayesian probabilistic basis. This consistency starkly contrasts with the hybrid and *ad hoc* nature of methods which have dominated this field in recent years.

M-Pos287

NESTED INTERACTION CAN DESCRIBE THE ATP-BINDING BY GroEL ((Nadja Hellmann and **Heinz Decker**)) Institute of Molecular Biophysics, University of Mainz,Jakob-Welder-Weg 26, 55128 Mainz, Germany

Several investigators published data concerning the ATPase activity of GroEL under different conditions, which is important for its role in the folding process [1,2,3]. The initial rates of hydrolysis change in cooperative manner with the substrate concentration. The phenomena were explained with a mixture of MWC-type and KNF-type interactions, including negative cooperativity between the 7-mers [1].We included the influence of KCl and GroES on the hydrolysis rate applying the nested MWC model, which has successfully explained the oxygen binding of hemocyanins [4,5]. In contrast to [1] we could describe the ATPase activity based on protein characteristic properties (binding constants and hydrolysis rates), which are not influenced by any effector and regulatory properties (conformational equilibria), which are modified by the presence of GroES and KCl. This description of cooperativity is in full accordance with the results from X-ray structures, that no strong evidence for inhibitory interaction (negative cooperativity) between the 7-mers can be found [6].This is another example for a certain principle, which is represented by the nested MWC-model: different conformations exist for the unligated protein-complex; regulation of function is established by enhancing the fraction of conformations with the right properties.

[1] Yifrach,O. et al, (1995), Biochemistry 34:5302-5308
[2] Yifrach,O. et al, (1994), JMB 243,397-401
[3] Kovalenko,O. et al (1994), Biochemistry 33, 14974-14978
[4] Decker,H. and R.Sterner (1990), J.Mol.Biol. 211:281-293
[5] Robert,C.H. et al, (1987), Proc. Natl. Acad. Sci. (USA) 84:1891-1895
[6] Boisvert,D. et al (1996), Nature Struc.Biol. 3:170-177

PROTEIN STRUCTURE AND FUNCTION

M-Pos288

HUMAN ORNITHINE TRANSCARBAMYLASE: STRUCTURE FUNCTION RELATIONSHIPS OF LATE ONSET MUTATIONS. ((**H. Morizono**, C. D. Listrom, M. Aoyagi, D. Shi, B. S. Rajagopal[1], M. T. Tuchman[1], N. M. Allewell)) Department of Biochemistry, University of Minnesota, St. Paul MN 55108. [1]Department of Pediatrics, University of Minnesota Medical School, Minneapolis, MN 55455.

Mutations in ornithine transcarbamylase (OTCase) are the most common cause of inherited urea cycle disorders, and can produce symptoms that range from milder "late onset" to fatal neonatal hyperammonemia. Three mutants associated with "late onset" OTCase deficiency (R40H, R277Q, R277W) with mutations distant from the predicted active site were expressed in *E. coli* and purified. R40H has properties very similar to wild type OTCase while both R277Q and R277W show a nearly 60 fold decrease in affinity for ornithine, an alkaline shift in the optimal pH for Vmax, and a greater susceptibility to thermal inactivation. The effects of mutation at position 277 may be due to interactions with a conserved aspartate at position 196. The results from purified R40H suggest this mutation may affect mitochondrial import or post-translational modification of the protein.
Supported by NIDDK 47870

M-Pos289

3-DIMENSIONAL STRUCTURE OF FROZEN-HYDRATED CHIP28 (AQP1) WATER CHANNEL BY ELECTRON CRYO-CRYSTALLOGRAPHY. ((**A. Cheng***, A. N. van Hoek†, M. Yeager*, A. S. Verkman†, and A. K. Mitra*)) , *Dept. of Cell Biology, The Scripps Research Institute, La Jolla, CA 92037, †Cardiovascular Research Institute, University of California San Francisco, San Francisco, CA 94143.

CHIP28 (AQP1), the channel-forming integral protein of relative molecular mass 28,000, belongs to the "aquaporin" family of proteins that facilitate rapid transport of water across plasma membranes of water-permeable cells. We reported previously the structure of deglycosylated, human erythrocyte CHIP28 (AQP1) at 5.8 Å resolution as viewed normal to the membrane plane (Mitra *et al.*, Nature Structure Biology 2, 726-729, 1995). For this purpose we applied electron cryo-crystallography to frozen-hydrated, highly-ordered, 2-dimensional (2-D) crystals of CHIP28 generated in synthetic lipid bilayers. We now present the 3-D structure determined by analyzing data generated from views of the 2-D crystals of CHIP28 tilted up to 45° in the electron microscope. The nominal resolution of the density map is 7Å in the plane of the bilayer and ~30 Å perpendicular to it. The 3-D structure confirms, as suggested earlier from the projection structure, the presence of multiple α-helices in each monomer enclosing an aqueous vestibule leading to the water-selective channel within the bilayer. The current resolution of the map does not rule out the existence of elements of β-structure. Within a tetramer, adjacent monomers interact at the opposite sides of the bilayer. Additionally, the 3-D density map suggests the presence of a pseudo 2-fold axis of symmetry relating the two homologous halves of a CHIP28 molecule.

M-Pos290

CYTOCHROME P450 RECOGNITION SITES FOR NADPH CYTOCHROME P450 REDUCTASE AND SUBSTRATES. ((**R. Dai**, R.C. Robinson and F.K. Friedman)) NCI, NIH, Bethesda, MD 20892

Mammalian cytochromes P450 contain functional domains which are responsible for substrate recognition and interaction with NADPH cytochrome P450 reductase. Although a number of amino acids which contribute to these functional interactions have been identified, the residues which comprise the corresponding binding sites remain to be ascertained. To identify the P450 binding regions for substrates and reductase, we utilized multiple sequence alignments along with the known structures of bacterial P450s, to generate a model for rat P450 2B1. Peptides corresponding to predicted reductase binding regions were synthesized and evaluated for their ability to disrupt the P450-reductase interaction as measured by inhibition of reductase-mediated benzphetamine demethylation by P450 2B1. The most potent peptide inhibitors were derived from combinations of the C- and L-helices, and the heme binding region. These results indicate that these predicted surface regions include recognition sites for reductase. In addition, several P450 2B1 substrates were docked into the substrate binding site of this model, and the strength of the observed substrate-P450 2B1 interactions were found to correspond to the known substrate specificity of this P450. This model thus successfully predicts both reductase and substrate binding domains of a mammalian P450.

M-Pos291

DISULFIDE STABILIZATION OF THE OXYGEN BINDING SITE IN *LIMULUS* HEMOCYANIN AND ITS SUBUNITS. ((R. Topham, L. Strong, S. Tesh and **C. Bonaventura**)) Chem. Dept., Univ. of Richmond, VA 23173 & Duke Univ. Nicholas School of the Environ. Marine Lab., Beaufort, NC 28516

Reduction of disulfide bonds in intact *Limulus* hemocyanin or its subunits results in pH and oxygen-dependent disruption of its active site. The active site lies in domain 2 and two disulfide bonds, presumably those involved in disruption of the active site, are attached to a loop of domain 3 that bridges both domains 1 and 2. An increase in pH from 7 to 9 markedly enhances the active-site disruption by disulfide-reducing agents. The pH dependence of the active site disruption is inferred to result from ionization of specific groups that alter the coordination of histidines to the active-site copper atoms. Candidate residues responsible for the pH-dependence of the active-site disruption are the free cysteines 208 and 213 that occur in the alpha helix that contains His 204, a ligand for copper A of the active site. Crystallographic studies have shown that oxygenation of *Limulus* II hemocyanin shifts the orientation of the histidine residues that ligand the copper atoms of the oxygen binding site. This may account for the faster active-site disruption seen in the presence of oxygen. The subunits of *Limulus* hemocyanin differ in their susceptibility to this mode of active-site disruption, indicating that their stereochemistry differs significantly with regard to the stability conferred by disulfide bonds. The subunits that form hexameric aggregates are relatively more resistant to modification by disulfide-reducing agents, showing that breaking of disulfide bonds has quaternary as well as tertiary consequences.

M-Pos292

HYDRODYNAMIC & PROTEOLYTIC FOOTPRINTING STUDIES OF CALCIUM-INDUCED INTERDOMAIN INTERACTIONS IN CALMODULIN ((**B. R. Sorensen** & M. A. Shea)) Dept. of Biochemistry, U. of Iowa College of Medicine, Iowa City, IA 52242-1109 (madeline-shea@uiowa.edu)

Proteolytic footprinting titrations of calmodulin (CaM) show that binding of calcium to the two high affinity sites in the C-terminal domain of CaM alters the conformation of the two vacant sites in the N-domain.[1,2] To better understand domain communication in CaM and to estimate the energetic costs, we use hydrodynamic techniques and residue-specific probes to compare calcium-dependent properties of the whole protein *versus* those of the isolated domains.

Gel permeation chromatography studies have shown calcium binding decreases the Stokes radius (R_s) of whole CaM[3] and the isolated domains by equivalent amounts (~1Å). This implies that ΔR_s is a function of the behavior of each domain, their interactions and orientation. Analytical ultracentrifugation studies of CaM and its domains (using a Beckman XLI) are underway to further explore the calcium-dependent hydrodynamic properties of this protein.

Footprinting titrations show that the proteolytic susceptibility of the isolated N- domain of CaM is intrinsically very low indicating that the induced susceptibility in the N-domain of whole CaM exceeds the intrinsic susceptibility of the isolated N-domain. This suggests that in whole CaM the N-domain is made more flexible or exposed by calcium binding to in the C-domain. By comparing the free energies of cooperative calcium binding between the isolated domains and the holo protein, we estimate the energy of interdomain interactions.

[1]Pedigo & Shea (1995). *Biochemistry* 34: 1179-1196; [2]Shea, Verhoeven & Pedigo (1996). *Biochemistry* 35 : 2943-2957; [3]Sorensen & Shea (1996) *Biophysical Journal* (in press).

M-Pos293

ON THE TRANSPORT MECHANISM OF THE SUGAR SPECIFIC OUTER MEMBRANE PROTEIN LamB ((N. Saint[1], M. Winterhalter[2], Y.F. Wang[1], and J.P. Rosenbusch[1])) [1]Dept. of Microbiology and [2]Dept. of Biophys. Chem., Biozentrum, CH-4056 Basel, Switzerland

Trimeric maltoporin (LamB protein) facilitates the diffusion of maltodextrins across the outer membrane of Gram-negative bacteria. The crystal structures of maltoporin from Escherichia coli in complexes with maltotriose and maltohexaose were determined to a resolution of 3.2 and 2.8 Å[1]. They reveal an extended binding site within the maltoporin channel. The hydrophobic face of the sugars are in van der Waals contact with the "greasy slide" which is composed of aromatic residues and guides the sugar into and through the channel constriction. The aromatic residues of the "greasy slide" (W74, Y6, W420, W358, F227), as well as a tyrosine (Y118) in the channel constriction were replaced one by one by alanine. Purified LamB protein as well as the mutants were reconstituted into artificial planar lipid bilayer and conductivity measurements were performed. Titration experiments with maltotriose and maltohexaose yielded the binding constant for the respective sugars. In addition the spectra of the current noise was analysed to yield on and off-rates of sugar ligands. The results are discussed with respect to the crystal structure and compared with swelling experiments of liposomes containing reconstituted LamB proteins.

[1] R. Dutzler et al., *Structure* 4, (1996) 127-134.

M-Pos294

COMPARISON OF T54 ALLELE WITH NORMAL A54 ALLELE OF HUMAN INTESTINAL FATTY ACID BINDING PROTEIN. ((**Fengli Zhang**[*], Christian Lucke[+], Leslie J. Baier[++], James C. Sacchettini[+], and James A. Hamilton[*])) [*]Department of Biophysics, Boston University School of Medicine, Boston, MA 02118; [++]Phoenix Epidemiology and Clinical Research Branch, NIDDK, NIH, Pheonix, AZ 85016; [+]Department of Biochemistry and Biophysics, Texas A&M University, College Station, TX 77845

The human intestinal fatty acid binding protein (I-FABP) is a small (131 amino acid) protein which binds dietary long-chain fatty acids in the cytosol of enterocytes. Recently, an alanine to threonine substitution at position 54 in I-FABP has been identified which affects fatty acid binding and transport, and is associated with the development of insulin resistance in several populations including Mexican-Americans and Pima Indians. To investigate the molecular basis of the binding properties of I-FABP, the 3D solution structures of both T54 and A54 alleles of human I-FABP, expressed and purified from *E. coli.* with and without ^{15}N-enriched media, are being studied by multidimensional NMR. The sequential assignments were completed by using two dimensional homonuclear spectra (COSY, TOCSY, and NOESY), and three dimensional spectra (NOESY-HMQC and TOCSY-HMQC). The tertiary structures of both alleles are being calculated by a distance geometry program DIANA based on NOE constraints obtained from NMR spectra. The up-down β-barrel structural motif is present in both I-FABP alleles. The NMR results show significant conformational variability of certain backbone segments around the postulated portal region for the entry and exit of fatty acid ligand. Detailed comparisons of the chemical shift values and the structures of the normal and the T54 allele of I-FABP will help understand the molecular basis of disorders of fatty acid metabolism in diabetes.

M-Pos295

CONVERTING TRYPSIN INTO ELASTASE. ((**Su-Hwi Hung and Lizbeth Hedstrom**)) Department of Biochemistry, Brandeis University, Waltham, Massachusetts 02254-9110

A trypsin mutant with chymotrypsin-like activity has been made by replacing the residues of the S1 binding site and two surface loops (residues 185-188 and 221-225) of trypsin with analogous sequences of chymotrypsin [Hedstrom, L., Perona, J. J., & William J. Rutter, 1994, *Biochemistry*, 33, 8757-8763]. In order to test whether the S1 binding site and loops 1 and 2 are general specificity determinants in trypsin family of serine proteases, the chymotrypsin-like trypsin mutant (Tr→Ch[S1+L1+L2+Y172W]) was further mutated by replacing the two surface loops with the analogous sequences of elastase (Tr→El[L1+L2]). Tr→El[L1+L2] does not confer elastase-like activity and the mutant is a nonspecific enzyme with kcat/Km's of 2.2 x 10^4 $M^{-1}s^{-1}$ and 1.2 x 10^5 $M^{-1}s^{-1}$ for the hydrolysis of MeOSuc-AAPA-SBzl and Suc-AAPF-SBzl, respectively. Mutations of Gly216Val and Gly226Thr were added to imitate the occluded S1 site of elastase. Tr→El[L1+L2+G216V+G226T] has elastase-like specificity. MeOSuc-AAPA-SBzl is hydrolyzed 160-fold faster than Suc-AAPF-SBzl (kcat/Km = 3.1 x 10^3 $M^{-1}s^{-1}$ vs. 19 $M^{-1}s^{-1}$) and 770-fold faster than Nα-CBZ-K-SBzl (kcat/Km is 3.9 $M^{-1}s^{-1}$). None of these Tr→El enzymes have significant elastase-like amidase activity. Interestingly, the circular dichroism (CD) spectrum of Tr→El[L1+L2+G216V+G226T] is similar to the CD spectrum of elastase at far UV range (250-190 nm) whereas the CD spectrum of Tr→El[L1+L2] is similar to the CD spectrum of Tr→Ch[S1+L1+L2+Y172W].

M-Pos296

MOLECULAR MODELING STUDIES OF THE NADPH BINDING DOMAIN OF RAT STEROID 5α-REDUCTASE. ((A. K. Bhattacharyya, M.F. Taylor, M. Wang, D. Isbell and D.C. Collins. (Spon. R.W. Hadley)). VA Medical Center, Departments of OB/GYN and Biochemistry, University of Kentucky, Lexington, KY 40536.

Previous studies [Bhattacharyya et al. (1995) Biochemistry 34, 3663-3669] have shown that the NADPH binding domain of rat liver microsomal steroid 5α-reductase resides in a highly conserved region of the polypeptide sequence (residues 160-190). The primary structure of the 31 amino acid peptide was used to produce a peptide structure *ab initio* using a molecular modeling approach. The Monamy secondary structure prediction was used to provide initial constraints, and subsequent energy minimization was performed using an Adopted-Basis Newton-Raphson protocol. The structure of NADPH was subsequently docked and showed that cofactor binding occurred within a cleft upon the surface of the peptide molecule, and appears to interact with charged residues on the same surface. Stacking is observed between 179Y and 187F which maximizes the hydrophobic interaction between these residues. The nicotinamide ring of NADPH is proximal to 179Y, with the distance between its hydroxyl moiety and C-4 of the nicotinamide ring being ~ 4.5 A°. Other potential interactions are electrostatic in nature involving negatively-charged phosphates on the NADPH and intermolecular ionic interactions between residues which may serve to stabilize the peptide structure. Site-directed mutagenesis studies indicated that the mutation Y179F results in a 40-fold increase in the Km for NADPH vs wild type, suggesting that the -OH functionality of this residue may be involved in cofactor binding, whereas the mutant Y179S resulted in enzyme that was inactive. Supported by Department of Veterans Affairs and NIH grant R01DK50083.

M-Pos297

Zn^{2+} PROMOTES THE SELF-ASSOCIATION OF HIV-1 INTEGRASE *IN VITRO*. ((S.P. Lee[#], J. Xiao[&], J.R. Knutson[&], M.S. Lewis[$], and M.K. Han[#])) [#]Department of Biochemistry and Molecular Biology, Georgetown University Medical Center, Washington, DC 20007, [&]Laboratory of Cell Biology, NHLBI, [$] Biomedical Engineering and Instrumentation Program, NIH, Bethesda, MD 20892

The Mg^{2+}-dependent 3'-processing activity of purified HIV-1 integrase is stimulated by the addition of exogenous Zn^{2+} [Lee and Han (1996) Biochemistry 35, 3837-3844]. This activation was hypothesized to result from integrase self-association. In this report, we examine the Zn^{2+} content of HIV-1 integrase by atomic absorption spectroscopy and by application of a thiol modification reagent, p-hydroxymercuriphenylsulfonate, with a metallochromic indicator, 4-(2-pyridylazo)resorcinol. We find that the Zn^{2+} content of HIV-1 integrase varies from 0.1 to 0.92 eq. Zn^{2+} per monomer depending on the conditions of protein purification. *In vitro* activity assays, time-resolved fluorescence emission anisotropy and gel filtration chromatographic analyses all indicate that EDTA yields an apoprotein which is predominantly monomeric and less active with Mg^{2+}. Further, sedimentation equilibrium studies reveal that reconstitution of the apoprotein with Zn^{2+} results in a monomer-tetramer-octamer transition. These results suggest that Zn^{2+} promotes a conformation with enhanced oligomerization and thereby stimulates Mg^{2+}-dependent 3'-processing. This may also imply that multimers larger than dimers (tetramers and possibly octamers) are required for *in vitro* activity of integrase in the presence of Zn^{2+} and Mg^{2+}. In contrast, the content of Zn^{2+} did not significantly affect the 3'-processing and strand transfer reactions with Mn^{2+} *in vitro*.

M-Pos298

THE VAST PROTEIN STRUCTURE COMPARISON METHOD
((J.F. Gibrat, T. Madej, J.L. Spouge, S.H. Bryant))
NCBI-NLM-NIH, Bethesda, MD 20894 (Sponsored by C.W.V. Hogue)

VAST (Vector Alignment Search Tool) is a protein structure comparison method that has recently been implemented at NCBI. This comparison algorithm is fast enough that it has been possible to do a pairwise comparison of all the domains in the Brookhaven Protein Data Bank. The results of this massive computation are available via the internet (http://www.ncbi.nlm.nih.gov/Structure/). An important feature and novelty of the VAST approach is the scoring scheme, which for a given structure ranks the others according to a statistically-derived measure of similarity. This poster presents an overview of VAST with an emphasis on the statistical basis of the scoring scheme.

M-Pos299

PROTEIN FINGERPRINTING: EXPLORING THE PROTEIN FOLD UNIVERSE AT WARP SPEED

((Malin M. Young, Irwin D. Kuntz)) Dept. of Pharmaceutical Chemistry, University of California, San Francisco, San Francisco, California 94143 USA

The recent exponential rise in the number of protein structures submitted to the Protein Data Bank (PDB) increases the need for a rapid, fully-automated method for accurate protein fold classification. Such a method would not only be useful for clustering the PDB into meaningful structural families, but it could also lead to a new global perspective of the protein fold universe. Identification of the dominant features of the fold universe could lead to a greater understanding of the forces which cause proteins to fold, and may answer the question why some folds are utilized in nature more than others. We have developed a method called *protein fingerprinting*, which has proven to be an accurate and extremely rapid protein fold classification scheme. With this tool, we have been able to do an all-by-all comparison of a large protein structure database. We clustered this database and used the pairwise similarities between cluster heads as distance constraints in a distance geometry calculation to place each cluster head relative to all others in a many-dimensional fold space. Projection of this space into three dimensions indicates that although there are several dominant features that distinguish protein fold families, there exist many minor characteristics that relate disparate protein structures. This may explain why, in clustering the PDB, protein fold families lack distinct boundaries.

M-Pos300

SOLUTION STRUCTURE OF THE C-TERMINAL DOMAIN OF RNA POLYMERASE II: CD OF LONG AND SHORT FRAGMENTS ((Ewa A. Bienkiewicz and Robert W. Woody)) Department of Biochemistry and Molecular Biology, Colorado State University, Fort Collins, CO 80523

The C-terminal domain (CTD) of RNA polymerase II consists of tandem copies of a heptapeptide with the $Y^1S^2P^3T^4S^5P^6S^7$ consensus sequence. This repeat resembles the SPXX motif found in some gene regulatory proteins that adopt a β-turn structure. We have studied CTD fragments using circular dichroism (CD) to test: (1) importance of the putative β-turn points, ie. Ser^2 and Ser^5, (2) dependence of the CTD structure on the length of the polypeptide, and (3) effect of phosphorylation on the CTD structure. The CD analysis pointed to polyproline II, type I β-turn, and tyrosine as the three major components contributing to the CD signal of CTD. The polyproline II-like conformation predominated in water and at lower TFE concentrations. In contrast, 90% and 100% TFE triggered a dramatic increase in β-turn formation with the concurrent increase in the Tyr CD signal. Replacement of Ser^2 and Ser^5 affected the CTD turn population in water and TFE. The CTD structure was chain-length dependent, with the β-turn component being favored in short fragments of CTD, and the polyproline II component predominating in the 56-residue CTD peptide. Phosphorylation of Ser^2 and Ser^5 did not trigger dramatic changes in the CTD structure, but it seemed to stabilize the β-turn conformation. Overall, these findings indicate that in the aqueous environment and by itself, CTD adopts a polyproline II-like structure. In addition, this study supports the prediction that CTD can assume a conformation characteristic of the SPXX transcription factor family, but only upon stabilization of the β-turn structure.
Supported by NIH Grant GM22994 (RWW) and by a CIRB fellowship (EAB).

M-Pos301

CYCLIC NUCLEOTIDE INDUCED CONFORMATIONAL CHANGE IN THE cGMP-DEPENDENT PROTEIN KINASE. ((Jinkui Zhao, Jill Trewhella)) Los Alamos National Laboratory, Los Alamos NM 87545, ((Robert Brushia, Donal Walsh)) University of California, Davis CA 95616, ((Sharron Francis)) Vanderbilt University, Nashville TN 37323.

Small-angle scattering data from type Iα cGMP-dependent protein kinase (PKG) titrated with cGMP (1 through 13 molar equivalents) shows a significant conformational change induced by cGMP-binding. PKG is a dimer with a regulatory and catalytic domain within each monomer component. There is one 'slow' and one 'fast' cGMP binding site on each monomer. A P(r) analysis of the scattering data indicates that the conformational change involves a shift of the molecular mass away from the center of the molecule, possibly due to the movement of the regulatory domain away from the catalytic domain. The radius of gyration of PKG increases dramatically by 30% from 45.4 to 59.4 Å upon addition of two or more molar equivalents of cGMP. This result may explain why PKG can be partially activated while the cAMP-dependent protein kinase (PKA) can not. In the activated state of PKA, the two catalytic subunits fully dissociate from the regulatory subunits and binding of all four cAMP's is needed for this activation. In the case of PKG, binding of cGMP at only two sites has already induced the change of the PKG conformation and hence could leave PKG in a partially activated state. Further study is needed to characterize the exact role of the slow and fast cGMP-binding sites.

M-Pos302

PLANAR LIPID BILAYER STUDIES OF DISULPHIDE BRIDGE ENGINEERED CRY1Aa, A *BACILLUS THURINGIENSIS* INSECTICIDAL TOXIN.

((**M. Juteau**[1], G. Préfontaine[1], P. Grochulski[1], R. Brousseau[1], R. Laprade[2], L. Masson[1] and J.L. Schwartz[1,2])) [1]BRI, National Research Council, Montreal and [2]GRTM, Université de Montréal, Que, Canada.

A major step in the mechanism of action of *Bacillus thuringiensis* Cry toxins involves the permeabilisation of target insect midgut cells. Based on Cry toxin structural data[1,2], it has been proposed that part of, or the entire α helix-rich Domain I contributes to the formation of membrane pores. Cry1Aa forms cation-selective channels in planar lipid bilayers[2]. In the present study, intramolecular disulphide bonds were introduced in Cry1Aa to cross-link Domain I's last helix with Domain II, or pairs of Domain I's α-helices together. Six double cysteine mutants were constructed, expressed in *E. coli*, purified and trypsin-activated using standard procedures[3]. They were tested in planar lipid bilayers for channel formation under oxidizing or reducing conditions. We demonstrate (i) that pore formation by Cry1Aa toxin requires the unfolding of the protein around the hinge region linking Domain I and Domain II, and (ii) that the α_4-α_5 hairpin plays a critical role in the channel's architecture.

[1]Li *et al*, Nature 353:825-821, 1991; [2]Grochulski *et al*, J. Mol. Biol. 254:1-18, 1995); [3]Masson *et al*, Biochem. J. 269:507-512

(Supported in part by NSERC)

M-Pos303

STRUCTURE-FUNCTION CHARACTERIZATION OF BINDING SITE MUTANTS OF ,eIF-4E. ((**D.E. Friedland**[‡], **M.L. Balasta**[‡], T. Spivak-Kroizman[‡], C. De Staercke[§], Y. Xie[§], **D.J. Goss**[‡] and C.H. Hagedorn[§],)) [‡]Chem. Dept., Hunter College of CUNY, NY, NY 10021, [§] Medicine Dept. and Genetics Program, Winship Cancer Center, Emory Univ. School of Medicine, Atlanta, GA, 30322.

eIF-4E is the predominant protein in mammalian cells that interacts with the m^7GTP cap structure of eukaryotic mRNA. Expression of recombinant $4E_{human}$ in *E. coli* has allowed large scale purification of a functional protein (1). Photoaffinity labeling was used to identify a binding site of ,eIF-4E for the m^7GTP cap structure (2). This site was mutagenized to assess the effect of individual amino acid substitutions to alanine on cap binding and protein structure (3). Previous fluorescence quenching studies with a variety of quenching agents have revealed that the binding site is negatively charged. Preliminary studies show that mutagenesis of a positively charged amino acid further enhances binding of the cap to the recombinant protein. Removal of a tryptophan, believed to be involved in stacking with the m^7GTP cap structure (previous studies), reduces the affinity of ,eIF-4E for m^7GTP Sepharose. Structure-function studies of a model m^7GTP mRNA cap binding protein may pave the way for developing molecules that regulate the expression of selected target mRNA.

(1) Hagedorn et.al. *Protein Expression & Purification* (in press)
(2) Friedland et. al. *Protein Science* (in press)
(3) Spivak-Kroizman et al. (in preparation)

DJG. NSF MCB 9600521 DEF. NSF DGE-9553549 CHH. NIH CA63640

M-Pos304

STUDIES ON THE MECHANISM OF GROEL-GROES BINDING

((**Abida Taher***, N. K. Steede*, Costa Georgopoulos# and Samuel J. Landry*))
*Dept. of Biochemistry, Tulane University School of Medicine, New Orleans, LA-70012 and # Departement de Biochemie Medicale, Universite de Geneve, 1211 Geneve 4, Switzerland.

We have shown previously by ^{1}H nuclear magnetic resonance that upon binding of GroES to GroEL, a mobile polypeptide segment of GroES (a.a. 17-32) becomes immobilized in the GroEL/ES/ADP complex, suggesting that this mobile segment interacts directly with GroEL. Mobility in this segment seems to be important because the corresponding segment of the homologous bacteriophage T4 co-chaperonin, Gp31, also displays conformational flexibility despite significant sequence divergence. By analysis of transferred nuclear Overhauser effects in NMR spectra, we find that synthetic peptides corresponding to the GroES and Gp31 mobile loops adopt a characteristic hairpin turn conformation in association with GroEL. Conservation of glycine residues at positions 23 and 24 in the mobile loop can be explained on the basis of either the ability of glycine to adopt turn-compatible phi/psi angles or simply its conformational flexibility. GroES mutants with glycine 23 replaced with serine and glycine 24 replaced with alanine have been created. They are being characterized in terms of their affinity for GroEL, function in chaperonin-assisted citrate synthase refolding, and GroEL-bound conformation for the corresponding peptides. Initial studies show that the Gly24>A mutant has reduced affinity to GroEL. We expect that functional differences between wild type and mutant GroES can be explained on the basis of differences in affinity for GroEL. Off rates for wild type and mutant GroES will be monitored by changes in steady- state anisotropy. The steady-state anisotropy should increase significantly upon binding of the 70 kDa GroES to the 840 kDa GroEL. We have introduced tryptophan in GroES by replacement of Tyr 71 which is on the lower inner surface of GroES dome, a site that we anticipated would contact hydrophobic sites on GroEL. Anisotropy measurement with this trp variant, however, did not reflect changes co-incident with ATP- dependent complex formation. This suggests that the tryptophan does not bury itself in the hydrophobic sites in the GroEL-GroES complex. We have created another trp variant of GroES, Val26>W. This valine lies in the mobile loop and is the least conserved residue in a cluster of three hydrophobic residues. This trp should experience a substantial change in local environment upon GroES binding to GroEL since the mobile loop appears to be the principle site of contact between GroEL and GroES.

M-Pos305

INTERACTION OF E. COLI MOLECULAR CHAPERONE DNAJ WITH DNAK AND/OR SUBSTRATES

((**Michael K. Greene**, Nancy K. Steede, Christi Magrath and Samuel J. Landry))
Department of Biochemistry, Tulane University School of Medicine, New Orleans, LA 70112

Escherichia coli molecular chaperones DnaK and DnaJ are heat shock proteins that cooperate in binding unfolded proteins. DnaJ also regulates the ATPase activity of DnaK. Our goal is to identify sites of contact between DnaJ and DnaK. Since wild type DnaJ contains no tryptophan residues, five aromatic amino acids were individually changed to tryptophan by site-directed mutagenesis. Three of the 5-OH-trp mutant proteins, Y31W, Y53W and F93W, were expressed in a trp auxotrophic strain with the growth medium supplemented with 5-hydroxytryptophan, and the 5-OH-trp-containing proteins were purified. Two of the trp substitutions, Y31W and Y53W are located in a conserved N-terminal domain (residues 1-75) which is characteristic of all DnaJ-like proteins. This J-domain is probably important for DnaK interaction. The third substitution, F93W, is in the second domain of DnaJ, the gly/phe rich region that we hypothesize is important for binding substrates. Preliminary characterization of these mutant proteins by equilibrium unfolding monitored by 5-OH-trp fluorescence indicates that the J-domain and gly/phe rich region act as independent folding units. The midpoint of the unfolding transitions for Y31W, Y53W and F93W were 2.0 M, 2.0 M and 0.6 M guanidine hydrochloride respectively. Interactive surfaces in DnaJ will be probed by analyzing changes in spectroscopic properties upon complex formation with unfolded protein substrates and/or DnaK.

M-Pos306

ANNEXIN V MUTANT STRUCTURES AND PROPERTIES

((C. Balch, M.B. Campos, J.R. Dedman, C.W. Li, T.R. Mealy, M.A. Swairjo, **B.A. Seaton**)) Structural Biology Group, Department of Physiology, Boston University School of Medicine, Boston MA 02118 (CWL, TM, MAS, BAS); Department of Molecular and Cellular Physiology, University of Cincinnati College of Medicine, Cincinnati OH 45267 (CB, MBC, JRD)

Annexins are a family of abundant and widely-distributed eukaryotic proteins. Their hallmark property is the calcium-dependent binding of phospholipid membranes. The in vivo properties of annexins are under investigation, but they have been implicated in many membrane-related processes including membrane trafficking, cytoskeletal interactions, and movement of ions across membranes. Our previous crystallographic studies demonstrated that a Ca^{2+}-bridging mechanism exists through the formation of a stable annexin-Ca^{2+}-phospholipid ternary complex. The mode of PS binding is notable as the polar head group binds at a novel dual Ca^{2+} site that may enhance PS recognition by annexins. A triggered surface exposure of a tryptophan sidechain also plays a role in membrane binding. Mutagenesis studies have been initiated to test the significance of various residues at the protein-membrane interface. We report herein the crystal structures of several interesting mutants and describe their altered properties in synthetic phospholipid vesicles.

M-Pos307

TUMOR NECROSIS FACTOR CHANNEL ACTIVITY: CELL AND MODEL MEMBRANE STUDIES. ((**Bernadine J. Wisnieski, Ylou Tseng** and Rae Lynn Baldwin)) University of California, Los Angeles, CA 90095.

Previously, we have shown that TNF-α and β have channel-forming activity, with a 2:1 selectivity for Na^+ over K^+. After pH-dependent insertion of TNF into the bilayer, channel opening and closing are controlled by *trans*-membrane voltage. Channel formation involves bilayer insertion of cracked or splayed trimers via the tip of the cone-shaped structure. Insertion is followed by rapid reacquisition of a sealed trimer-like state. X-ray data on TNF:receptor co-crystal complexes indicate that receptor binding aligns the TNF trimers tip-down toward the surface of the cellular bilayer, a finding that agrees with the orientation of bilayer insertion that we have observed with receptor-free bilayers. After 10 min of TNF treatment, $^{22}Na^+$-uptake by human U937 histiocytic leukemia cells is increased 2- to 3-fold. Real-time image analysis of U937 histiocytic leukemia cells that are loaded with Na^+-specific and K^+-specific fluorescent dyes shows that TNF elicits a decline in intracellular K^+ as well as an increase in intracellular Na^+. These data provide a mechanistic explanation for the observations of K.J. Tracey and co-workers, i.e., that skeletal muscle fiber depolarization occurs both in TNF-treated isolated rat muscles and in muscles isolated from animals that receive i.v. injections of TNF. [Supported by grants ACS IM-716 and USPHS GM22240 (BJW)]

M-Pos308

BINDING OF Zn^{2+}, BUT NOT Ca^{2+}, INVOLVES THE THIOL GROUP OF HUMAN CALCYCLIN. ((J. Kordowska and C.-L. A. Wang)) Muscle Research Group, Boston Biomedical Research Institute, 20 Staniford St., Boston, MA 02114.

Calcyclin (CaCY) contains two EF-hand type Ca^{2+}-binding sites, but it shows rather weak binding (K_a=4x10^4 M^{-1}) toward Ca^{2+}; on the other hand, CaCY binds 2 mol/mol of Zn^{2+} with a much higher affinity ($K_a \geq 1x10^7$ M^{-1}). Zn^{2+} induced a greater Tyr fluorescence enhancement than did Ca^{2+}; when CaCY labeled with IANBD at the single cysteine (Cys-3) was used, binding of the two kinds of metal ions resulted in opposite changes in the extrinsic fluorescence intensity. Thiol-blocked CaCY exhibited a lowered affinity toward Zn^{2+}, but binding of Ca^{2+} was not affected. To probe the location of the respective binding sites of these ions we have examined the accessibility of Cys-3 in the presence of Zn^{2+} or Ca^{2+} by reacting with 5,5'-dithio-bis(2-nitrobenzoic acid) (DTNB). Freshly reduced CaCY incubated in EDTA, $CaCl_2$ or $ZnCl_2$ was mixed with DTNB, and the release of NbS^- was monitored spectrophotometrically by measuring the absorbance at 412 nm as a function of time. The reaction profiles followed pseudo first-order kinetics and the rate constants were obtained by curve fitting. The reactivity of the thiol group of CaCY was fastest in its Ca^{2+} saturated form, suggesting that upon Ca^{2+} binding the SH group becomes more exposed to the solvent. This agreed with our earlier observation that labeling of CaCY was facilitated by $CaCl_2$. Zn^{2+} binding, on the contrary, decreased the reactivity of thiols by 3-fold as compared to the metal-free form and by at least 10-fold as compared to the Ca^{2+} saturated form, indicating that thiol groups are involved in Zn^{2+} binding. Thus Ca^{2+} and Zn^{2+} most likely do not bind at the same sites in human CaCY. Supported by grants from NIH.

M-Pos309

INHIBITION OF COAGULATION FACTOR Xa BY ANTITHROMBIN INCLUDES WATER-LINKED TRANSITIONS.((Maria P. McGee and Jie Liang)) Department of Medicine, Bowman Gray School of Med., Wake Forest University, Winston-Salem, NC 27157 and National Center for Supercomputing Applications, University of Illinois at Urbana-Champaign, IL 61801.

The osmotic stress(OS) technique was applied to investigate water transfer during inhibition of FXa (coagulation factor Xa) by aTIII (antithrombin III). This reaction includes a rapid bimolecular association and a slower "monomolecular" conformational transition manifested by exponential decay of FXa activity. OS was induced in water-permeable spaces with inert cosolutes excluded from these spaces. Water volumes transferred during the reaction were calculated from changes in free energy of activation with osmotic stress. Reaction rates were measured in mixtures with FXa(10nM), aTIII(10-400nM) and ~400nM heparin. Pseudo-first order rate coefficients, k_{obs}, increased with aTIII concentration, approaching asymptotically to a maximum. Limiting k_{obs} values increased 3-4 fold with osmotic stress indicating water transfer from protein to bulk during the slow conformational transition. Second order rate coefficients were 1.6± 0.5 and 1.0± 0.0 x 10^{6}M^{-1} s^{-1} with and without OS. With cosolutes of radius 3.0-26.5Å, volumes transferred were correlated to cosolute size. For cosolutes with radius, 17.2 and 26.5Å volumes were large, 1,241 and 3,360 waters, suggesting that these cosolutes probe intermolecular spaces. In contrast, cosolutes with ~3.0, 5.8 and 8.0 Å radius, detected volumes of 73, 130, and 251 waters, consistent with volumes in protein water-permeable spaces. This was further confirmed by alpha-shape analyses of hydration fingerprints in active and latent aTIII conformers. Computations of volumes excluded by a 3.0Å probe, detected an excess of 59 waters in the active as compared to the latent conformer. Taken together, these results demonstrate that conformation changes of aTIII are water-linked and associated with the slow, first-order reaction step.

M-Pos310

A NEW THERMODYNAMIC APPROACH TO SITE-DIRECTED MUTAGENESIS: UNFOLDING OF THE LYSOZYME PHAGE T4 WILD-TYPE R96 AND TEMPERATURE-SENSITIVE MUTANT R96H (ARG → HIS). ((P.W. Chun)) Dept. of Biochemistry and Molecular Biology, University of Florida, Gainesville, Florida 32610

The Planck-Benzinger thermal work function, $\Delta W(T) = \Delta H(T_o) - \Delta G(T)$, represents the strictly thermal components of any intra- or intermolecular bonding term in a system, that is, energy other than the inherent difference of the 0 K portion of the interaction energy. The latter, the temperature-invariant enthalpy, $\Delta H(T_o)$ is the only energy term at absolute zero Kelvin. The magnitude of $\Delta H(T_o)$ or $\Delta H_o(T_o)$, the temperature-invariant enthalpy, is determined by the type of macromolecular interaction taking place under experimental conditions, and thus, this thermodynamic function should be particularly applicable to studies involving a site-directed mutagenic approach to the examination of structure-function problems in protein. The temperature-invariant enthalpy, $\Delta H(T_o)$, for wild-type R96 and temperature-sensitive mutant R96H of the phage T4 lysozyme unfolding has been evaluated at two different pH values. The $\Delta H(T_o)$ value for R96 was 12.32 kcal mol^{-1} at pH 3.0 and 7.35 kcal mol^{-1} at pH 2.0. For the temperature-sensitive mutant R96H at pH 3.0, $\Delta H(T_o)$ = 7.61 kcal mol^{-1}. At pH 2.0, $\Delta H(T_o)$ = 2.4 kcal mol^{-1} for R96H. This difference in $\Delta H(T_o)$ implies that a structural alteration in the temperature-sensitive mutant R96H makes this form more accessible to solvent or solvent additives. With decreasing pH, the melting temperature $<T_m>$ decreases, as does the stability of the molecule, in both the wild-type R96 and mutant R96H. At both pH 2.0 and 3.0 for the mutant R96H in which arginine is replaced by histidine (a single amino acid mutation), there is a reduction in the temperature-invariant enthalpy of 5 kcal mol^{-1} from that of the wild-type R96. The energy required to unfold the R96H mutant is quite small at pH 2.0, especially when compared to wild-type.

M-Pos311

CHARACTERIZATION OF TRUNCATED FORMS OF HUMAN TISSUE FACTOR-SURFACTANT MIXED MICELLES BY ANALYTICAL ULTRACENTRIFUGATION AND EPR SPECTROSCOPY. ((David Cipolla*, Steven Shire#, Jun Liu#, Narendra Bam*, Latoya S. Jones* and Theodore W. Randolph*)) *Aradigm Corp., Hayward, CA 94545; #Pharm R&D, Genentech, Inc., SSF, CA 94080 and *Chemical Engineering Dept., University of Colorado-Boulder, Boulder, CO 80309-0424.

Human tissue factor (TF) is a blood coagulation protein which exists as a glycosylated integral membrane protein, and functions as a cofactor in the coagulation extrinsic pathway . The extrinsic pathway does not require factor VIII, and therefore TF may be useful as a therapy for hemophiliac patients with antibodies or inhibitors to factor VIII. In order for TF to function in this pathway it needs to be incorporated into a membrane structure. We have investigated the interaction of recombinant human TF that lacks the cytoplasmic domain with the surfactants octylglucoside and C12E8. These surfactants are at concentrations greater than the critical micelle concentration. Activity of relipidated TF was assessed by its ability to activate factor X as well as the ability to form a clot in factor VIII deficient human plasma. These activity assays suggest that surfactant micelles are required for successful relipidation and activity of TF. In order to obtain an estimate of how many TF molecules on the average are associated with each surfactant micelle we have obtained estimates of molecular weight of the surfactant-TF complexes by analytical ultracentrifugation. Our data suggest that no more than one TF is associated per C12E8 or octylglucoside micelle. The EPR label partitioning method of Bam *et al.* confirmed the results of the C12E8 and Tween 20 ultracentrifugation studies. Control experiments with recombinant TF that also lacks the transmembrane domain show little interaction with the surfactants.

M-Pos312

SELECTIVE INTERACTIONS IN THE INTERVENING SEGMENT OF THE NBF-1 DOMAIN OF CFTR. ((Shoshana Barnoy, Peter McPhie, George Lee, Ofer Eidelman, and Harvey B. Pollard)) Dept. of Anatomy and Cell Biology, USUHS and LCBG & LBP, NIDDK, NIH, Bethesda, MD.

The nucleotide binding fold domain (NBF-1) of CFTR is the locus of ΔF508, the main mutation in cystic fibrosis. Even though NBF-1 had been assumed to be principally cytosolic, it lately was found[1,2,3] also to cross the membrane. Recently, we have shown that the 20 kDa rNBF-1 interacts with phospholipids in a PS-specific manner. In order to identify the site responsible for NBF-1 interactions with phospholipids, we have synthesized two contiguous sequences of the Intervening Segment between the Walker A and the C motifs: I_α (477-508) and I_β (509-539). I_α was found to interact with chromaffin granules and with liposomes. I_α caused aggregation and permeabilization of PS- and PS:PC-, but not of pure PC-, LUVs. Furthermore, I_α caused fusion of PS containing LUVs. I_β was found by spectroscopic methods to interact with I_α but not with membranes. I_α-induced membrane aggregation, permeabilization, and fusion were inhibited by I_β. We conclude that: (a) I_α resembles NBF-1 in regards to the effects and specificity of phospholipid interactions, and (b) I_β modifies I_α interactions and thus might regulate these interactions *in vivo*.

[1]Arispe et al., (1992) PNAS 89:1539. [2]Clancy et al, (1995) Pediatric Pulmonology Supp. 12: LB#8. [3]Gruis et al, (1995) Pediatric Pulmonology Supp. 12: 180.

M-Pos313

PURIFICATION OF CYTOCHROME P450 2B1, NADPH CYTOCHROME P450 REDUCTASE, AND CYTOCHROME b_5 FROM RAT LIVER ((N.A. Rodionova and W.R. Laws)) Department of Biochemistry, Mount Sinai School of Medicine, New York, NY 10029.

We are examining the protein-protein interactions between the members of the cytochrome P450 system in liver reticulocytes. Current purification protocols for these membrane proteins are optimized with respect to one or two components. We report a procedure to recover cytochrome P450 2B1, the NADPH cytochrome P450 reductase (reductase), and cytochrome b_5 (b_5) from the same preparation of rat liver microsomes. Cholate-extracted proteins are first fractionated on an octylamino-Sepharose (hydrophobic) column oy buffers differing in their cholate and deoxycholate content. Purification of each protein then requires only a single additional step. P450 2B1 can be purified using a DEAE Sepharose FF column using a linear NaCl gradient. Fractions enriched in b_5 are loaded onto a DEAE Sepharose CL-6B column and eluted by a linear gradient of NaSCN. Reductase fractions are directly applied to a 2',5'-ADP Sepharose 4B affinity column; after washing off all other proteins, the reductase is eluted by AMP. In the absence of protease inhibitors during the affinity step, the soluble portion of the reductase (70 kDa) can also be recovered; separation of the intact reductase from the soluble form can be accomplished by sizing chromatography. Preliminary characterizations of the these proteins and their complexes by steady-state and time-resolved fluorescence and by analytical ultracentrifugation will be presented. Supported by NIH Grant AA09953

M-Pos314

5-FLUORO-TRYPTOPHAN SUBSTITUTED SOLUBLE TISSUE FACTOR: ANALYSIS OF STRUCTURE AND FUNCTION USING FLUORESCENCE AND ^{19}F NMR. ((**J. Zemsky**[1], E. Rusinova[1], L. Luck[2] and J.B.A. Ross[1]))
[1]Biochemistry Department, Mount Sinai School of Medicine, New York, NY 10029 and [2]Clarkson University, Potsdam, NY 13699.

Formation of a complex between membrane bound tissue factor and factor VIIa (VIIa) results in the activation of the extrinsic blood coagulation cascade. A soluble version of tissue factor (sTF), capable of activating VIIa, has been used in structure/function studies of the complex. Crystal structures exist for sTF alone and in complex with VIIa. Structural information has also been gathered for sTF using analytical ultracentrifugation and absorbance and fluoresence spectra. To further our knowledge of sTF in complex with VIIa, we generated sTF in vivo replacing tryptophan with 5-Fluoro-tryptophan (5F-Trp). 5F-Trp has greater absorbance than tryptophan from 280 nm to 310 nm. Above 305 nm, the fluoresence of a protein containing 5F-Trp can be selectively excited to examine the role of the labeled protein in a complex. We have observed that certain Trp residues became fluorescent in 5F-Trp sTF. Additionally, 5F-Trp can be used as a site specific NMR probe. 5F-Trp sTF has four well resolved peaks in the ^{19}F NMR spectrum. The use of 5F-Trp sTF will enhance our knowledge of the solution conformations of the sTF - VIIa complex. Supported by NIH grants GM-39750 and HL-29019.

M-Pos315

CORRELATION BETWEEN EXCLUDED VOLUME COMPUTATIONS AND OSMOTIC STRESS MEASUREMENTS.((**Jie Liang** and Maria P. McGee)) National Center for Supercomputing Applications, University of Illinois, Urbana-Champaign, IL and Department of Med., Bowman Gray School of Med., Wake Forest University, Winston-Salem, NC.

In this report we illustrate a new approach to structure function studies by measuring water-permeable spaces in I (active) and L (latent, inserted) conformers of aTIII (human antithrombin). The x-ray structures of each conformer are analyzed for water spaces, using alpha-shape fom computational geometry. Water transfer is measured experimentally using OS (osmotic stress technique) and kinetics of FXa (coagulation factor Xa) inhibition by aTIII. The limiting step of this reaction includes insertion of the initially solvent-exposed reactive loop of aTIII (I configuration), into a β-sheet structure in the protein core. The alpha-shape approach allows analytical evaluation of protein spaces that are permeable to water but excluded by solutes larger than water. This is achieved by transforming atomic coordinates into geometrical constructs (weighted Voronoi diagram and weighed Delaunay complex) to which exact topological theorems can be applied. In computation-based analyses, spherical probes of radius= 3.0 and 5.8Å are used to locate and measure excluded spaces on functional domains of the aTIII structures. Regions experiencing most changes in water excluded volume are found to coincide with functional domains of aTIII: residues in the reactive loop, its insertion region and the the heparin binding site.The difference in probe-excluded volume between the I and L conformers is within the limits predicted by OS measurements, indicating that loop insertion accounts for a significant proportion of the water transferred. The computed and the functional values also correspond in the direction of the water transfer and in the reaction step involved. These studies demonstrate that alpha-shape and OS technologies can be combined to reveal new structure-function relationships in large and structurally complex proteins.

M-Pos316

S100B OLIGOMERIZATION STATE AT NANOMOLAR CONCENTRATION ((**Alexander C. Drohat**[‡], Elizabeth Nenortas[§], Dorothy Beckett[§], and David J. Weber[‡])) [‡]Dept. of Biochem. and Molec. Biol., Univ. of MD Sch. of Med., Balt., MD 21201, and [§]Dept. of Chem. and Biochem., Univ. of MD Balt. Co., Baltimore, MD 21228

S100B is a Ca^{2+}-binding protein which forms noncovalently associated homodimers, S100B(ββ), and disulfide-linked dimers, S100B(β-β), of the 91 residue S100β subunit. The solution structure of apo-S100B(ββ) shows that the subunits, each comprising two helix-loop-helix Ca^{2+}-binding domains (EF-hands), associate in an antiparallel manner to form a tightly packed hydrophobic core at the dimer interface which extends into each subunit and involves 6 of 8 helices and the C-terminal loop [Drohat *et al.* (1996) *Biochemistry 35*, 11577-11588]. The C-terminal loop, however, is known to participate in the binding of S100 proteins to target proteins, and its participation in the dimer interface of apo-S100B(ββ) raises questions of physiological relevance of dimeric S100 proteins. Using large-zone analytical gel filtration chromatography with ^{35}S-labeled S100B, we determined that S100B exists as a noncovalently associated dimer, S100B(ββ), at 1 nM subunit concentration (0.5 nM dimer), in the presence or absence of saturating levels of Ca^{2+}. This implies a dissociation constant in the picomolar concentration range or lower, and suggests that S100B exists as dimeric S100B(ββ) at physiological concentrations in reducing environments, in the presence or absence of Ca^{2+}, and that the noncovalent dimer is the form of S100B presented to various target proteins.

Supported by NIH (R29GM52071 to DJW and R29GM46511 to DB), ACS (JFRA-641 to DJW), SRIS and DRIF funding from the State of Maryland (to DJW), and a DuPont Professorship (to DB).

M-Pos317

THE ROLE OF CYSTEINE RESIDUES IN S100B DIMERIZATION AND REGULATION OF TARGET PROTEIN ACTIVITY

((**Aimee Landar**, Emily H. Cornwall, John J. Correia, Alexander C. Drohat, and David J. Weber, Danna B. Zimmer)) Dept. of Pharmacology, University of South Alabama, Mobile, AL 36688.

In the present study, a recombinant S100B protein and mutant S100Bs containing two, one or no cysteine residue(s) have been used to determine the contribution of cysteine residues to S100B dimerization and interaction with the intracellular target proteins aldolase, phosphoglucomutase, and the microtubule associated tau protein. Mutation of C68 to valine or C84 to serine, C68 to valine and C84 to serine, or C68 to valine and C84 to alanine did not significantly alter S100B activation of aldolase. However, mutation of C84 to serine resulted in calcium-independent S100B activation of phosphoglucomutase and a loss of S100B inhibition of tau phosphorylation by Ca^{2+}/calmodulin-dependent protein kinase II. The altered functionality of the C84S mutant with phosphoglucomutase and tau was not due to altered physical properties or dimerization state. All of the mutants exhibited heat stability and calcium dependent conformational changes which were identical to recombinant S100B. In addition, S100B proteins containing two, one or no cysteine residue(s) behaved as dimers in ultracentrifugation experiments in the presence or absence of calcium as well as in the presence or absence of reducing agent. These results demonstrate that dimerization is not calcium-or sulfhydryl-dependent; a conclusion which is supported by size exclusion chromatography and dynamic light scattering experiments. In summary, cysteine residues are not necessary for the noncovalent dimerization of S100B, but are important in certain S100B target protein-interactions.

Supported by NIH (NS 30660-DBZ, GM 52071-DJW), NSF (BIO-920038-DBZ, BIR-9216150), and SRIS and DRIF funding from the State of Maryland (DJW).

M-Pos318

THE FAMOUS SERINE PROTEASE "CATALYTIC TRIAD" IS A PAIR-Rufus Lumry, Chemistry Departmentt. University of Minnesota, Minneapolis, Minnesota 55455

The serine-protease family like most other enzyme families is characterized by highly conserved B-factor pattern demonstrating a high degree of palindromy between the two functional domains. As usual each domain has a single chemically-functional residue attached loosely to its knot, two to a catalytic unit. These are palindrome partners and in trypsin are his57and ser195. Asp102 is very close to his 57 and it is often suggested that it too is chemically functional but asp102 and its paliodrome partner ser139, have the lowest atom B factors in the protein which means they are corresponding parts of the two knots. To participate in the chemical events of catalysis they must be labilized by knot disruption, the rate-limiting step in melting. This is most unlikely. Rather as knot residues they are parts of the hard platforms by which the force generated by matrix contraction is delivered along the reaction coordinate to supply transient mechanical free energy for activated-complex formation. Thermal fluctuations cannot be given a vector direction but nature has discovered that PV fluctuations can be controlled and directed using knot-matrix constructions. It appears that all modern enzymes in the absence of a common initial guiding principle have evolved to the point that improvements in mechanical activation are the major criterion for natural selection in all.

The "catalytic triad" has figured strongly in attempts to explain tryptic catalysis by familiar thermal activation on the assumption of a rigid protein. Matrices of enzymes become hard on contraction but are liquidlike otherwise and this is easily seen by examining their B factors since these reflect the amount and distribution of free volume. The functional-domain pairs of modern enzymes are so closely tailored in size, conformation and free volume distribution as to suggest a miniature tuning fork. The palindromic patterns reflect a high degree of non-crystallographic symmetry, usually a two-fold dyad axis, as required by a dynamic mechanism. The "tuning-fork" frequency appears to be about 10^9 sec^{-1}. (details in Methods in Enzymology 259, chap. 29 (1995) and Protein-solvent Interactions, ed. R. Gregory, Dekker, 1994; chaps. 1 and 3) Supported by the Lumry Family foundation.

M-Pos319

CHARACTERIZATION OF THE ZINC-INDUCED STRUCTURAL TRANSITION OF $p13^{suc1}$ BY EXTRINSIC FLUORESCENCE METHODS. ((P. Neyroz, C. Menna, B. De Gregorio, and L. Masotti)) Dipartimento di Biochimica *"G.Moruzzi"*, Università di Bologna, Italy.

$p13^{suc1}$ acts in the fission yeast cell division cycle as a component of $p34^{cdc2}$. Although the relevance of its biological function is widely recognized, the underlying molecular mechanism is not yet understood clearly. The zinc-induced oligomerization transition of $p13^{suc1}$ has been studied in solution by extrinsic fluorescence methods. The protein (13kDa) has been primarily labelled with lucifer yellow and dansyl chloride. The measured lifetimes of the two derivatives of $p13^{suc1}$ are 14.5 ns and 8.4 ns, respectively. Steady-state anisotropy measurements obtained in 50mM Tris-HCl (pH 8) in the absence and in the presence of zinc ions reveal a change from 0.073±0.003 to 0.115±0.006. In the interval of concentrations from 0 to 2 mM zinc, the steady-state anisotropy increases following a sigmoidal profile with a transition midpoint at 0.4 mM and reaching a plateau at 1mM zinc. Similar results have been obtained with both the two extrinsic fluorescence derivatives of $p13^{suc1}$. The time-resolved anisotropy decay of lucifer yellow-$p13^{suc1}$ measured at high zinc concentration excludes that $p13^{suc1}$ can oligomerize to form a stable hexamer as has been proposed for its human homologue $p9^{CKS2}$. Nonlinear least-squares analysis of the steady-state anisotropy data provides an association free energy change in the absence of zinc, $\Delta G°_{ass}$, of -3.46 kcal/mol. Indeed, the existence of a finite fraction of $p13^{suc1}$ dimer in zinc-free buffer is revealed by the combination of gel-filtration chromatography, gel-electrophoresis and glutaraldehyde cross-linking techniques. At 1mM zinc the stability of the dimer form is much higher with a free energy of association of -12.1 kcal/mol. Anisotropy measurements performed at pH 5.6 provide strong evidences for the involvement of residues His-26 and His-40 of $p13^{suc1}$ in coordinating the zinc ions. Finally, the zinc-induced dimer formation is confirmed in solution by energy-transfer experiments using the FITC- and TRITC-$p13^{suc1}$ donor-acceptor pair. This work was supported by the italian Research National Council (C.N.R.) grant n. 95.02368.CT04 to P.N..

M-Pos320

BIOSYNTHETIC INCORPORATION OF 7-AZATRYPTOPHAN INTO THE CHANNEL-FORMING DOMAIN OF COLICIN E1)

((**M.J. Weller**, A.R. Merrill, F.-L. Yeh, A.G. Szabo)) Dept. of Chemistry and Biochemistry, University of Windsor, Windsor, Ontario, Canada, N9B 3P4; Univ. of Guelph, Guelph, ON, CANADA N1G 2W1.

Colicin E1 is a toxin-like protein secreted by strains of E. coli carrying a colicin-encoding plasmid. The COOH-terminal channel-forming domain of colicin E1 forms a lethal ion channel which depolarizes the cytoplasmic membrane of target bacterial cells. Before the channel-forming domain is inserted into the membrane, it must undergo a structural change, similar to unfolding. Several single tryptophan (Trp) mutants of the channel-forming domain have been studied by fluorescence, providing valuable insight into the colicin protein (Merrill et al. (1994) Biochemistry 33:1108). Recently, it has been shown that tryptophan analogues such as 5-hydroxytryptophan and 7-azatryptophan (7AW) can be incorporated into proteins in place of Trp (Ross, J.B.A et al., Proc. Natl. Acad. Sci. (USA) 89:12023-12027, 1993). 7AW can be selectively excited in the presence of Trp and thus provides a fluorescent probe suitable for monitoring local conformational changes. 7AW is a stronger base than L-Trp, and therefore it is more sensitive to pH changes in its chemical environment. Thus, 7AW acts as an excellent intrinsic probe of protein structure and protein-protein interactions. In order to probe structural changes and dynamics of colicin E1, the tryptophan residues of the channel-forming domain were replaced with the analogue, 7-azatryptophan (7AW). The specific incorporation of 7AW was achieved by expressing the protein in Trp auxotrophic strains of E. coli, CY15077 and W3110 A33, grown in 7AW containing media. Steady-state and time-resolved fluorescence spectroscopy will be used to probe and elucidate structural changes which occur in the channel forming domain upon low pH activation prior to membrane insertion.

M-Pos321

Correlation of structure and function of Crotonase mutants using time resolved fluorescence.

S. Barker[1], A.G. Szabo[1], P.J. Tonge[2], and T.E. Dahms[3]. [1]Department of Chemistry and Biochemistry , University of Windsor, Windsor, ON. Canada, N9B 3P4; [2]Department of Chemistry SUNY, Stoney Brook, NY 11794-3400; [3]Department of Biology, Purdue University, West Lafayette, IN.

The enzyme Crotonase (enoyl -CoA hydratase) catalyses the hydration of ∝β unsaturated CoA thiol esters. The catalytic properties of the enzyme on a series of CoA thiol esters has been extensively studied and the ∝-proto n abstraction is viewed as an important step in its dehydration mechanism. Very little information regarding changes in the enzyme structure have been uncovered. The single tryptophan in crotonase offers a potentially useful spectroscopic probe of the local structure changes occurring on binding the enzyme substrate. The mutant E164Q has been shown to bind substrates with comparable efficiency to the wild type enzyme. However activity is reduced 1000 fold. In this work the fluorescence behavior of the tryptophan has been used to provide information on structural differences between the two enzymes in both the free and complexed forms.

M-Pos322

SECONDARY AND TERTIARY STRUCTURE CHANGES OF RECONSTITUTED P-GLYCOPROTEIN.

((**N. Sonveaux**#, A.B. Shapiro*, E. Goormaghtigh#, V. Ling* and J.M. Ruysschaert#)) #From the Laboratoire de Chimie Physique des Macromolécules aux Interfaces, Université Libre de Bruxelles, B-1050 Brussels, Belgium and * the British Columbia Cancer Research Centre, Vancouver, BC V5Z1L3 Canada.

The structure of purified P-glycoprotein functionally reconstituted into liposomes was investigated by attenuated total reflection Fourier transform infrared spectroscopy. A quantitative evaluation of the secondary structure and a kinetic of ^{2}H/H exchange of the P-glycoprotein were performed both in the presence and in the absence of MgATP, MgATP-verapamil and MgADP. This approach was previously shown to be a useful tool to detect tertiary structure changes resulting from the interaction between a protein and its specific ligands, as established for the Neurospora crassa H^+-ATPase. ^{2}H/H exchange measurements provided evidence that a large fraction of the P-glycoprotein is poorly accessible to the aqueous medium. Addition of MgATP induced an increased accessibility to the solvent of a population of amino acids, while addition of MgATP-verapamil resulted in a subtraction of a part of the protein from access to the aqueous solvent. No significant changes were observed upon addition of MgADP or verapamil alone. The secondary structure of P-glycoprotein was not affected by addition of ligands. The variations observed in the ^{2}H/H exchange rate when P-glycoprotein interacted with the above ligands therefore represented tertiary structure changes. Fluorescence quenching experiments confirmed that MgATP-induced changes are to be found in the tertiary structure of the enzyme.

M-Pos323

INVESTIGATION OF THE DYNAMIC PROPERTIES OF TRYPTOPHAN-SHIFTED MUTANTS OF *B. STEAROTHERMOPHILUS* PHOSPHOFRUCTOKINASE USING TRYPTOPHAN FLUORESCENCE

((**M. Riley-Lovingshimer** and G. D. Reinhart)) Texas A&M University, Dept. of Biochemistry/Biophysics, College Station, TX 77843

Phosphofructokinase (PFK) from *B. stearothermophilus* is a homotetramer containing a single tryptophan per subunit. PFK is allosterically activated by MgADP and inhibited by phospho(enol)pyruvate (PEP). In the native position the tryptophan shows no fluorescence response to ligand binding. Site directed mutagenesis has been used to generate two "tryptophan-shifted" mutants. In one mutant the tryptophan (position 179) has been changed to phenylalanine and phenylalanine (position 230) has been changed to tryptophan. These mutations move the tryptophan to the opposite side of the subunit approximately 20 Å from the allosteric binding site according to the x-ray crystal structure of Fru-6-P/MgADP bound wild type enzyme. A fluorescence intensity increase is observed upon the binding of PEP (22%), a decrease in intensity is observed upon the binding of MgADP (20%), and no change is observed with the binding of the substrate Fru-6-P. The other "tryptophan-shifted" mutant contains a tyrosine at position 179 and a tryptophan substituted for tyrosine at position 164. The new position of the tryptophan is approximately 6 Å from the Fru-6-P binding site as shown in the x-ray crystal structure of the wild type. The fluorescence intensity of this mutant decreases with the binding of Fru-6-P (25%) and steady state polarization increases from 0.335 to 0.355. The kinetic properties of both mutants are similar to those of the wild type enzyme. These new mutants will allow, for the first time, extensive probing of conformational changes induced by ligand binding using steady-state and time-resolved fluorescence techniques. Supported by NIH grant GM33216.

M-Pos324

TRYPTOPHAN-SHIFTED MUTANTS AS PROBES OF THE ALTERED ALLOSTERIC REGULATION EXHIBITED BY THE E187A MUTANT OF *E. COLI.* PHOSPHOFRUCTOKINASE

((**T.C. Pham**, F. Janiak-Spens, and G.D. Reinhart)) Dept. of Biochem. and Biophys., Texas A & M Univ., College Station, TX 77843-2128. (Spon. by T.O. Baldwin)

Possessing a unique tryptophan per subunit, *E. coli.* phosphofructokinase (PFK) is a convenient system to study allosteric regulation via fluorescence spectroscopy. In the wild-type enzyme, this tryptophan (position 311) is located equidistant (20Å) from both the allosteric and the active sites; making it possible to monitor ligand binding to either site. Lau and Fersht reported (*Nature* 326: 811-812, 1987) that an alanine substitution for a glutamate (position 187) at the allosteric site causes phophoenolpyruvate (PEP) to become a weak activator whereas PEP is a strong inhibitor of the wild-type enzyme. MgADP, a strong activator of the wild-type enzyme, appears to have no allosteric influence. We have demonstrated that MgADP still binds to this E187A mutant using fluorescence polarization and kinetic assays. In both cases, the ligand binding affinities are comparable to the wild-type enzyme. To better probe the environment around the allosteric site of this E187A mutant, "tryptophan-shifted" double mutants were made in which the native tryptophan is mutated to a phenylalanine or a tyrosine and the native phenylalanine or tyrosine is changed to a tryptophan. These mutants generally retain the catalytic and regulatory properties of the wild-type enzyme. We have made the triple mutant W311F/F188W/E187A and in preliminary studies, the fluorescence of this mutant is responsive to the binding of MgADP. We are in the process of making other triple mutants, specifically W311Y/Y55W/E187A and W311Y/Y319W/E187A. Time-resolved fluorescence studies of these mutants should provide information regarding the nature of the changes coming from the E187A mutant in the allosteric binding region. Supported by grant GM33216 from NIH.

M-Pos325

ANESTHETIC INDUCED CONFORMATIONAL CHANGES IN THE NICOTINIC ACETYLCHOLINE RECEPTOR PROBED BY FOURIER TRANSFORM INFRARED (FTIR) DIFFERENCE SPECTROSCOPY

((**Stephen E. Ryan** and John E. Baenziger)) Department of Biochemistry, University of Ottawa, Ottawa, Canada K1H 8M5.

The effects of various local anesthetics on the carbamylcholine (Carb) induced structural changes in the nicotinic acetylcholine receptor (nAChR) have been probed using FTIR *difference* spectroscopy. The difference between spectra recorded in the presence and absence of Carb reveal a number of highly reproducible infrared bands identifying changes in both secondary structure and the structure and/or environment of individual amino acids upon transition from the resting to the desensitized state. In the presence of the local anesthetics dibucaine, proadifen, tetracaine and procaine, at concentrations near those reported for binding to the non-competitive inhibitor (NCI) site, only tetracaine induced band intensity variations characteristic of the stabilization of the nAChR in its resting state. In contrast, increased concentrations of the afore mentioned anesthetics induced dose dependent band intensity variations characteristic of the stabilization of the nAChR in its desensitized state. Significantly, the difference spectra also display features consistent with the competitive displacement of anesthetic from the neurotransmitter binding site upon the addition of Carb. These results suggest that these anesthetics stabilize the nAChR in its desensitized state through interactions with the neurotransmitter binding site rather than with the NCI site.

M-Pos326

EXAMINATION OF THE CALCIUM BINDING AFFINITY OF EF-HAND TYPE PROTEINS BY X-RAY CRYSTALLOGRAPHIC ANALYSIS OF A SERIES OF PARVALBUMIN MUTANTS. M. Susan Cates*, Qi Li **, Emai L. Ho*, Michael B. Berry*, James D.Potter**, and George N.Phillips, Jr.*
*W.M. Keck Center for Computational Biology, Dept. of Biochemistry and Cell Biology, Rice University, MS 140, Houston, TX, 77005-1892
**Dept. of Molecular & Cellular Pharmacology, University of Miami School of Medicine, Miami, FL. 33136

Three mutants of carp parvalbumin have been created to determine the effect of individual residues in the protein's EF-hand domains (CD and EF) on Ca2+ binding affinity/specificity. The first of these, F102W, has a phenylalanine to tryptophan mutation which acts as a fluorescence reporter of Ca2+/Mg2+ binding. The crystal structure of this mutant has been determined and is essentially identical to the wild type structure, with only minor rearrangements necessary to accommodate the bulkier tryptophan residue. A second mutant, PVEF (EF site active), has the F102W mutation plus a glutamate to alanine mutation, E51A, which inactivates the CD Ca2+ binding site. Crystals of this mutant have been grown in the presence of Ca2+ and diffract to 2.0 A with cell constants a=33.3 A, b=33.3 A, c=297.3 A, alpha=beta=90.0 degrees, gamma=120.0 degrees, and space group P6122 or P6522. We are currently in the process of collecting a complete data set from these crystals. A third mutant, PVEF E101D, has the same mutations as PVEF plus a glutamate to aspartate mutation, E101D . .The Ca2+ affinity of PVE101D is reduced by 100 fold compared to PVEF and the Mg2+ affinity is increased 10 fold. The structure of this mutant has been determined in the Mg2+ bound state at a resolution of 2.0 A (space group P21 with cell constants: a=35.2 A, b=50.2 A, c=55.4 A, alpha=gamma=90.0 degrees, beta=99.2 degrees). Initial analysis of the PVEF E101D/Mg2+ structure indicates considerable rearrangement of the inactivated CD site (which may represent the apo-state of this site) and more subtle rearrangements of the remaining mutated EF site to accommodate Mg2+.

This work was supported by National Library of Medicine Medical Informatics Training grant no. 1T15LM07093 and the W.M. Keck Center for Computational Biology.

M-Pos327

STRUCTURE-FUNCTION RELATIONSHIP IN THE ANTIFREEZE ACTIVITY OF ENGINEERED ALANINE-LYSINE COMPOUNDS. ((A. Wierzbicki*, C. A. Knight#, D. D. Muccio†, J. D. Madura*, and J. P. Harrington*)) *Department of Chemistry, University of South Alabama, Mobile, Alabama 36688, #National Center for Atmospheric Research, Boulder, Colorado 80307, †Department of Chemistry, University of Alabama, Birmingham, Alabama, 35294

Our studies of shorthorn sculpin antifreeze protein have revealed an unusually strong structure-function relationship in the antifreeze activity of this protein. The enantioselective recognition and binding between the protein and the ice surface on (2-1 0) planes of ice along [122] direction utilizes both α-helical protein backbone matching to the specific ice surface and matching of lysine residues side chains with specific water molecules positions in the ice surface. We have engineered and analyzed for antifreeze activity several alanine-lysine based polypeptides, which structure was inspired by the sculpin antifreeze protein structure. We will present our ice growth, circular dichroism, molecular modeling and dynamics studies of these polypeptides, which will provide a new insight into the nature of the structure-function relationship of Type I antifreeze proteins. Strategies for the design of antifreeze polypeptides will be also discussed.

M-Pos328

CLONING AND EXPRESSION OF PEPTIDES FOR STRUCTURE AND FUNCTION STUDIES IN MUSCLE. ((I. Vainshtein[1], B. Tripet[1], J. E. Van Eyk[1], R.T. Irvin[2] and R.S. Hodges[1])) Dept. of Biochemistry and MRC Group in Protein Structure and Function[1] and Dept. of Medical Microbiology and Immunology[2], University of Alberta, Edmonton T6G 2H7, Canada. (Spon. C.E. Hill)

Cloning and expression of peptides is an alternative approach to synthetic peptide chemistry for the study of protein structure and function, especially when large quantities of N^{15} and C^{13} labeled peptides are needed for NMR studies. We have cloned and expressed a fragment of skeletal troponin I (95-131) and a peptide of myosin (633-644) which represent linear amino acid sequences of two important binding sites involved in muscle regulation. These peptides were shown to interact with theN-terminus of actin and an anti-TnI monoclonal antibody B4 which mimics the conformation of this region of actin (*Van Eyk et al., Prot. Sci., 1995*). Synthetic oligonucleotides corresponding to these amino acid sequences with methionines and restriction sites at both ends were inserted into the expression vector pRLDE (*Tripet et al., Prot. Eng., 1996*). This vector contains one strand of coiled-coil dimerization domain (E-coil) which allows rapid detection and purification of fusion-peptides. Fusion-peptides from bacterial cell lysates were purified using K-coil (the second strand of dimerization domain) affinity chromatography and showed 90% purity judged by reversed-phase HPLC. Molecular masses of expressed peptides were confirmed by electrospray mass spectrometry. The advantages of this tag system is that the fusion-peptides can be used directly in biosensor studies for quantitative measurements of their interactions with receptors. For NMR studies peptides can be cleaved off from the tag using cyanogen bromide digestion. Results using these fusion-peptides will be discussed.

M-Pos329

PROPERTIES OF THE PORES FORMED BY PARENTAL AND CHIMERIC *BACILLUS THURINGIENSIS* INSECTICIDAL TOXINS IN PLANAR LIPID BILAYER MEMBRANES. ((J. Racapé[1], D. Granger[1], J.-F. Noulin[1], V. Vachon[1], C. Rang[2], R. Frutos[2], J.-L. Schwartz[1,3] and R. Laprade[1])) [1]GRTM, Université de Montréal, Montreal, Que., Canada, [2]BIOTROP-IGEPAM, CIRAD, Montpellier, France, and [3]BRI, NRCC, Montreal, Que., Canada.

Bacillus thuringiensis toxins are widely used for the biological control of insect pests. Their three-dimensional crystal structure reveals three domains. Domain I, located at the N-terminal end of the molecule and composed of a group of α-helices, is probably involved in the formation of a pore in the luminal membrane of the midgut epithelial cells of susceptible insects. The middle and C-terminal moieties, domains II and III, are composed mainly of β-sheets and appear to be involved in the specificity of the toxins by mediating their interaction with receptor proteins on the surface of these membranes. To investigate the role of domain I, the properties of Cry1C were compared with those of two genetically engineered chimeric toxins: Cry1Ac-1C, in which domain I was replaced by that of Cry1Ac, and Cry1C-1E, in which domains II and III were replaced by those of Cry1E. All three proteins formed cation-selective channels in artificial lipid bilayer membranes with multiple conductance states ranging from about 10 to 300 pS in 300 mM KCl. In agreement with a strong cation selectivity, the conductance of the pores formed by Cry1C, in the presence of ions of different sizes, depended mainly on the size of the cation. While Cry1C and Cry1C-1E formed predominantly channels of about 30, 110 and 150 pS, Cry1Ac-1C formed, in addition, a large proportion of channels of 290 pS. These results provide further evidence in favor of the hypothesis that domain I plays a determining role in pore formation, at least in receptor-free artificial membranes.

M-Pos330

LIGAND-INDUCED CONFORMATIONAL CHANGES IN LAC REPRESSOR MONITORED BY FLUORESCENCE OF SINGLE TRYPTOPHAN PROBES. ((J.K. Barry and K.S. Matthews)) Dept. of Biochemistry and Cell Biology, Rice University, Houston, TX 77251.

The *lac* repressor protein is a transcriptional regulator whose affinity for a specific DNA sequence (operator) is regulated by the presence of inducer sugars. Protein affinity for operator and inducer is reciprocally regulated by stabilizing different protein conformations. The operator-bound conformation can also be mimicked by high pH. Regions in the *lac* repressor which are involved in these changes include the monomer-monomer interface and the inducer binding site. To determine the character and extent of these different conformations, *lac* repressor mutants with single tryptophan substitutions were generated for use as intrinsic fluorescent probes. The two native tryptophans, W220 and W201, were mutated to tyrosine to allow introduction of single tryptophans at selected sites. The sites selected in the subunit interface of the core domain were H74W, Q117W, E100W and F226W. Residues selected near the inducer binding pocket include Y273W and F293W. In addition, Y7W, L62W, and K325W were generated to probe other regions of the protein, and the single native tryptophans, W220 (W201Y) and W201 (W220Y), were also examined. Ligand binding properties of all these substitution mutants have been measured. Conformational changes have been explored using steady state and time-resolved fluorescence measurements combined with measurements of fluorescence quenching. Fluorescent properties vary among these mutant proteins, and these properties are also affected by inducer, operator, or high pH depending upon where the tryptophan is placed. The composite picture that emerges provides further insight into the relationship between structure and function in this key regulatory protein.

M-Pos331

EFFECT OF SODIUM N-DODECYL SULPHATE ON STRUCTURE AND OXYGENATION OF HEMOGLOBIN. ((J. Masoudy, A.K. Bordbar, O. A. Amire, A.A. Saboury and A.A. Moosavi-Movahedi)) Institute of Biochemistry and Biophysics, University of Tehran, Tehran, Iran.

The effect of sodium n-dodecyl sulphate (SDS) on structure and function of hemoglobin was investigated by various experimental techniques, such as, tonometry, isothermal titration microcalorimetry, ultraviolet spectroscopy and equilibrium dialysis.

The results show that the oxygen affinity of hemoglobin improved as SDS concentration increased up to 0.20 mM SDS. At 0.40 mM SDS concentration, the oxygen affinity was completely lost; which is markedly consistent with the mid-point or 50% of the denaturation process of hemoglobin as deduced from spectroscopic data. Analysis of the binding and microcalorimetric data indicated predominant unfolding at 0.40 mM SDS concentration, which is consistent with the conclusion that the nature of the binding sites have changed from electrostatic to hydrophobic.

M-Pos332

CONFORMATIONAL CHANGES IN AEROLYSIN DURING INTOXICATION PATHWAY ((**V. Cabiaux**, J.T. Buckley, J.M. Ruysschaert, M.W. Parker and G. Vandergoot)) Department of Physical Chemistry of Macromolecules at Interfaces, Free University of Brussels CP206/2, 1050 Brussels, Belgium. (Spon. By F. Homblé).

Aerolysin is secreted as a dimeric protoxin. Proteolytic cleavage at the C-terminus leads to mature aerolysin, which is able to form an heptameric oligomer. The oligomer is the insertion-competent form of the toxin that produces a channel. Using FTIR and CD spectroscopies, we have analyzed the structural consequences of activation, oligomerization and membrane insertion. In order to uncouple activation from oligomerization, we used three mutants which are unable to oligomerize. Our results show that activation induces a significant change in secondary structure, characterized by a decrease in random structure and an increase in beta sheets content. This change was not observed when the propeptide was covalently linked to the protein. Moreover, the conformational change is not restricted to the regions surrounding the cleavage site but is transmitted throughout the protein. During the subsequent oligomerization of the wild type toxin, secondary structure was not affected, eventhough a change in tertiary structure could be detected. Oligomerization also led to a dramatic change in both the kinetics and extent of deuterium/hydrogen exchange. The change in tertiary structure was confirmed by near UV CD. Analysis of the heptamer after reconstitution in DMPC vesicles showed that secondary structure is not affected by membrane insertion. Oriented ATR-FTIR measurements indicated that a large proportion of the alpha helices have their axis oriented parallel to the normal to the plane of the membrane, whereas both parallel and perpendicular orientations were found for the beta sheets elements.

M-Pos333

DESTABILISATION OF THE N- and C-TERMINAL DOMAINS OF CALMODULIN BY SELECTIVE POINT MUTATIONS. ((J.P.Browne, M.Strom, S. R. Martin, and P. M. Bayley)). Div.Phys.Biochem., N.I.M.R., Mill Hill, London NW7 1AA, U.K.

Single residue mutations have been made of the hydrophobic Ile or Val residue in position 8 of the binding loop in sites I, II, III, and IV of *Drosophila* calmodulin. This residue is part of the hydrophobic core of either calmodulin domain, and is involved in the structural link of two calcium binding sites via a short anti-parallel β-sheet. In the apo-form, the replacement of Ile (or Val) by Gly causes a substantial unfolding of the domain carrying the mutation. At 25°C this corresponds to a loss of ≈ 15-20 helical residues, i.e., approximately half of the domain's α-helical secondary structure. In the presence of calcium this deficiency in α-helix is restored for the mutants at site I, II, or III, but not at site IV, which requires the further binding of a high affinity target peptide to re-establish the native conformation. The extent of the destabilisation is seen in the depression of the melting temperature of individual domains, which can be as large as 80 degrees in the case of Ca_4-CaM(V136G). In spite of the magnitude of these effects, the affinity of the mutants for calcium, and the affinity for a target peptide from skeletal myosin light chain kinase, are only slightly reduced compared to wild-type calmodulin. Also, the secondary structure is largely preserved in the presence of 15% v/v of the helicogenic solvent trifluoroethanol. These results indicate that the stability of the conformation of calmodulin can be dramatically reduced by a single mutation of a highly conserved residue, but that the binding to a target sequence can readily compensate for this, and maintain the wild-type properties. The fact that residues forming the β-structure are strongly conserved in nature suggests that the conservation of the conformational integrity of not only the holo-form, but also the apo-form of calmodulin is important to the maintenance of its biological function.

HEME PROTEINS I

M-Pos334

EVIDENCE FOR TERTIARY COOPERATIVITY WITHIN QUATERNARY "T" HEMOGLOBIN. ((Jo M. Holt, Yingwen Huang, Alexandra L. Klinger, Ilia G. Denisov & Gary K. Ackers)) Dept. of Biochemistry & Molecular Biophysics, Washington University School of Medicine, St. Louis, MO 63110

The contribution to the free energy of ligand binding cooperativity by each intermediate ligation species of human hemoglobin (Hb) has been measured (Ackers et al., 1992; Huang & Ackers, 1996; Huang et al., 1996). The resulting distribution of energies among the ligation microstates, coupled with the determination that the asymmetric doubly-ligated molecule remains in the "T" quaternary structure (LiCata et al., Proteins, 1993), demonstrates that cooperativity occurs upon ligation *without a quaternary structure change* (termed tertiary constraint). The correlation of configuration-specific energetics over a number of Hb systems prepared with a range of O_2 analogs and with O_2 itself has provided a set of rules, or "molecular code", which translates the site-specific binding events into quaternary and tertiary structural transitions. The correlation of the tertiary cooperative free energy with solution parameters and allosteric effectors will be reviewed and contrasted with other Hb systems that do not appear to exhibit tertiary cooperativity. Supported by NIH R37-GM24486, P01-HL51084 & NSF DMB9107244.

M-Pos335

FTIR SPECTRA OF CARBONMONOXYHEMOGLOBIN LIGATION INTERMEDIATES.

((Ilia G. Denisov, Jo M. Holt, Yingwen Huang, and Gary K. Ackers)) Department of Biochemistry and Molecular Biophysics, Washington University School of Medicine, St.Louis, MO 63110

FTIR spectra of all possible configurational isomers of ligand binding intermediates were used to monitor the T→R conformational transition of human hemoglobin A (Hb) caused by CO binding. The intermediates were obtained as pure species or as hybrids using the replacement of Fe by Co in the α- or β-subunits. Relative to fully ligated tetramers, the shape of the CO stretch band is perturbed mainly by Fe/Co substitution and/or by the ligation state of the neighboring subunit within the same dimer. The quaternary structural change is followed by alterations in the -SH stretch bands. Among the doubly ligated intermediates species [22], [23], and [24] more closely resemble the R-like spectra than does [21] (which hardly differs from the singly ligated species). These findings are consistent with the thermodynamic analysis of Huang and Ackers (1996, Biochemistry,35:704). The results of simultaneous analysis of all spectra (CO stretch, -SH stretch, and -CN stretch in CN-metHb intermediates) in relation to alternative models (yielding different numbers of linearly independent components) are discussed with respect to possible local and large scale conformational changes of the Hb tetramer corresponding to each ligand binding event. Supported by NSF Grant DMB9107244 and NIH Grants R37-GM24486 and P01-HL51084.

M-Pos336

THE CONTRIBUTIONS TO COOPERATIVITY BY SINGLY AND DOUBLY OXYGENATED HEMOGLOBIN INTERMEDIATES ((**Alexandra L. Klinger** and Gary K. Ackers)) Dept. of Biochemistry & Molecular Biophysics, Washington University School of Medicine, 660 S. Euclid Ave., Box 8231, St. Louis MO 63110

Understanding the molecular mechanisms by which hemoglobin (Hb) binds O_2 cooperatively is contingent upon determining the roles of the eight partially oxygenated intermediates in this process. Traditional O_2 binding studies can only provide information on the statistical average of the intermediates that comprise each stage of oxygenation; all species with the same number of bound O_2 are spectroscopically indistinguishable. Binding studies of Fe^{2+}/Co^{2+} hybrid Hbs, however, allow resolution of ligation microstates, since the spectral changes upon oxygenation of Co^{2+} hemes are distinct from those of Fe^{2+} hemes. We have expanded upon the pioneering hybrid Hb work of Yonetani and coworkers [Imai et al., 1980] with O_2 binding studies of three doubly-substituted hybrid species in which the normal Fe^{2+} porphyrin is substituted with Co^{2+} porphyrin, i.e., in both α and β subunits of the same dimer, both α subunits, or both β subunits. Nonlinear regression analysis of the resulting concentration dependent isotherms has resolved the binding free energies for all significantly populated, spectroscopically distinct ligation intermediates of these hybrid species. A recently developed method [Huang & Ackers, 1996)] allows for thermodynamic transformation of the cooperative free energies (ΔG_C) for the Fe^{2+}/Co^{2+} hybrid systems to those of normal Fe^{2+} HbA_0. We find good agreement of the resulting ΔG_C values that, for the first time, have been measured by direct O_2 binding with those measured by differences in dimer assembly free energies [Huang *et al.*, 1996], and to those predicted from the "consensus partition function" in conjunction with previous O_2 binding work [Ackers *et al.*, 1992]. Support: NSF DMB9107244, NIH R37-GM24486 and P01-HL51084.

M-Pos337

DO DIFFERENT HEMOGLOBIN LIGATION SYSTEMS FOLLOW A COMMON COOPERATIVE MECHANISM? ((**Yingwen Huang** and Gary K. Ackers)) Dept. of Biochemistry & Molecular Biophysics, Washington University School of Medicine, 660 S. Euclid Ave., St. Louis, MO 63110.

A commonly used strategy for elucidating the cooperative mechanism of hemoglobin is to study analogs of oxygenation intermediates whose properties can't be directly evaluated. A long standing question regarding this strategy is whether a common mechanism exists among different analog systems. Do the structural differences of the analog intermediates perturb the allosteric behavior of the Hb system so that it follows a qualitatively different mechanism? Here we present an analysis of these questions using 6 ligation analog systems (Fe/FeCN, Fe/Mn(III), Co/FeCO, Co/FeCN, Fe/FeCO, Zn/FeO_2) whose cooperative free energies (ΔG_c) have been resolved for all ten ligation species. At the level of equilibrium binding, a common mechanism requires a common molecular partition function, which defines fixed relationships between the ligand-driven free energies of cooperativity. All six of the analog systems studied conform to a consensus partition function deduced previously [Ackers, G. K., et al. (1990) *Science* 255:54] from studies of the three initially resolved systems (Fe/FeCN, Fe/Mn(III), Co/FeCO).Within the framework of the fixed relationships, magnitudes of the detailed energy components were found to vary within reasonable limits. To account for such variations, a strategy was developed [Huang and Ackers (1996) *Biochemistry* 35:704] to evaluate the energetic perturbations of metal substitutions. After "correcting" for such effects the ΔG_c values of Zn/FeO_2, Co/FeCO, and Co/FeCN species were transformed into those of Fe/FeO_2, Fe/FeCO, and Fe/FeCN, respectively. The later three systems show consistent distributions of ΔG_c. Binding isotherms simulated using the resolved microstate ΔG_c values for the Fe/FeO_2 and Fe/FeCO systems were in close agreement with the directly-measured isotherms for O_2 and CO binding, respectively. Supported by NSF Grant DMB9107244 and NIH Grants R37-GM24486 and PO1-HL51084.

M-Pos338

TERTIARY AND QUATERNARY ALTERATIONS IN HEMOGLOBIN UPON COBALT SUBSTITUTION MONITORED BY UVRR SPECTROSCOPY. ((G. Heibel, **L.A. Dick**, and T.G. Spiro)) Chemistry Department, Princeton University, Princeton, NJ 08544-1009. (Spon. by T.G. Spiro.)

The end states of hemoglobin's [Hb] allosteric transition are well studied, but intermediate states of the cooperative mechanism are not yet completely understood due to their transient nature. A useful tool for probing intermediate states is to substitute other metals for Fe^{2+}, thereby altering the electronic structure and ligand binding properties to mimic Hb's natural intermediate forms. In this study, the effects of cobalt substitution on the protein structure are investigated by monitoring tryptophan and tyrosine residues with ultraviolet resonance Raman (UVRR) spectroscopy.

Co^{2+} binds CO with very low affinity, so substituted hemes mimic unligated or deoxy heme. Tetra substituted CoHb is T state, like deoxy FeHb, but shows highly perturbed quaternary contacts in comparison. Markers of tertiary and quaternary structure reveal that Hb is R state when Co is substituted into either α or β chains, and Fe in the remaining chains is ligated by CO. Addition of the allosteric effector, IHP, switches symmetric hybrids to a weakened T state relative to FeHb. Because the perturbation is minimized when the CO ligated hemes are in the α chain (αFeCOβCo), the Fe-His bond must be extensible by T state induced forces generated in the α chains.

Our most recent investigations include the asymmetric substituted species, $(\alpha\beta Co),(\alpha\beta FeCO)_2$, which show unusually strong thermodynamic stability (G.K. Ackers *Biophys. Chem.* **37**, 371).

M-Pos339

ROLE OF DISTAL HISTIDINE IN PROPAGATING STRUCTURAL INFORMATION IN HEMOGLOBIN

((**Ramadas Nirmala** and Joseph Rifkind)) Laboratory of Cellular and Molecular Biology, Molecular Dynamics Section, National Institute on Aging, National Institutes of Health, 4940 Eastern Avenue, Baltimore, Maryland 21224

Structural fluctuations in hemoglobin are necessary for binding oxygen, since the crystal structures do not show any access to the ligand pocket. EPR and Mossbauer experiments show that structural flunctuations are propagated between the heme pockets. In order to understand this process molecular dynamics simulations were carried out on a methemoglobin dimer. Analysis of the trajectory reveals that the distal histidine undergoes conformational change leading to the formation of a bishistidine complex. This structural change in the distal pocket is propagated to the interface as evidence by the increase in the compactness of the interface and the accompanying conformational change in the backbone of the G helix at the interface. The communication is effectively achieved by the correlated motion of the G-H helices at the interface and the E helix enclosing the distal pocket. These results demonstrate how conformational changes are propagated from the ligand pocket. It also indicates the importance of considering the $\alpha_1\beta_1$ interface in understanding hemoglobin function.

M-Pos340

ENTHALPY CHANGES OF THE STEP-WISE LIGATION OF HEMOGLOBIN. ((J.A. Foltz, K. Franklin, H.S. Zahwa, **M.D. Chávez**, and R.L. Berger)) Blood Research Detachment, Walter Reed Army Institute of Research, Washington, D.C. 20307-5100

Direct measurement of the heat of ligation for the carbon monoxide - hemoglobin reaction has been obtained at 4°C, 25°C, and 40°C. Previous studies have shown that the heat of ligation to be approximately equal for each of the four ligation steps of hemoglobin. Under isoionic (no salt, inorganic phosphates, buffers) conditions, direct enthalpy measurements using a DSFC-100 microcalorimeter have determined the enthalpy change for the first ligation step to be dramatically greater than the average heat of ligation at all three temperatures (-33.0 kcal/mol vs. -13.7 kcal/mol). Clearly, a dramatic loss of enthalpy occurs as complete ligation of the hemoglobin takes place. Potential sources of this loss include the T-R transition and the release of Böhr protons. Studies by Imai[1] have shown that third ligation step produces the greatest amount of Böhr proton release. However, because of the relatively small differences, it is unlikely that the Böhr proton release alone can account for the large differences found at all three temperatures. This result implies that anionic ligands such as chloride may play a more significant role in the energetics of the ligation of hemoglobin than previously thought.

[1]Imai, K. (1979) J. Mol. Biol. **133**, 233-247.

M-Pos341

A TWO-STATE ALLOSTERIC MODEL CAN EXPLAIN HEMOGLOBIN KINETICS. (E. R. Henry, C. M. Jones, J. Hofrichter and W. A. Eaton) Laboratory of Chemical Physics, Building 5, NIDDK, NIH, Bethesda, MD 20892-0520.

The nanosecond-millisecond kinetics of ligand binding and conformational changes in hemoglobin have been analyzed by extensive computer modelling. Time-resolved optical spectra following nanosecond photodissociation of the heme-carbon monoxide complex were used to determine these kinetics. An extension of the two-state allosteric model of Monod, Wyman, and Changeux (MWC) was used to fit the data. The extension accounted for geminate ligand rebinding and nonexponential tertiary relaxation within the *R* quaternary structure. Use of a linear free energy relation between quaternary rates and equilibrium constants considerably simplified the model. Recent experimental and theoretical results on the stretched exponential time course for conformational relaxation in myoglobin also play an important role (Hagen and Eaton, *J. Chem. Phys.* **104**, 3395, 1996). Monte Carlo simulated annealing techniques were used to find global minima in parameter space. With the same set of kinetic parameters the model, described by 85 coupled differential equations, accounts for a demanding set of complex kinetic data, as well as the equilibrium data of Perrella et al. (*Biophys. Chem.* **37**, 211, 1990) on ligand binding and the distribution of ligation states. The present results, together with those from single crystal oxygen binding studies (see poster by Mozzarelli et al), indicate that the two-state MWC allosteric model has survived its most critical testing.

M-Pos342

THE STRUCTURAL BASIS FOR SICKLE CELL DISEASE ((Frank A. Ferrone and Rossen Mirchev)), Department of Physics and Atmospheric Science, *Drexel University*, Philadelphia, PA 19104

Sickle hemoglobin molecules assemble into polymers composed of 7 helically twisted double strands. Intermolecular contacts involving the mutation sites within the double strands are well established. We show that the same contact sites are present at the polymer surface on 4 of the 14 molecules, and demonstrate that the identical contact geometry can be achieved between polymers as found within the double strands. This provides a structural rationale for the heterogeneous nucleation process which lead to the exponential rate of polymer growth that characterizes the kinetics of gelation. This also gives a structural basis for the cross-linking which solidifies the polymer gel. In the absence of these surface contact regions sickle cell disease would be a much milder syndrome.

M-Pos343

SITE SPECIFIC MUTATIONS PROVIDE INSIGHT INTO THE FUNDAMENTAL ENERGETICS OF SICKLE HEMOGLOBIN ASSEMBLY ((Dan Liao*, Zhonglin Hu*, Zhiqi Cao*, Rossen Mirchev*, Jose Javier Martin de Llano §, Juha-Pekka Himanen§, James M. Manning § and Frank A. Ferrone*)) *Department of Physics and Atmospheric Science, *Drexel University*, Philadelphia, PA 19104 and §Department of Biology, *Northeastern University* Boston, MA 02115

We have begun a study of site specific mutations on the kinetics of homogeneous and heterogeneous nucleation as a means of gaining insight into fundamental energies of assembly. Because the kinetics are modeled in terms of fundamental thermodynamics, and because the nucleus size and polymer size are so different, it becomes possible to resolve individual site contact energies. So far we have employed this procedure for the mutants HbS (β88L→A) and (β95K→I). Contact energy is unchanged in the (β88L→A) mutant, with all solubility changes arising from vibrational entropy, while contact energies are different in the mutant (β95K→I). Because the solubility is so much greater than HbS, nonideality effects are enhanced, and deficiencies in the treatment of heterogeneous nucleation become apparent. We are addressing these experimentally by measurements in the presence high MW dextrans, and these results will also be discussed.

M-Pos344

THE OXYGEN AFFINITY OF HEMOGLOBIN CRYSTALS IS NOT ALTERED BY ALLOSTERIC EFFECTORS. (A. Mozzarelli, C. Rivetti, G. L. Rossi, W. A. Eaton and E. R. Henry) Institute of Biochemical Sciences, University of Parma, 43100 Parma, Italy and Laboratory of Chemical Physics, Building 5, NIDDK, NIH, Bethesda, MD 20892-0520.

Rivetti et al (*Biochemistry* **32**, 2888, 1993) explained the low oxygen affinity and lack of a Bohr effect in hemoglobin crystals by postulating high and low affinity tertiary conformations within the *T*-state, corresponding to broken and unbroken intersubunit salt bridges. In solution both are populated, while in the crystal only the low affinity conformation exists. Binding of allosteric effectors in the crystal should therefore not influence the oxygen affinity. We tested this hypothesis by measuring oxygen binding curves of single crystals of hemoglobin in the *T* quaternary structure in the presence of the "strong" allosteric effectors, inositol hexaphosphate and bezafibrate. We find that they change the oxygen affinity of the crystal by less than 10% (compared to a 10-30 fold reduction in solution), as predicted by the model of Rivetti et al. We also find that the crystal binding curve is non-cooperative, which is a critical requirement of the two-state allosteric model of Monod et al. Cooperative interactions within the *T* quaternary structure are not masked by a fortuitous compensation from a difference in the affinity of the α and β subunits. We demonstrated this by calculating the separate α and β subunit binding curves using geometric factors from the X-ray structures of deoxygenated and fully oxygenated *T*-state molecules determined by Paoli et al. (*J. Mol. Biol.* **256**, 775, 1996).

M-Pos345

A NEW ROLE OF ANIONS ON THE ALLOSTERIC EQUILIBRIUM OF HEMOGLOBIN REVEALED BY THE HYDRATION EFFECT ON ALLOSTERIC REGULATION. (**M.F.Colombo**, F.A.V.Seixas and G.O.Bonilla-Rodrigues) Depart.de Física, IBILCE, UNESP, Campus de São José do Rio Preto, SP, Brazil, 15054.000.

The hydration change accompaning the quaternary transition of Hb, Δn_w, depends on the concentration of anions that bind preferentially to deoxy-Hb. Human Hb-A_0 and bovine Hb bind only about 10 H_2O molecules per tetramer when oxygenated in 10 mM Hepes without Cl^- or DPG. In the presence of 0.1 M Cl^- or 1mM DPG, Hb-A_0 binds ~70 H_2O molecules and bovine-Hb ~ 50. To uncover the mechanism by which these anions increase the hydration change associated with Hb oxygenation, we measured the dependence of Δn_w on Cl^- and DPG concentrations. For bovine Hb, Δn_w^{bov} varies from 10 to 50 H_2O molecules/tetramer within the range of 10 to 100 mM Cl. DPG alters Δn_w^{bov} similarly within 10 to 50μM DPG at [Hb]= 60μM heme. This change in Δn_w indicates that Hb undergoes conformational changes upon deionization. Since the binding of Cl^- or DPG restores the full value of Δn_w, and, as both anions bind preferentially to the deoxy (T) form of Hb we assume that a new T^o is stabilized in a non-ionic solution. The transition from T to T^o would involve the DPG binding site whose stability ought to be crucially dependent on the partial neutralization of their positive charges by anion binding or anion condensation. In the absence of neutralization these charges would tend to separate driving the conformational change. This interpretation explains the decreased value of Δn_w, because a significant fraction of the hydration change following the T to R transition is due to the exposure of those charges. Moreover, assuming the equilibrium between T and T^o we determined that an apparent number of 1.6 Cl^- (or 1 DPG) binds preferentially to the T form in relation to T^o form. It is noticeble that 1.6 Cl^- (and 1 DPG), is released in the T to R transition induced by oxygenation. Supported by FAPESP, CAPES and CNPq.

M-Pos346

NEAR UV MAGNETIC CIRCULAR DICHROISM STUDIES OF THE R-T TRANSITION IN CARP HEMOGLOBIN ((**D. J. Vitale**, R. M. Esquerra, D. B. Shapiro, R. A. Goldbeck, L. J. Parkhurst*, D. S. Kliger)) University of California, Santa Cruz, Santa Cruz, CA 95064-1077; *University of Nebraska, Lincoln, NB 68588-0304.

As hemoglobin changes its conformation between the tense and relaxed quaternary states, the amino acid residues within the dimer joint region experience a shift in their environment. These differences can be observed for aromatic residues using magnetic circular dichroism in the near UV region. The MCD spectral contributions from tryptophan in the joint region show particular sensitivity to this altered environment; the spectrum of the T state is subtracted from the R state spectrum to yield a difference spectrum which clearly shows the spectral shift of the Trp MCD bands. The heme prosthetic group also has a large MCD in the near-UV region. However, we have been able to eliminate its contribution to the difference spectrum by keeping the ligation of the heme constant while varying quaternary state. To achieve this, we took advantage of the Root effect, which allows the conformation of the protein to be held constant regardless of the heme ligation. We present an analysis discussing our MCD results for four equilibrium carp Hb species, R0, R4, T0, and T4, (ligand = CO) in terms of tertiary and quaternary interactions in the joint region. These results will be prerequisite to interpreting near-UV time-resolved MCD studies of the R-T transition that are in progress.

M-Pos347

THE CORRELATION BETWEEN INTERACTIONS WITH OXYGEN AND ALLOSTERIC EFFECTORS AND THE QUATERNARY STRUCTURE/OXYGEN AFFINITY OF α-NITROSYL HEMOGLOBIN ((Yuxiang Zhou, Antonio Tsuneshige, & Takashi Yonetani)),Department of Biochemistry & Biophysics, University of Pennsylvania Medical Center, Philadelphia, PA 19104-6089, USA

The heme coordination structure of the α-subunits of α-nitrosyl hemoglobin [α(Fe-NO)$_2\beta$(Fe)$_2$] is in a dynamic equilibrium between the 6- and 5-coordinates, which exhibit characteristic EPR spectra (Spectra A and B, respectively). This coordination equilibrium, which is caused by the reversible breakage of the heme Fe-His(F8) bond in the α-subunits, is a function of interactions with ligands such as O_2, CO, and NO in the β-subunits and interactions with allosteric effectors such as H^+ and IHP. Thus, α(Fe-NO)$_2\beta$(Fe)$_2$, which is in an extremely low affinity ***Super-T*** structure (predominantly 5-coordinate α-hemes) in the absence of O_2, is reversibly converted to a high-affinity ***R*** structure (predominantly 6-coordinate α-hemes) in the presence of O_2, rendering it to be an extremely efficient O_2 carrier with a low O_2 affinity, allosteric sensitivity, and cooperativity. Therefore, a-nitrosyl hemoglobin formed under physiological conditions can deliver O_2 to tissues more efficiently than hemoglobin. Supported by HL14508 and GM48130.

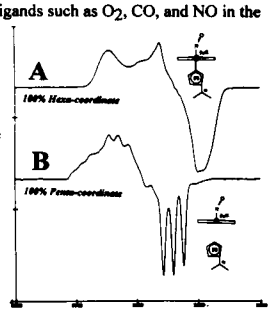

M-Pos348

MANOMETRIC MEASUREMENTS OF OXYGEN BINDING BY WHOLE BLOOD AND HEMOGLOBIN SOLUTIONS. ((O.O. Abugo, **V.W. Macdonald**, R.L. Berger, and J.R. Hess)) Blood Research Detachment, Walter Reed Army Institute of Research, Washington, D.C. 20307.

An automated instrument for manometric determination of oxygen equilibrium curves (OECs) of whole blood and hemoglobin was used to measure OECs without dilution under physiological conditions of 37°C, 5% CO_2, and constant pH. Manometric titration was done by step-wise addition of H_2O_2 in the presence of catalase. Oxygen affinities of human, swine, and rat whole blood, expressed as the oxygen partial pressure at half saturation (P_{50}), obtained with this method were 28.8±1.9 (n=30), 33.0±1.7 (n=9) and 42.9±2.9 (n=11) Torr, respectively. The classical Bohr effect for whole blood was observed across these species. Concentrated solutions of hemoglobin crosslinked between alpha chains at α-Lys^{99} with bis(3,5-dibromosalicyl) fumarate ($\alpha\alpha$Hb, 6.5 g/dl) and hemoglobin A_0 (HbA_0, 7.5 g/dl) exhibited shifts in oxygen affinity in proportion to the amounts of methemoglobin formed at different catalase concentrations during the measurement intervals. P_{50}s ranged from 43.7 Torr when met$\alpha\alpha$Hb increased from 1.4% to 6.2% during OEC runs, to 16.7 Torr when met$\alpha\alpha$Hb increased to 58%. Similar shifts in P_{50} occurred with increased metHbA_0 formation (18.2 Torr at 4.9% metHbA_0 versus 5.5 Torr at 58%). These shifts in P_{50} were attenuated when metHb was preformed by autoxidation and OECs determined at constant metHb concentrations. P_{50}s obtained for DPG depleted red cells and HbAo solutions at low metHb concentrations had similar values. The P_{50}s obtained by spectrophotometric determinations of dilute Hb samples (Hemox-Analyzer) were similar to those obtained by manometric titration at higher methemoglobin concentrations. These effects of metHb formation on oxygen affinity are consistent with accumulation of high affinity R-state conformations and suggest that the true oxygen affinity for these hemoglobins may be lower than previously reported. These results stress the need for physiologically accurate OEC's for whole blood and acellular hemoglobin solutions in order to determine blood oxygen content.

M-Pos349

BARLEY HEMOGLOBIN: REACTIONS WITH OXYGEN AND CARBON MONOXIDE. ((S.M.G. Duff, R.D. Hill and **J.B. Wittenberg**)) Dept. of Plant Science, Univ. of Manitoba, Winnipeg, Manitoba, Canada 3RT 2N2 and Dept. of Physiology and Biophysics, Albert Einstein College of Medicine, Bronx, N.Y., 10461.

Barley (*Hordeum*, a monocot) seed tissue expresses a non-symbiont plant hemoglobin during hypoxia at a concentration of about 20 μM. In order to obtain sufficient quantities of the protein, it has been expressed as a recombinant protein in *E. Coli* using puC19 as the vector, isolated and purified. The partition coefficient, M, expressing the relative affinities for O_2 and CO, was determined spectrophotometrically in a Hb solution equilibrated with mixtures of O_2 and CO. M = 1.52 at 20° C. Carbon monoxide combination and dissociation rate constants and the oxygen dissociation rate constant were determined by stopped flow spectrophotometry at 20° C. The determined rate constants are: carbon monoxide combination 2.1 x 10^5 $M^{-1}s^{-1}$, carbon monoxide dissociation 0.0016 s^{-1} and oxygen dissociation 0.028 s^{-1}. From these values we calculate the carbon monoxide affinity 7.6 nM, the oxygen affinity 11.6 nM and the oxygen combination rate constant, 2.4 x 10^6 $M^{-1}s^{-1}$. Extraordinarily great oxygen affinity is due largely to very slow oxygen dissociation. In fact, this latter rate is among the slowest known. Supported by Research Grants OGP4689 and STR 149182 from the Natural Science and Engineering Council of Canada.

M-Pos350

EXPRESSION AND CHARACTERIZATION OF HUMAN HEMOGLOBIN WITH α-GLOBIN PRODUCED IN *ESCHERICHIA COLI*.

((M.T. Sanna[@], A. Razynska[#], M. Karavitis[#], A.P. Koley[^], F.K. Friedman[^], I.M. Russu[+], W.S. Brinigar[^]and C. Fronticelli[#])[#] [#]University of Maryland, [^]National Cancer Institute, [+]Temple University, [@]Wesleyan University.

Recombinant mutant hemoglobins have been widely used in the study of structure -function relationships in hemoglobin. Hemoglobin with mutations in the α-chains have been less available than mutations in the β-chains. Accordingly we have developed an efficient expression system for α-globin, that can produce a human hemoglobin in which only the α-chains are recombinant. This allows the assignment of any observed difference exclusively to the recombinant chains. Oxygen binding isotherms of native and recombinant HbA, yielded similar thermodynamic parameters. The sensitivity to effectors (Cl^- and 2,3-Diphosphoglycerate), the Bohr effect, the CO binding kinetics and the dimer-tetramer association constants were the same in the two proteins. CD spectra indicate correct heme insertion and heme pocket refolding. NMR spectra of the deoxy and carboxy derivatives indicated the correct refolding of the $\alpha_1\beta_1$ and $\alpha_1\beta_2$ interfaces; however differences in the α-chain heme pockets are observed and, very likely, are not the result of heme inversion. The α-globin can fold with the heme in the absence of the partner chains, as opposed to β-globin. The CO binding kinetics is the same as the native α-chains, however, an additional faster binding component is present. Also, the ellipticity of the Soret CD spectrum was decreased, suggesting the presence of alternate conformations in the isolated recombinant α-chains in the absence of native β-chain.

M-Pos351

EFFECTS OF CYSTEINE SUBSTITUTIONS IN THE β-CHAINS OF HUMAN Hb.

((M. Karavitis[#], G. Vasquez[#], W. Nie[#], W. Brinigar[*], G. Gilliland[#], and C. Fronticelli[#])) [#]University of Maryland and [*]Temple University.

Recombinant human β-globin genes bearing the mutations C112G and C93A+C112G have been constructed, expressed, the proteins refolded with native α-chains and purified. X-ray structures of the deoxy forms were refined to 2Å resolution. Comparison with HbA shows that a water molecule occupies the void created by the C112G substitution. In turn, the βC93A substitution removes conformational constraints imposed on the β146H, which then can rotate away from β94D, thus weakening this important T-state salt bridge. The functional properties of the βC112G mutant are essentialy those of HbA. In the absence of Cl^-, β(C93A+C112G) also behaves much like HbA. However, in the presence of 100 mM Cl^-, the Bohr effect is significantly decreased below pH 7.5. There does not appear to be any preferential binding of Cl^- to the double mutant at pH 6.5. These results suggest that there is an intricate interplay between the Bohr effect and the differential binding of anions to R and T states of hemoglobin.

M-Pos352

SPECTROSCOPIC INSIGHT INTO THE ROLE OF Ca^{+2} IONS IN THE STABILIZATION OF THE MULTIMERIC *LUMBRICUS* HEMOGLOBIN

(J.P. Harrington[a], J.M. Friedman[b] and R.E. Hirsch[b]) [a]University of South Alabama, Mobile, Al. and [b]Albert Einstein College of Medicine, Bronx, N.Y.

Studies of several independent groups have provided evidence that alkali and alkaline cations reduce the subunit dissociation of LtHb, reduce the rate of autoxidation, lower the rate of conversion of the high spin metHb form to the more unstable low spin hemichrome state, and increase LtHb's resistance to thermal denaturation. The relevant role of Ca^{+2} ions in affecting stabilization within the heme environment (reducing autoxidation and hemichrome formation), and inducing greater resistance to urea and thermal unfolding has been investigated via spectrophotometric studies which demonstrated that 1)the presence of Ca^{+2} ions resulted in an increased urea unfolding midpoint for LtHb($D_{1/2}$=4.8 M, no Ca^{+2} and $D_{1/2}$=5.4, 10mM Ca^{+2}), as well as a steeper transition reflecting a more cooperative unfolding process than in the absence of Ca^{+2}ions; 2) thermal resistance to LtHb unfolding is evident even at 0.1 mM Ca^{+2}; 3) similar resistance to thermal unfolding was also found with the calcium binding analogs Gd^{+3} and Tb^{+3} (0.02mM); 4) the presence of 0.1mM Gd^{+3}, Tb^{+3}, and Yb^{+3} resulted in the reduction of autoxidation of LtHb; and 5) the interactions of the heme-containing trimer (abc chains) and the monomeric d chains, analyzed by front-face fluorescence spectroscopy, revealed an effective binding role for Ca^{+2} at the interface of these functional important subunits. Further studies are also underway using several calcium binding analogs (Gd^{+3}, Tb^{+3}, Yb^{+3}) as probes in an attempt to identify and differentiate structural and functional roles associated with Ca^{+2} binding sites within the LtHb molecule.

M-Pos353

POLARIZED LIGHT SCATTERING FROM SICKLE HEMOGLOBIN POLYMERS

((Daniel B. Kim-Shapiro[*] and Patricia G. Hull[*]) Department of Physics, Wake Forest University, Winston-Salem, NC 27109 & [*]Department of Physics, Tennessee State University, Nashville, TN 37209

The Mueller scattering matrix has been calculated for sickle cell hemoglobin fibers using coupled-dipole theory. The complex polarizability of the fiber is calculated using the absorption spectrum of hemoglobin to obtain the imaginary part and a Kramer-Kronig transform to obtain the real part. The anisotropy in the polarizability is calculated based on previous work using linear dichroism.[1] The results of the polarized light scattering calculations are compared to previous measurements of total intensity light scattering and circular intensity differential scattering (CIDS) of sickle red blood cells.[2] Calculations of CIDS are found to be very sensitive to structural and optical parameters and reasonable agreement between experimental measurements and calculations are obtained. Further measurements and calculations should provide new information concerning the structure and mechanism of formation of the sickle cell hemoglobin polymer and gel.

1. Eaton, W.A. & Hofrichter J. (1981). *Methods in Enzymology*, **76**, 175-261.
2. Gross, C.T., Salaman, H., Hunt, A.J., Macey, R.I., Orme., F. & Quintanilhia, A.T. (1991). *Biochim. Biophys. Acta*, **1079**, 152-160.

[*] The biophysicist formerly known as Daniel B. Shapiro.

M-Pos354

GENERAL SOLID PHASE METHODS FOR CROSSLINKING PROTEINS: HEMOGLOBIN-ENZYME COMPLEXES

((K. Bobofchak, J. S. Brunzelle, S. Kondubhotla and K. W. Olsen)) Department of Chemistry, Loyola University, 6525 N. Sheridan Rd., Chicago, IL 60626

Preparing multi-enzyme complexes is hindered by low yields. A solid-phase method, in which alternating protein and linker reagents are applied to a column, has the potential for improving yields. The reactions can be forced to completion by adding excesses of each reagent. Two general methods have been developed to form hemoglobin-enzyme complexes. In the first, HbA is bound to the solid support through a disulfide bridge to the reactive β-93 Cys residue. Enzymes, such as catalase, can then be added using either a general or an affinity crosslinker. Removing the complex from the resin can be accomplished by the addition of a reducing agent, such as β-mercaptoethanol. In the second method, peanut agglutinin (PNA) was bound to a lactose affinity matrix and then activated using sulfosuccinimidyl-4-(p-maleimidophenyl)butyrate (S-SMPB), a heterofunctional reagent that reacts with lysine and cysteine. Since PNA has no cysteine, there was no PNA-PNA crosslinking with S-SMPB. After washing the column with buffer to remove the excess S-SMPB, HbA was added. After reaction and washing to remove excess HbA, the PNA-HbA complex was eluted by adding lactose. SDS-PAGE and UV/Vis spectroscopy demonstrated the presence of the PNA-HbA complex.

M-Pos355

THE EFFECT OF IONIC STRENGTH ON THE ACID-INDUCED TRANSFORMATIONS OF MYOGLOBIN

((Qun Tang, William A. Kalsbeck, and David F. Bocian)) Department of Chemistry, University of California, Riverside, CA 92521-0403 (Spon. by R. Cardullo)

The 426 nm absorbing deoxyheme intermediate (I'-form) occurs in the pathway of the acid unfolding of deoxymyoglobin from the native N-form to the unfolded U-form. In order to elucidate the factors which control the formation of the I'-form, a detailed series of equilibrium and slow kinetic (>2 s) experiments were performed. Equilibrium pH titrations reveal that the I'-intermediate forms at successively higher pH as the ionic strength increases. pH-jump experiments (pH 6.9 to 3.2 and pH 4.4 to 3.2) indicate that the rate of formation of the intermediate is dramatically affected by the ionic strength conditions. If the ionic strength is held constant during the pH-jump, the I'-intermediate forms slowly (~35 s) and the formation rate is independent of ionic strength. If the ionic strength is jumped from low to high values during the pH-jump, the formation rate of the I'-intermediate monotonically increases. Conversely, if the ionic strength is jumped from high to low values during the pH-jump, the rate monotonically decreases. In both types experiments where the pH and ionic strength are simultaneously jumped, the rate of formation of the I'-intermediate is independent of the initial and final ionic strength and depends only on the difference. The kinetic and equilibrium data are well accounted for with a simple three-state model in which the N-form is transformed into the I'-form via a single transition (T) state and the free energy of the various forms depends linearly on the ionic strength.

M-Pos356

TIME-RESOLVED FLUORESCENCE DECAY OF A SINGLE TRYPTOPHAN ON THE RECOMBINANT CARDIAC TROPONIN C ((C.K. Wang[#] and B.S. Hudson[*&]) [#]Dept. of Physio. & Biophys., U. of Washington, Seattle, WA & [*&]Dept. of Chem., U. of Oregon, Eugene, OR.

To investigate effects of Mg^{2+} and Ca^{2+} on the environment of a specific site on cardiac troponin C, nine rCTnCs have been prepared from *E. Coli*, respectively. Each rCTnC contains only one tryptophan residue at different sites. A cavity-dumped dye laser synchronously pumped by a mode-locked Nd:YAG was used to excite the tryptophan on rCTnC. Each protein was excited and its emission was detected at 295 and 340 nm, respectively. Results are given as follows.

Protein	Mutation site	Emission Peak	Lifetimes*			Sensitive to	*Three conditions
Y5W	N-helix	338 nm	M	M	M	none	in the column are
M60W	C-helix	345 nm	M	M	M	Ca	apo-, Mg^{2+}, and
F74W	Ca-Loop II	340 nm	S	S	S	none	Mg^{2+}/Ca^{2+},
Y150W	H-helix	344 nm	M	S	S	Mg & Ca	respectively. M
C35S,Y5W	N-helix	340 nm	M	M	M	none	stands for multiple
C35S,V44W	B-helix	330 nm	M	M	M	Ca	lifetimes, and S
C35S,M60W	C-helix	340 nm	M	M	M	Ca	for single lifetime.
C35S,F77W	D-helix	323 nm	M	M	M	Ca	
C35S,Y150W	H-helix	345 nm	M	S	S	Mg & Ca	

Emission peak of Trp residue on rCTnC in column 3 was obtained from steady-state fluorescence measurements with excitation at 295 nm, 20°C, and pH 7.2. Single lifetime for F74W, Y150W, and C35S,Y150W is 6 - 7 ns. Multiple lifetimes for the rest of mutants are in the range of 1 - 4 ns. The observed single lifetime may result from electron transfer quenching of Trp fluorescence by proximal residue(s). It is surprised to see single lifetime of mutant F74W being insensitive to cations, however, suggesting that Trp74 side chain may point outward and interact with proximal residue(s) in helix A. Similar interpretation may be applied to Trp150 interacting with residue(s) in helix E. We studied recombinant rabbit sTnC, and same results were observed. I^- quenching results showed that Trp74 is more accessible than Trp150. (Supported by NIH HL52558)

M-Pos357

TIME-RESOLVED FLUORESCENCE STUDIES ON MUTANTS OF FRUCTOSE-6-PHOSPHATE, 2-KINASE:FRUCTOSE-2,6-BISPHOSPHATASE

((**M. K. Helms**, T. L. Hazlett, K. Uyeda and D. M. Jameson)) University of Hawaii, Honolulu, HI 96822; University of Illinois, Urbana-Champaign, IL 61801; and University of Texas Southwestern Medical Center, Dallas, TX, 75216.

Fructose-6-phosphate, 2-kinase:Fructose-2,6-bisphosphatase is a bifunctional enzyme which catalyzes the synthesis and degradation of fructose-2,6-bisphosphate. The enzyme from rat testes is a homodimer, with subunits of M, 55,000. The kinase activity resides in the N-terminal domain, whereas the phosphatase activity resides in the C-terminal domain. The wild-type enzyme has four tryptophan residues at positions 15, 64, 299 and 320. Mutants were constructed containing single tryptophan residues at positions 15 and 64 in the kinase domain and 299 and 320 in the phosphatase domain to act as fluorescent reporter groups of conformational changes as well as for distance measurements. The double tryptophan mutants, 15/64; 299/320; 15/299 and 64/299, were also constructed. Multifrequency phase and modulation fluorometry was used to determine the lifetimes and mobilities of the tryptophan residues in these various mutants. The lifetime data of the single tryptophan mutants were best fit to Gaussian distribution models, with centers of 4.72 ns (W15), 5.16 ns (W64), 6.73 ns (W299) and 3.89 ns (W320). The global rotational relaxation times, corresponding to the overall protein tumbling, were in the range of 200 to 250 ns in all cases, indicating that the proteins were non-spherical. The W299/320 mutant showed relatively low polarizations compared to all other mutants, suggesting that the tryptophans in these positions are close enough to result in depolarization due to energy transfer. These observations are consistent with the recently determined X-ray structure of the protein (Hasemann, C. et al. (1996) Structure 4, 1017-1029). (This work was supported by grants from the Department of Veteran's Affairs and National Institutes of Health (DK16194 and RR03155).)

M-Pos358

FLUORESCENCE AND CIRCULAR DICHROISM STUDIES OF THE EQUILIBRIUM UNFOLDING PROPERTIES OF SIX SINGLE-TRYPTOPHAN MUTANTS OF *E. COLI* ADENYLATE KINASE **Tim Fulmer***†, Ruth Pionke*, Michael Glaser*, William Mantulin*† *Department of Biochemistry, University of Illinois, Urbana, IL; †Laboratory of Fluorescence Dynamics, Department of Physics, University of Illinois, Urbana, IL.

The enzyme adenylate kinase (AK) from *E. coli* (MW 23.5 kD) is a monomeric protein that has been cloned, overexpressed, and purified to homogeneity. It is a highly flexible protein with significant domain movements upon substrate binding. The wild type AK is devoid of tryptophan. We have constructed six single-tryptophan mutants of the enzyme useful for spectroscopic studies. The equilibrium unfolding properties of the six single-tryptophan mutants were studied in the presence of a variety of perturbants that included chemical denaturants, high temperature, and hydrostatic pressure. Both steady-state and time-resolved fluorescence methods, as well circular dichroism spectroscopy, were used to characterize both partially and fully denatured states of the mutants. The single-tryptophan mutations leave the wild-type enzyme's function and global structure largely unperturbed. Hence, the single tryptophan residues may be used as reporter groups of the various local microenvironments of the wild-type enzyme. Far-UV circular dichroism was used to follow changes in the protein's global secondary structure, while fluorescence variables such as polarization and lifetime monitored both local and global changes in the protein's tertiary structure. In the presence of chemical denaturants the folding transition was found to be reversible, but less so with pressure and high temperature suggesting that side-reactions (aggregation) may compete with the refolding step. A set of equilibrium unfolding curves for each showed interesting differences depending on which fluorescence variable was monitored as a function of the denaturant used. The curves can be rationalized based on the coordinates of single-tryptophan residue, available from high-resolution x-ray crystal structures. Finally, free energies of unfolding for all six mutants were estimated by applying the linear free energy model to the chemical denaturation curves. (This work was supported by the NIH RR 03155.)

M-Pos359

SM-MLCK binding to bovine calmodulin: evidence for 2:1 complex formation.

((**A.G. Szabo**[1], W. A. Stephenson[1], R. Fischer[2] and M. Berchtold[2])) [1]Dept. of Chemistry and Biochemistry, University of Windsor, Windsor, ON. Canada N9B 3P4; [2]Institute of Veterinary Biochemistry, University Zurich-Irchel, Switzerland.

There have been a very large number of studies of the binding of peptides to calmodulin (CAM.) (A. Crivici & M. Ikura, Annu. Rev. Biophys. Biomol. Struct. 1995, 24:85-116). The peptides studied are usually identified as corresponding to domains of target enzymes to which CAM binds with nanomolar dissociation constants and modulates their activity. Recently it has been shown by some of us (R. Fischer et al. J. Biol. Chem. 1996, 271: 25067-25070) that the c-terminus of the Ras-like GTPase Kir/Gem also binds to CAM in a Ca^{2+} dependent manner. In the current study the change in the tryptophan fluorescence of the peptide was utilized to follow the binding to Bovine CAM. The studies show strong evidence that the peptide forms a 1:1 complex with a nanomolar dissociation constants and a 2:1 complex with a K_d in the micromolar range.

This data is present and discussed in terms of binding to target proteins

M-Pos360

CHARACTERIZATION OF CALMODULIN BINDING TO NITRIC OXIDE SYNTHASE BY FLUORESCENCE ENERGY TRANSFER ((**P.B.O'Hara**, A.Barczak, P.Kim)) Amherst College,Department of Chemistry, Amherst MA 01002

Nitric oxide synthase (NOS), the only known calmodulin (CaM) dependent redox protein, catalyzes the synthesis of NO, an important signal molecule in neuronal, endocrine and epithelial cells. In this study, fluorescence resonance energy transfer has been used to determine the structure of CaM when bound to both intact NOS and a NOS peptide fragment; KRRAIGFKKLAEAVKFSAKLMQC, which corresponds to the CaM binding domain. The fluorescent energy donor, AEDANS, [5-((((((acetyl)amino)ethyl)amino) napthalene)-1-sulfonic acid] and the fluorescent energy acceptor DDP, [N-(4-dimethylamino-3,5-dinitrophenyl)maleimide] are bound covalently through thiol side groups at positions 34 and 110 in the mutant protein T34C;T110C CaM. The relatively low degree of quenching in the uncomplexed CaM (7%- donor acceptor distance of 41 Å as determined from both lifetime and intensity quenching using Forster theory), is consistent with the long distance predicted from the crystal structure of Ca-CaM. Fluorescence of the donor is quenched to a large extent, 86%, upon binding to the NOS peptide. Again, Forster theory allows the calculation of a new donor acceptor distance of approximately 21 Å. This is interpreted as a collapse of the open structure of Ca-CaM about the basic amphiphillic helix of the NOS peptide in a manner consistent with structures determined by NMR and X-ray crystallography for CaM binding to peptides derived from other target proteins. The characterization of the fluorescence quenching of labelled CaM with intact NOS is complicated by the intrinsic fluorescence of the NOS derived from its flavin group. A model developed to interpret the changes in flavin fluorescence induced by CaM binding will be presented. Taking those changes into account, the quenching of the AEDANS donor suggests that the interaction of the CaM with the intact protein is similar to that derived from the NOS binding peptide.

M-Pos361

S100 PROTEIN-LIGAND INTERACTIONS: CALORIMETRIC AND FLUORESCENCE STUDIES

((**William Kirk***, Miklos Nyitrai‡, Franklyn Prendergast*))
*†*Mayo Foundation, Rochester Minn 55905, and ‡ Univ Medical Sch. of Pecs, Pecs Hungary. † sponsoring member*

Bovine brain S100A protein binds Ca^{2+} and displays a characteristic absorption difference spectrum, which has been interpreted as due to conformational changes upon cation binding. We, however, can account for this spectrum entirely in terms of the ^1L_b transition of *trp* coupled weakly via an exciton interaction to two near degenerate levels of a nearby *tyr* residue for which transition a particular Franck-Condon progression is suppressed by 'quenching' the local E field upon Ca^{2+} binding.

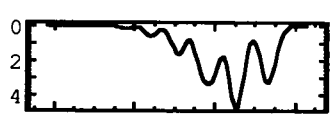

Tb^{3+} binding and stoichiometry is monitored by energy transfer from the *trp*, while the stoichiometry of Ca^{2+} binding and the respective affinity constants are measured by means of isothermal titration calorimetry.

M-Pos362

Ligand-induced Conformational Changes in Stromelysin: Theory and Experimental Fluorescence Studies. John H. Van Drie, Roger A. Poorman, Gary L. Petzold, and Dennis E. Epps Pharmacia and Upjohn, Kalamazoo MI 49001

Ligand-induced conformational changes in stromelysin (STR) were suggested by NMR, crystallography, and peptidic SAR experiments. To define the details of these putative conformational changes, the "Flory chain dynamics" computational technique was applied to a model of the three-dimensional structure of STR. The modelling results indicated that the motions of largest amplitude occur in the loop 135-145 which lies at the bottom of the "right-hand side" (P2'-P3') of the active site cleft. The NMR structure of U-99533/STR complex revealed that all three tryptophan residues of STR lie within 15 Å of the catalytic Zn binding site, with one of them, Trp-104, being proximal to the right-hand side of the inhibitor binding site. The fluorescence of the tryptophans might, therefore, report ligand-induced conformational changes in the 135-145 loop. Using fluorescence quenching, polarization, bisANS binding, and dynamic measurements, we were able to observe significant changes induced in the intrinsic tryptophan fluorescence by any one of three hydroxamate inhibitors, Batimistat, U-99533, and Celltech CT1418, which bind in P2'-P3', but no change was observed for the ligand CGS27023A which is thought to bind in P1-P1'. Binding of the high affinity inhibitor, Batimistat, produced by far the most significant changes in conformation, including an 80% increase in the average polarization of the STR Trp's, and a 100-fold increase in the K_d for bisANS binding, which was also shown by activity measurements to be a weak ($K_i \approx 20\ \mu M$) competitive inhibitor of STR catalytic activity. The significance of these results for drug design is discussed.

M-Pos363

TIME-RESOLVED FLUORESCENCE STUDIES OF FLAVINS IN NEURONAL NITRIC OXIDE SYNTHASE. ((K. Brunner, E. Pitters[†], A. Tortschanoff, C. Warmuth, H.F. Kauffmann, M. Auer[‡], B. Mayer[†] and A.J. Kungl[‡])) Dept. Phys. Chem., A-1090 Univ. Vienna; [†]Dept. Pharmcol. & Toxicol., A-8010 Univ. Graz; [‡] Sandoz Res. Inst., A-1235 Vienna.

Neuronal nitric oxide synthase (nNOS) is a homodimer containing one FAD and one FMN per monomer. According to current models, the flavins act as acceptors and donors in the electron transport chain from NADPH in the reductase domain to the heme in the oxidase domain. We have investigated the steady state and picosecond time-resolved fluorescence of FAD and FMN in nNOS during the stepwise reconstitution of the enzyme by molar excess of its cofactors and substrate. Typical flavin fluorescence emission was found at 526 nm when excited at 367 nm, a laser wavelength chosen to allow the monitoring of NO_x production *via* nitrosation of diaminonaphthalene *in situ*. The fluorescence intensity increased upon addition of Ca^{2+}/calmodulin. In addition the maximum shifted slightly to shorter wavelengths when NADPH was added. Three exponential terms were needed to fit the fluorescence decay of nNOS adequately: a very short component of 25 ps (13 %), a medium lifetime of 390 ps (7 %), and a long lifetime of 3.65 ns (79 %). We interpret the short fluorescence lifetime as being due to charge transfer quenching, probably electron transfer, by a very close acceptor. A significant increase in the mean lifetime $<\tau>$ from 2.91 ns to 3.53 ns was obtained when Ca^{2+}/calmodulin was added, but did not further change when the substrate arginine and the electron donor NADPH were added. Obviously the flavins become more exposed, i.e. less quenched, when Ca^{2+}/calmodulin was added. The fluorescence anisotropy of the flavins in nNOS decayed fast to zero with rotational correlation times ϕ_1 = 93 ps (30 %) and ϕ_2 = 480 ps (70 %). Addition of Ca^{2+}/calmodulin changed the mean rotational correlation time $<\phi>$ from 364 ps to 197 ps. $<\phi>$ remained constant when arginine was added, but increased to 264 ps upon addition of NADPH. The fast decay of the flavin fluorescence anisotropy refers to a fast rotational motion of these chromophores which is uncoupled from the overall rotation of the enzyme. Binding of both Ca^{2+}/calmodulin and NADPH influence this rotational dynamics and may therefore be required for optimum positioning of the flavins in the course of electron transfer.

M-Pos364

PICOSECOND TIME-RESOLVED FLUORESCENCE STUDIES CHARACTERIZE THE BINDING BETWEEN THE NOVEL FLUORESCENT ANTI-ANGIOGENIC DRUG PNU151484 AND HUMAN BASIC FIBROBLAST GROWTH FACTOR.

((Moreno Zamai [1,2], Valeria R. Caiolfa[2], Dina Pines[1], Ehud Pines[1] and **Abraham H. Parola[1 *]**)) [1] Department of Chemistry, Ben-Gurion University of the Negev, P.O. Box 653, 84 105 Beer-Sheva, Israel.and the [2] Department of Experimental Oncology, PPC-Oncology, Pharmacia & Upjohn, via Giovanni XXIII, 20014 Nerviano, Milano, Italy.

PNU151484, an anti-angiogenic compound named suradista, exerts its activity by interacting with heparin binding growth factors. The in-vitro complex formation between PNU151484 and human recombinant basic fibroblast growth factor (bFGF) was studied due to its relevance to tumoral angiogenesis. Titration experiments were followed by quantitative high performance affinity chromatography, ps time-resolved fluorescence emission and anisotropy studies in PBS (pH 7.1) at 20 °C. Affinity chromatography revealed a dissociation constant of 1.5×10^{-7} M. The binding isotherm, constructed by the method of fluorescence lifetime titration, yielded a dissociation constant of 1.0×10^{-7} M. Time-resolved decay of anisotropy study resulted in a similar dissociation constant after correction for drug dimerization at the relatively higher drug concentration employed. PNU151484:bFGF is a tight complex with a 1:1 stoichiometry, and studies of solvent effect on the drug's lifetime highlights the mode of interacion of suradista with HBGFs. Since it does not cause protein aggregation, suradista has a potential clinical applicability.

M-Pos365

FLUORESCENCE SPECTROSCOPY STUDIES OF INTEGRATION HOST FACTOR PROTEIN COMPLEXED WITH DNA

(I.Iliescu and I.Mukerji) Department of Molecular Biology and Biochemistry, Wesleyan University, Middletown, CT 06459-0175

Integration Host Factor(IHF) is a small heterodimeric protein which has been implicated in gene activation and transcription, due in part to its ability to bind and bend DNA. A prokaryotic histone-like protein, IHF has a high degree of homology with the HU protein and both proteins are thought to bind to the minor groove of DNA via two β-ribbon arms that extend from an α-helical core. Unlike HU, however, IHF can bind to DNA in both a sequence specific and non-specific manner. We have employed fluorescence measurements of the four Tyrosine (Tyr) residues present in the protein to elucidate the differences in protein conformation that result from the two modes of binding to DNA. Previous fluorescence and UV resonance Raman investigations have indicated that the Tyr residue (β93) located near the carboxy-terminus of the IHF β subunit is stabilized in the ionized form. This residue yields a distinct peak in the emission spectrum that is readily monitored and is spectroscopically distinguishable from the two Tyr residues located in the β-ribbon arms. Fluorescence quenching experiments, using acrylamide and iodide as the quenching agents, were performed on free IHF and on IHF complexed with specific and non-specific DNA to assess the role of the Tyr residues in DNA binding. To understand the function of the β93 Tyr residue with regard to protein stability and DNA binding properties, a pH titration of IHF was performed both in the presence and absence of DNA. Preliminary results reveal that in the absence of DNA the pKa is less than 9.0.

M-Pos366

THE DIMMER SWITCH IN PHOTOSYSTEM II: MODEL OF THE XANTHOPHYLL-CYCLE DEPENDENT ENERGY DISSIPATION MECHANISM. ((A.M. Gilmore[1], V.P. Shinkarev[2], T.L. Hazlett[3], Govindjee[2])). [1]ANU/RSBS Canberra ACT 0200 Australia; [2]CBCB, UIUC, Urbana, IL 61801 USA; [3]LFD, UIUC, Urbana, IL 61801.

The special carotenoid pigments of the 'xanthophyll cycle' play an important, yet still unresolved, photoprotective role by mediating the dissipation of excess absorbed light energy in photosystem II in all higher plants [Gilmore (1997) Physiol. Plant. (in press)]. In this poster, we describe how stoichiometric modeling of photosystem II chlorophyll *a* fluorescence lifetime distribution data has elucidated the mechanism of xanthophyll cycle-dependent energy dissipation. Consistent with our earlier reports, both the primary photochemistry and the xanthophyll cycle dependent energy dissipation function independently of the LHCIIb complexes of the peripheral photosystem II antenna. These analyses support that in a singe pH-activated event, one of the deepoxidized β-cyclic endgroup structures (3S or 3'R configuration) of a zeaxanthin or antheraxanthin molecule can bind to one stereospecific site in the inner antenna complexes (CP26 or CP29) of a photosystem II unit. This binding event effectively causes the unit to 'switch' to an increased rate constant of heat dissipation and a decreased fluorescence lifetime. The data also clearly indicate that both zeaxanthin and antheraxanthin function with equal effect in the energy dissipation mechanism. Further the model explains why extremely low concentrations of xanthophylls containing a β-cyclic endgroup structure analogous to antheraxanthin or zeaxanthin (such as lutein or diatoxanthin) can cause large decreases in the photosystem II chlorophyll *a* fluorescence yield when the chloroplast thylakoid lumen pH falls below 5. The data and model interpretation highlight the *in vivo* significance and photoprotective function of the xanthophyll cycle in higher plants and algae. (AMG supported by ANU/RSBS, AMG and G supported by Training Grant (DOE 92ER20095, DOE/NSF/USDA), VPS Supported by USDA Grant #94-37306-0343, TLH supported by NIH Grant #RR03155)

M-Pos367

THE INTERACTION OF FLUORESCEIN-TAXOL WITH MICROTUBULES FROM ABSORPTION AND FLUORESCENCE SPECTROSCOPY. ((M.P. Lillo[1], A.A. Souto[2], J.Evangelio[3], M. Abal[3], I. Barasoain[3], F. Amat[2], J.M. Andreu[3] and A.U. Acuña[1])) [1]Instituto Química-Física, [2]Instituto Química Orgánica, [3]Centro Investigaciones Biológicas, CSIC, E-28006 Madrid (Spain)

Flutax (7-alanyl-fluorescein-taxol) and **2'-acetyl-flutax** (2'-acetyl-7-alanyl-fluorescein-taxol are members of a series of novel fluorescent derivatives of taxol, sinthesized recently in our laboratory (A.A. Souto et al. (1995) Angew. Chem. Int. Ed. Engl. 34, 2710-2712). Flutax biological activity is similar to that of taxol, inducing the assembly of microtubules and inhibiting the cell cicle. 2'Acetyl-Flutax is biologically inactive. A detailed spectroscopic study of these taxol derivatives and their interaction with microtubules has been performed (steady-state and fluorescence time-resolved techniques). The sensitivity of the fluorescein chromophore to the properties of its microenvironment was used to characterize the flutax binding site in GDP-tubulin (TB), and in Flutax-induced microtubules (MTB) (see fig). Spectroscopic studies of cellular microtubule are in progress. [Supported by DGICYT Grants PB93-126, PB950116].

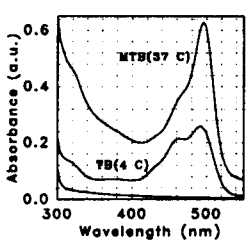

M-Pos368

ANALYSIS OF FLUORESCENCE ANISOTROPY DECAY: SPECIFIC ASSOCIATIONS BETWEEN LIFETIMES AND ROTATIONAL CORRELATION TIMES ((C. Bialik, B. Wolf, J.B.A. Ross, and W.R. Laws)) Dept. of Biochemistry, Mount Sinai School of Medicine, New York, NY 10029.

As usually applied, the analysis of time-resolved fluorescence anisotropy decays assumes that, in the case of multiple intensity decay times, each lifetime is associated with each rotational correlation time. We have been studying the use of alternate analysis models where the associations can be stated explicitly. For the situation of two lifetimes and two correlation times, nine association models exist. We have used all nine models to analyze synthetic data generated by all nine models for six different fluorescence intensity weightings. In addition, two experimental systems[1] that should reflect two of the models were studied. In general, the model used to generate the synthetic data was the best at recovering the parameters. Closely related associations were sometimes able to analyze the data successfully. However, the 'correct' model was always better as the intensity contribution of one lifetime component became small. For the experimental systems, all but three models were eliminated based on fit statistics and/or recovery of parameters without physical relevance. Of the three acceptable models, one had the expected associations for the experimental system and the other two were closely related. This analysis approach therefore shows promise in helping to determine the size, shape, and dynamics characteristics of biological macromolecules in solution. Supported by NIH Grant GM39750.

[1] Two Trp residues in liver alcohol dehydrogenase and a mixture of indole and β-cyclodextrin.

M-Pos369

RESOLUTION OF PROTEIN TRYPTOPHAN FLUORESCENCE SPECTRA INTO ELEMENTARY COMPONENTS. COMPARISON WITH STRUCTURAL CHARACTERISTICS OF INDIVIDUAL INDOLIC FLUOROPHORES. ((E.A. Burstein, Ya.K. Reshetnyak)) Institute of Theoretical and Experimental Biophysics, Russia Acad. Sci., Pushchino, Moscow Region, 142292, Russia. (Spon. by B. Ehrenberg)

The overwhelming majority of proteins exhibit smooth non-structured spectra of tryptophan fluorescence, which often contain more than one component. For resolving the protein fluorescence spectra into elementary components some algorithms, based on quite different mathematical approaches, were used. The histogram obtained demonstrates the most probable position of the spectral components. In the next stage, it was found correlations between spectral properties and some features of microenvironment of individual indolic fluorophores, obtained from the database of the protein atomic coordinates (PDB-bank), such as solvent exposure of tryptophan residues, relative polarity and flexibility of fluorophore environment, steric relations between various indole atoms and potential donor and acceptors in hydrogen bonding, existence of hydrogen bonds in the ground state, presence and distance to quenching groups and heavy atoms etc. The approaches described was used to test the hypothesis about the discrete structural-physical and spectroscopic states of tryptophan in protein. This work was supported by the RFBR Grant 95-04-12938

M-Pos370

BAND-SHAPE ANALYSIS OF FLUORESCENCE DECAY-ASSOCIATED SPECTRA; TRYPTOPHAN IN PROTEINS. (([1]Piotr Targowski and [2]**Lesley Davenport**)) [1]Institute of Physics, Nicolas Copernicus University, Torun, Poland and [2]Department of Chemistry, Brooklyn College of the City University of New York, Brooklyn, NY 11210.

Analytical expression of a fluorescence spectrum based on a semiclassical quasi-molecular model, which accounts for intermolecular interactions with the fluorophore surroundings, can provide direct information on purely electronic (0-0) transition energy of a fluorophore (following excitation to the Franck-Condon state and further thermal and orientational relaxation). In this approach high amplitude oscillations of the fluorophore in the averaged force field of the surroundings are decisive in shaping the profile of the spectrum. We have applied this analytical model in the characterization of decay-associated spectra (DAS) resolved from heterogenous fluorescence intensity decay profiles of tryptophan-containing proteins. As one example of this approach, we have examined our previously reported DAS (*Davenport, et al., Biophys. J. (1996) 70, A306*) for apo β_2-tryptophan synthase, a single Trp containing protein. The resolved DAS, associated with three fluorescence lifetimes, suggest different protein conformers. Our analyses clearly demonstrate different 0-0 transition energies for all components, but similar effective environmental interaction potentials, suggestive of similar short-range interactions but heterogeneous long-range effects. Other multiexponential proteins are under investigation. Details of the model will be discussed, and other protein examples shown. This work was supported in part by Polish Gov. through KBN Grant 2 PO3B 124 09 and PSC-CUNY Award Program.

M-Pos371

THE PEPTIDE BOND QUENCHES INDOLE FLUORESCENCE. ((Yu Chen, Bo Liu, Hong-Tao Yu, and Mary D. Barkley*)) Department of Chemistry, Louisiana State University, Baton Rouge, LA 70803-1804.

The effect of the peptide bond on protein fluorescence is an important unresolved question in tryptophan photophysics. Definitive evidence for the peptide group as a weak quencher of indole fluorescence was obtained from solute quenching studies with a series of model compounds. Two amides are required for detectable quenching of 3-methylindole fluorescence and the quenching rate depends on the distance between amides. The bimolecular rate constants k_q of malonamide, N-acetylasparagine, N-acetylglycinamide, and N-acetylglutamine are 33×10^7, 8.8×10^7, 6.6×10^7, and 2.2×10^7 $M^{-1}s^{-1}$, respectively. Transient absorption and temperature dependence of the fluorescence lifetime measured in the absence and presence of quencher gave strong circumstantial evidence for electron transfer as the quenching mechanism. Triplet yields were measured for five indole derivatives using transient absorption. Intersystem crossing rates were calculated from triplet yield and fluorescence lifetime data. Intersystem crossing in indoles is independent of temperature in aqueous solution. The peptide group does not change the value of k_{isc} of 3-methylindole. The temperature dependence of the fluorescence lifetime of 3-methylindole was determined in the presence of N-acetylglycinamide, ethylacetate, and $GdCl_3$. Two separate Arrhenius terms were resolved for water quenching and solute quenching. The activation energies for solute quenching by N-acetylglycinamide, ethylacetate, and $GdCl_3$ are 2.5 ± 0.3, 0.0, and 6.0 ± 0.5 kcal/mol, respectively. The strategy of using the temperature dependence of the fluorescence lifetime to calculate the rates of individual nonradiative processes is discussed.

M-Pos372

EVIDENCE OF ^1L_b FLUORESCENCE FROM INDOLE-POLAR SOLVENT PI-COMPLEXES IN THE SUPERSONIC JET ((**Kurt W. Short** and Patrik R. Callis)) Department of Chemistry and Biochemistry, Montana State University, Bozeman, MT 59717.

Indole, the chromophore of the amino acid tryptophan, has two close-lying π-π^* electronic transitions. They are from the electronic states known as ^1L_a and ^1L_b to the ground state. In a gas phase supersonic jet environment, bare indole is known to have fluorescence from the ^1L_b state. Indole is believed to form two different 1:1 gas phase complexes with small polar solvents, known as sigma- and pi-complexes respectively. For indole-water and indole-methanol the sigma-complex is known to emit from the ^1L_b state. The fluorescence of the pi-complex of indole with these solvents has been controversially assigned as coming from the ^1L_a state. This is because the published dispersed fluorescence spectra of the 1:1 complexes appear broad and somewhat featureless. However, we present here two-photon fluorescence excitation spectra and high resolution one-photon dispersed fluorescence spectra which show that the 1:1 pi-complex of indole, with water and with methanol, has fluorescence emission from the ^1L_b state. This result also agrees with recent ab initio calculations (see the poster by David Hahn and Patrik Callis) which suggest that, in the excited state, the lowest level of the ^1L_a state does not shift in energy below that of the ^1L_b state for a 1:1 pi-complex of indole with water.

M-Pos373

AB INITIO STUDY OF EXCITED STATE INDOLE-WATER COMPLEXES. ((**David K. Hahn** and Patrik Callis)) Department of Chemistry and Biochemistry, Montana State University, Bozeman, MT 59717.

We have conducted an ab initio investigation of the intermolecular potential energy surface between water and indole in its ^1L_a and ^1L_b excited electronic states. Geometry optimizations of the π and σ complexes were performed using the CIS method with basis sets ranging in size from 4-31G to 6-31G(p,d), while vibrational modes and frequencies were obtained at the CIS/4-31G or CIS/4-31G(p,d) level. In keeping with the findings of jet-cooled spectra, the intermolecular geometry of either excited state complex was found to differ considerably from the ground state, while the ^1L_a π complex was found to be only .5 kcal/mol more stable than the ^1L_b π complex (see the poster by Short and Callis). Computed intermolecular modes allow for the assignment of the ^1L_b pi and sigma complexes to their respective origins in the indole-water fluorescent excitation spectra. The computed frequencies of the ^1L_b complexes were found to be in fair agreement with experiment.

M-Pos374

SPECTROSCOPY OF INDOLE, 4-FLUOROINDOLE, AND 2-METHYL-INDOLE IN ARGON AT 20K, INCLUDING SHARP PHOSPHORESCENCE.
((**Bruce J. Fender** and Patrik R. Callis)) Department of Chemistry and Biochemistry, Montana State University, Bozeman, MT, 59717.

Indole is the chromophore of the amino acid tryptophan and accounts for the majority of uv absorption in proteins. Indole entrained in Ar at 20K fits mainly into six different "sites" within the matrix, spanning an energy of 213 cm^{-1}. These sites are produced by different orientation of the Ar with respect to indole, and each site has a different solvation leading to a different ^1L_a-^1L_b energy separation. Exploration of these sites has found a variety of spectral changes: shifting and intensity changes of vibronically coupled lines, varying frequencies of the out-of-plane vibrations, and exceptionally sharp phosphorescence (~10cm^{-1}). The research has also expanded to include 4-fluoroindole (4FI) (chromophore of 4-fluorotryptophan) and 2-methylindole (2MI) in Ar at 20K, whose fluorescence excitation (with polarization), fluorescence, and phosphorescence spectra also have very sharp lines (10 cm^{-1}). For 4FI the ^1L_a origin is located 1520 cm^{-1} above the ^1L_b origin and the spectra contain a FC progression of the ν_{25} (ν_{26}) vibration, not seen in indole. For 2MI our data suggests that the orientation of the ^1L_a and ^1L_b transition dipoles is not 90°, but a smaller angle and the ^1L_a origin is not located yet.

M-Pos375

PHOSPHORESCENCE EMISSION FROM TRYPTOPHAN AND SOME TRYPTOPHAN ANALOGS IN SUGAR MATRICES AT AMBIENT TEMPERATURE
((Colin McCaul and **Richard D. Ludescher**)) Department of Food Science, Rutgers, The State University, New Brunswick, NJ 08903-0231

L-Tryptophan and the tryptophan analogs 4-F-Tryptophan, 5-F-Tryptophan, 6-F-Tryptophan, and 5-Br-Tryptophan were dispersed in amorphous galactose or arabinose matrices at molar ratios in the range from 10-100 parts per million; matrices were generated by freeze drying concentrated aqueous solutions of the sugars + probes. The luminescence properties of the probes were characterized by comparing relative phosphorescence and fluorescence emission spectra and time-resolved phosphorescence emission decay kinetics. All probes were phosphorescent in the rigid environments of the sugar matrices, although the emission maxima of the spectra varied depending upon the type and position of the fluorine or bromine atom. All probes exhibited complex multi-exponential decay kinetics indicating that the probes occupied many different micro-environments within the sugar matrices. This study suggests that these probes may have utility in studies of the dynamics of amorphous carbohydrates in the solid state and in studies of the internal dynamics and function of proteins both in solution and in the solid state. (Research supported by grant #9502626 from the USDA.)

M-Pos376

BIOSYNTHETIC INCORPORATION OF 7-AZATRYPTOPHAN INTO THE CATALYTIC DOMAIN OF *PSEUDOMONAS AERUGINOSA* EXOTOXIN A.
((**F.-L. Yeh** and A.R. Merrill)) Guelph-Waterloo Centre for Grad. Work in Chem., Dept. of Chem. & Biochem., Univ. of Guelph, Guelph, ON, CANADA N1G 2W1.

Pseudomonas aeruginosa exotoxin A (ETA), is a mono-ADP-ribosyl transferase (ADPRT) that catalyzes the transfer of the ADP-ribosyl moiety of NAD^+ onto eukaryotic elongation factor-2 (eEF-2). This transfer inactivates eEF-2 resulting in the inhibition of protein synthesis causing host cell death. The use of intrinsic tryptophan fluorescence to study toxin-eEF-2 interaction is inherently limited since the spectral properties of the various tryptophan residues in both proteins cannot be distinguished. To aid in the study of this protein-protein interaction by tryptophan fluorescence, we replaced the tryptophans in the catalytic domain of exotoxin A (PE24) with the analogue, 7-azatryptophan (7-AW). This analogue possesses a red-shifted absorbance spectrum and hence can be distinguished from that of L-tryptophan. The specific incorporation of 7-AW was achieved by expressing the protein in a tryptophan auxotrophic strain of *E. coli*, BL21 (*λDE3*), in media containing 7-AW. The red shift in the absorbance and fluorescence emission spectra of analogue-incorporated PE24, upon comparison to the wild type protein, confirmed the presence of 7-AW. The selective excitation of the tryptophan analogue within the PE24 catalytic domain will facilitate the investigation of the protein-protein interaction between PE24 and eEF-2 as well as the mechanism of catalysis [supported by MRC, ARM].

M-Pos377

TWO-COLOR TWO-PHOTON EXCITATION OF FLUORESCENCE.
((**J.R. Lakowicz**, I. Gryczynski, Z. Gryczynski and H. Malak)) Center for Fluorescence Spectroscopy, University of Maryland at Baltimore, Dept. of Biochem. & Molec. Biology, 108 N. Greene St., Baltimore, Maryland 21201

NIR and UV train of pulses from fundamental and harmonic outputs of pyridine 2 dye laser were combined together and provided fluorescence excitation when synchronized in time and space. Each of the beams individually did not excite the investigated fluorophores. Excitation was also not observed for unsynchronized pulses. The observed fluorescence intensity depends on the product of NIR and UV beam intensities $I_{FL} \sim I_{NIR} \times I_{UV}$. Observed fluorescence anisotropies were characteristic of two-photon excitation and were 4/7 for parallel transitions. The fluorescence depends on relative polarizations of NIR and UV beams, being strongest for parallel and 1/3 of maximum value for the perpendicular configu-ration. Two-color two-photon (TCTP) excitation has many potential applications in microscopy, spectroscopy and optical data storage. TCTP can be also used with laser beams with slightly different repetition rates. In this case the signal will appear as pulses at the difference frequency. The significant advantage of TCTP excitation is that the signal appears against a dark background.

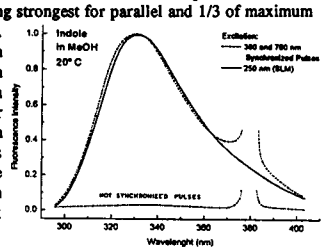

M-Pos378

SINGLE PROTEIN MOLECULE REACTION BY TWO-PHOTON EXCITED FLUORESCENCE.
((**Osman Akcakir** and Enrico Gratton)) Laboratory for Fluorescence Dynamics, Dept. of Physics, University of Illinois at Urbana-Champaign, Urbana, IL 61801.

2-photon fluorescence excitation occurs in a small volume (~0.1fl), it has excellent background rejection, and it can detect single molecules. The study of protein reactions at the single molecule/protein level is a promising tool to address many fundamental issues regarding protein conformation and dynamics. In particular, we are interested in the observation of proteins in different conformational substates. For example, by analyzing the kinetics of single protein ligand binding, information on the statistical distribution of conformational substates at the single protein level may be obtained. Two major technical problems confront research in this area: 1) immobilization of proteins in a matrix in which native conformations occur and the background fluorescence is sufficiently low for single molecule detection, and 2) heat induced denaturation or heat induced substates changes upon excitation of the single fluorescing protein. Progress to overcome these obstacles by suitable choice of host environment will be discussed. Supported by NIH grant RR03155.

M-Pos379

MULTIPHOTON EXCITATION OF MOLECULAR FLUOROPHORES AND NATIVE BIOLOGICAL ABSORBERS.
((Chris Xu, Jason B. Shear*, Marius Albota, and Watt W. Webb)) Applied Physics, Cornell University, Ithaca, NY 14853

Our measurements of two-photon excitation (TPE) cross sections, in addition to the common biological indicators, now include many important native biological absorbers, such as green fluorescent proteins (GFPs), NADH, NADPH, FAD and FMN. Knowledge of these TPE spectra (from 700 nm to 990 nm) not only indicated exciting opportunities for TPE but also provided new insight into the photodamage mechanisms of living biological preparations in the near infrared. The measured TPE spectra of both wild type GFP and GFP S65T are similar to the corresponding one-photon spectra. However, an extremely large TPE cross section was discovered for EGFP. Results for NADPH are nearly identical to NADH. The TPE spectrum of FAD is similar to FMN, although the action cross sections of FAD are approximately 9 times smaller than FMN (presumably due to quenching of fluorescence by the adenine). The pursuit of lower background in fluorescence detection has led to the determination of the two-photon scattering cross section of liquid water. Quantitative comparisons between two-photon scattering of liquid water and two-photon excited dye fluorescence show that the relative scattering background is typically reduced by orders of magnitude in two-photon excitation as compared to single photon excitation with confocal detection.

*Present address, department of chemistry, University of Texas, Austin, TX 78712.
Supported by the Developmental Resource for Biophysical Imaging and Opto-electronics funded by NSF(DIR8800278), NIH(RR04224) and NIH(RR07719).

M-Pos380

CLINICAL SENSING OF THE ANTICANCER DRUG HYCAMTIN IN WHOLE BLOOD AND PLASMA BY TWO-PHOTON FLUORESCENCE

Thomas G. Burke[1,2], Henryk Malak[3], Ignacy Gryczynski[3], Zihou Mi[2], and Joseph R. Lakowicz[3]

[1]Division of Medicinal Chemistry and Pharmaceutics, College of Pharmacy, and the Markey Cancer Center, University of Kentucky, Lexington, KY 40506-0286, [2]Division of Pharmaceutics, College of Pharmacy, The Ohio State University, Columbus, OH, 43210, and [3]Center for Fluorescence Spectroscopy, Department of Biological Chemistry and Medical Biotechnology Center, University of Maryland School of Medicine, Baltimore, MD 21201

Recent FDA-approval of Hycamtin (topotecan; 9-dimethylaminomethyl-10-hydroxycamptothecin) and Camptosar (CPT-11) along with the accelerated clinical development of related camptothecin drugs provides new hope for the successful treatment of human cancer, including neoplasms for which no effective treatments currently exist. Current clinical efforts worldwide are aimed at optimizing the therapeutic efficacies of the camptothecins, with the major focus on the determination of the most effective dosing schedules. To this end, technological advances which provide a direct and rapid means of measuring plasma drug levels (*i.e.* such that correlations between plasma drug levels and clinical responses can be sought) would be of great utility. Here we report on the direct fluorescence detection of Hycamtin in human plasma and whole blood at micromolar levels using two-photon excitation at 730 or 820 nm. Two-photon fluorescence techniques were also shown to be useful in directly studying SN-38 binding interactions in human plasma samples. Since skin, blood and other tissues are translucent at long wavelengths, our results suggest the attractive possibility of homogeneous or noninvasive clinical sensing of camptothecins *in situ* using two-photon excitation.

M-Pos381

EXCITED-STATE INTERACTIONS OF 2-AMINOPURINE ((E. Rachofsky, W. R. Laws, and J. B. A. Ross)) Dept. of Biochemistry, Mount Sinai Sch. Med., New York, NY 10029.

2-aminopurine (2AP) is a highly fluorescent analogue of adenine which can be incorporated into both single- and double-stranded nucleic acids with minimal perturbation of their native structure. The fluorescence emission of 2AP is sensitive to the local environment, and may therefore provide an invaluable probe of DNA-protein and RNA-protein interactions, as well as of the enzymology of nucleic acid metabolism. The time-dependent decay of fluorescence emission of 2AP in aqueous solution is a single exponential; in oligonucleotides it is multi-exponential. We have investigated the processes underlying the complexity of the decay law by steady-state and time-resolved fluorescence spectroscopy of model systems. Results demonstrate that 2AP in glycerol has an emission spectrum similar to that observed in oligonucleotides. Fluorescence decays obtained at multiple wavelengths show that 2AP in glycerol can undergo a time-dependent spectral shift due to dipolar relaxation of the solvent. This process results in an emission decay which is qualitatively similar to that observed in oligonucleotides. It is also shown that at pH ≤ 2.5, 2AP can undergo protonation during the lifetime of the excited state; this process also results in a multi-exponential decay function. Either or both of these excited-state processes may be responsible for the complexity of the emission decay in oligonucleotides. Supported by NIH Grant GM39750.

VISUAL RECEPTORS

M-Pos382

ACTIVATION OF THE PHOTOTRANSDUCTION CASCADE IN RETINAL RODS BY 2-PHOTON EXCITATION OF RHODOPSIN USING 1064 nm ILLUMINATION. ((M. Gray-Keller[a], W. Denk[b] and P. Detwiler[a])) [a]Dept. Physiol. and Biophy., Univ. of Washington, Seattle, WA. [b]Bell Labs, Lucent Technologies, Murray Hill, NJ.

Isolated rod outer segments (ROS) from Gecko lizard dialyzed in whole-cell voltage clamp with internal solution containing 1 mM GTP and 5 mM ATP maintain an inward dark current that is suppressed by light activation of rhodopsin. To compare the properties of light responses evoked by diffuse and local illumination, 2-photon absorption was used to restrict rhodopsin activation to ~0.1 fL volume by delivering brief pulses of 1064 nm light from a diode pumped Nd:YAG laser. The small amplitude responses to attenuated laser pulses varied with the square of the light intensity and dropped off precipitously with slight changes in focus consistent with 2-photon rather than single-photon activation of rhodopsin. The activation kinetics of responses evoked by 2-photon excitation were faster than the activation kinetics of similar amplitude responses evoked by single-photon excitation using diffuse 520 nm illumination. The rising phase of the responses evoked by stronger 1064 nm pulses was markedly bitemporal, expressing a slower component that differed in time course from the initial fast component; this was not observed in the responses to intense flashes of 520 nm light. Since the focal volume of 2-photon excitation only intersects a few disks it will be possible to use this method of local illumination to probe saturation effects in the biochemical cascade as they occur in a single disk under dark and light adapted conditions.

M-Pos383

LOW TEMPERATURE SPECTROSCOPY OF A VIOLET CONE OPSIN PROTEIN. ((**Bryan W. Vought***, Barry E. Knox#, and Robert R. Birge*)) *Dept. of Chemistry, Syracuse Univ. Syracuse, NY 13244 USA and #Dept. of Mol. Bio. and Biochem., SUNY Health Science Center, Syracuse, NY 13210 USA. (Spon. by Dr. Bruce Parsons)

The violet opsin cone opsin protein (λ_{max}=425 nm) from *Xenopus laevis* has been studied by low temperature uv-vis spectroscopy. This represents the first time that an expressed S-family cone pigment has been studied at low temperatures. This violet cone opsin has 76.3% identical and 89.6% similar homology with the human blue cone (another S cone pigment). The S family of cone pigments present a problem for current theories concerning spectral tuning. Group S is the only group of pigments blue shifted from the absorption maximum of a retinal Schiff base in solution (λ_{max}=440 nm). Other mechanisms must play a role in the spectral shifting of the blue pigments. The current study probes the origin of these perturbations.

M-Pos384

CHROMOPHORE MOVEMENTS IN THE EARLY PHOTOLYSIS INTERMEDIATES OF RHODOPSIN ((S. Jäger,[¶] J. W. Lewis,[¶] T. A. Zvyaga,[§] I. Szundi,[¶] T. P. Sakmar,[§] and D. S. Kliger[¶])) [¶]Department of Chemistry and Biochemistry, University of California, Santa Cruz, CA 95064, USA; [§]The Howard Hughes Medical Institute, Laboratory of Molecular Biology and Biochemistry, Rockefeller University, 1230 York Ave., New York, New York 10021.

Rhodopsin has been selectively mutated to vary the original distance between the Schiff base proton and its counterion, Glu113. Time resolved absorption spectra of COS cell rhodopsin and the mutant pigments were used to determine the reaction schemes and spectra of their early photolysis intermediates batho, bsi and lumi. This information, along with previously obtained linear dichroism data, was used to deduce chromophore movements in the early photolysis intermediates. This study links chromophore motions to previously suggested trigger mechanisms which eventually lead to the activation of the visual pigment rhodopsin.

M-Pos385

THE EFFECTS OF OCTANOL ON THE KINETICS OF THE LATE PHOTOINTERMEDIATES OF RHODOPSIN. ((**T.L. Mah**, I. Szundi, J.W. Lewis, S. Jäger, and D.S. Kliger)) University of California, Santa Cruz, Santa Cruz, CA 95064.

At 20°C and 35°C, membrane suspensions of unperturbed rhodopsin and rhodopsin perturbed with 2.5 mM octanol are photolyzed at 477 nm and changes in absorbance are monitored at times ranging from 1 μs to 80 ms after excitation. The data is analyzed utilizing a global exponential fitting procedure followed by Singular Value Decomposition. Both fit a recently proposed model involving the photointermediate Meta-I_{380} [Thorgeirsson *et al.* 1993. *Biochemistry* 32:13861-13872.]. Comparison of the microscopic rates shows that the alcohol enhances the formation of Meta-II via Meta-I_{380}. Activation and equilibrium thermodynamic parameters obtained from Arrhenius plots suggest that octanol reduces the entropy increase in forming both Meta-I_{380} and Meta-II; it also reduces the free energy barrier between Lumi and Meta-I_{380} and between Meta-I_{480} and Meta-II. To help determine whether octanol affects the protein directly or indirectly through the lipid bilayer, similar experiments are conducted with and without octanol of rhodopsin solubilized in 0.13% dodecyl maltoside. Again, the alcohol accelerates the kinetics, suggesting that a direct protein interaction exists in addition to effects dependent on membrane free volume.

M-Pos386

HISTIDINE-166 IS A CRITICAL RESIDUE FOR BOTH ACTIVE SITE PROTON TRANSFERS AND PHOTOTAXIS SIGNALING BY SENSORY RHODOPSIN I. ((**Xue-Nong Zhang** and John L. Spudich)) Department of Microbiology & Molecular Genetics, University of Texas Health Science Center, Houston TX 77030.

Photoinduced deprotonation of the retinylidene Schiff base (SB) in the SRI-HtrI complex results in formation of the signaling state S373. Here we report identification of a residue, His166, critical to this process, as well as to reprotonation of the SB during the latter half of the SRI photocycle. Each of the residue substitutions A, D, G, S, V, or Y at position 166 greatly reduces the flash yield of S373, to values ranging from 2% of wild-type for H166Y and 23% for H166V. Accumulations of long-lived K and L-like protonated SB species are observed for H166X mutants after the flash. The yield of S373 is restored to wild-type levels in HtrI-free H166L by alkaline deprotonation of Asp76, a SB proton acceptor normally not ionized in the SRI-HtrI complex, showing that proton transfer occurs from the SB in H166L when an acceptor is made available. The flash yield and rate of decay of S373 of the mutants are pH-dependent even when complexed with HtrI, which confers pH-insensitivity to wild type SRI, suggesting partial disruption of the complex has occurred. The rates of S373 reprotonation at neutral pH are also prolonged in all H166X mutants, with half-times from 5 s to 160 s (wild type, ~ 1 s). All mutations of His166 tested profoundly alter phototaxis signaling. No response (H166D, H166L), dramatically reduced responses (H166V), or inverted responses to orange light (H166A, H166G, H166S and H166Y) or to both orange and near-UV light (H166Y) are observed. The location of His166 predicted from the bacteriorhodopsin structure (corresponding to Val177), facing away from the retinal pocket on helix F, argues against His166 as a primary proton acceptor. Our conclusion is that His166 (i) plays a role in the pathway of proton transfers both to and from the SB in the SRI-HtrI complex, and (ii) is important in phototaxis signaling. Consistent with involvement of the His imidazole moiety, addition of 10 mM imidazole to membrane suspensions containing H166A receptors accelerates S373 decay 10-fold at neutral pH, while negligible effect is seen on wild type SRI.

M-Pos387

THE FIRST AND SECOND CYTOPLASMIC LOOPS OF THE G-PROTEIN RECEPTOR, RHODOPSIN, INDEPENDENTLY FORM β-TURNS. ((Philip L. Yeagle, James L. Alderfer, Alexender C. Salloum, Laith Ali, and **Arlene D. Albert**)) Department of Biochemistry, School of Medicine and Biomedical Sciences, University at Buffalo, Buffalo, NY 14214 and Department of Biophysics, Roswell Park Cancer Institute, Buffalo, NY 14263

The cytoplasmic face of the transmembrane protein, rhodopsin, is built of one carboxyl terminal and three cytoplasmic loops connecting six of the seven transmembrane helices. Neither the high resolution, three dimensional structure of this G-protein receptor nor any other cell surface receptor is known. In this work, the structure of peptides containing the amino acid sequence of the first and second cytoplasmic loops of rhodopsin have been determined. Both loops show ordered structures in solution. In both loops the ends of the transmembrane helices unwind and form a β-turn. The conformations of the two loops are remarkably similar, even though their sequences are not. These data suggest a structural motif for short loops in transmembrane proteins. The well-ordered structures of these loops, in the absence of the transmembrane helices, indicate that the primary sequences of these loops stabilize the β-turn. These data further suggest that the loops may contribute to the folding of such membrane proteins during their synthesis and insertion into membranes.

This work was supported by National Institutes of Health Grant EY03328 and in part by CA16056.

M-Pos388

STATE-DEPENDENT DISULFIDE CROSS-LINKING IN RHODOPSIN. ((**Masahiro Kono**, Hongbo Yu, and Daniel D. Oprian)) Graduate Department of Biochemistry and Volen Center for Complex Systems, Brandeis University, Waltham, MA 02254.

Rhodopsin is perhaps the best-studied member of the G-protein coupled receptor superfamily. However, high resolutioqn structures of the inactive and active states are still lacking. Our approach to understanding better rhodopsin structure has recently focused on identifying nearby residues in its tertiary structure by expressing the protein as two complementary fragments and forming disulfide cross-links between cysteines residing on separate fragments. These cross-links are readily assayed on western blots. Cross-linked samples have electrophoretic mobilities equal to that of the full length protein under non-reducing conditions; whereas, uncross-linked samples will migrate much more rapidly.

Using this technique, we show that specific disulfide cross-links are formed in rhodopsin in a state dependent manner. A Cys in the 3rd transmembrane helix forms a disulfide bond with a Cys in the 5th helix in the dark; whereas, upon exposure to light, it forms a cross-link with cysteines in the C-terminal tail. Thus, activation of the protein involves movement of the 3rd helix relative to the 5th and 7th helices.

M-Pos389

INTERACTION OF NUCLEOSIDE DIPHOSPHATE KINASES WITH MEMBRANES OF THE BLEACHED BOVINE RETINAL ROD OUTER SEGMENTS. EFFECTS OF pH, SALTS AND GUANINE NUCLEOTIDES. ((N.Ya. Orlov* and N. Kimura**)) *Institute of Theoretical and Experimental Biophysics, Russia Acad. Sci., Pushchino, Moscow Region, 142292, Russia and **Tokyo Metropolitan Institute of Gerontology, 35-2, Sakaecho, Itabashi-ku, Tokyo-173, Japan (Spon. by A.A. Orlova)

Soluble nucleoside diphosphate (NDP) kinases (the enzyme in bovine retinal rod outer segment (ROS) preparations and rat recombinant NDP kinase) were found to exhibit pH- and salt-dependent equilibrium binding to the bleached bovine photoreceptor membranes. Bound enzymes were released by submicromolar concentration of GTP-γ-S. AppNHp was ineffective up to 50 mM. The membranes containing ROS GTP-binding protein transducin (Gt) were able to bind NDP kinases even at low membrane concentration just as GTP-γ-S prevented the binding (high-affinity, GTP-γ-S sensitive binding). In contrast, binding of the enzymes to the Gt-depleted membranes occurred only at much higher membrane concentrations and was insensitive to GTP-γ-S. Addition of purified Gt to the Gt-depleted membranes restored the high-affinity, GTP-γ-S sensitive binding of NDP kinases. The results strongly suggest that Gt is involved in the high- affinity, GTP-γS-sensitive interaction of the soluble NDP kinases with the bleached ROS membranes. The possible role of the interaction discovered in extremely rapid formation of Gt active state in living ROS is discussed.

M-Pos390

EVIDENCE FOR THE DIMERIZATION OF THE NA-CA,K EXCHANGER OF PHOTORECEPTORS ((**A. Schwarzer**, V. Hagen, P.J. Bauer)) Inst. f. Biol. Informationsverarbeitung, Forschungszentrum Jülich, D-52425 Jülich, Germany.

We have examined the previously reported association of the Na-Ca,K exchanger from bovine rod photoreceptors (Biophys. J. **68** (1995) A19) using cysteine-specific cross-linking and Western blot analysis with monoclonal antibodies. In the plasma membrane, the exchanger could be almost completely cross-linked by cupric phenanthroline mainly to a complex of apparent m.w. of 490 kDa. Minor bands were also observed at 420 kDa and 340 kDa. Cysteine-specific reagents, like N,N´-p-phenylenedimaleimide (pPDM), gave similar cross-links, but cross-linking was not complete. Neuraminidase treatment of the exchanger, followed by pPDM cross-linking resulted in a decrease in the apparent m.w. of 50 kDa for the monomer and of 85 kDa for the main cross-link. To analyse the cross-links of the exchanger, we have synthesized the cysteine-specific reagent DL-1,4-bis-maleimido-2,3-butanediol (BMBD). This compound yielded cross-links, that were stable under reductive conditions, but could readily be cleaved with $NaIO_4$. After purification, monomer and BMBD cross-linked exchanger were separated by SDS-PAGE, followed by oxidative cleavage of the cross-links and SDS-PAGE analysis of the bands. On Western blots, only exchanger-specific antibodies labeled the cleaved products of the 490 kDa complex at 250 kDa, the apparent m.w. of the monomer. Re-probing with antibodies against the cGMP-gated channel subunits gave no labeling. These results strongly suggest, that the Na-Ca,K exchanger forms dimers in the plasma membrane of rod photoreceptors. Supported by the Deutsche Forschungsgemeinschaft (Ba 721/1-1).

M-Pos391

EXCITATORY EFFECTS OF ACTIVATORS OF PKC ON RHABDOMERIC PHOTORECEPTORS. ((**Maria del Pilar Gomez** and Enrico Nasi)) Department of Physiology, Boston University School of Medicine and Marine Biological Laboratory, Woods Hole, MA.

Visual excitation in rhabdomeric photoreceptors is mediated by PLC activation and the consequent hydrolysis of PIP_2. Much attention has been devoted to IP_3 and Ca_i whereas little is known about the possible involvement of the DAG branch in the generation of the light response. We have tested the effects of several DAG surrogates in isolated *Lima* and *Pecten* photoreceptors. Extracellular application of (-)indolactam V (20-100 μM) from a holding potential of -50 mV evoked an inward current, several hundred pA in amplitude, accompanied by an increase in membrane conductance. The relatively inert stereoisomer (+)indolactam had no effect, nor did DMSO at concentrations up to five-fold higher than those used to dissolve indolactam. The phorbol ester PMA also elicited similar currents, but with greater potency (1 μM extracellular or 500 nM intracellular). Like the photocurrent, the PMA-induced current became outward at V_m =+30 mV. The DAG analog OAG dialyzed into the cytosol (50-100 μM) also caused inward currents with an abrupt onset. The induction of an increase in membrane conductance by all these compounds was accompanied by a pronounced depression of responsiveness to light. Light-activated single-channels were recorded in the rhabdomeric lobe; an increase in current fluctuations could subsequently be elicited in the dark by PKC activators applied either locally in the cell-attached mode, or by perfusion of inside-out patches after excision. Single-channel activity was obtained by application of the catalytic subunit of PKC to excised patches in the presence of ATP. Taken together, these results support the notion that the DAG branch of the PLC signalling pathway may play an important role in visual excitation, probably in synergy with IP_3-mediated Ca release. Supported by NIH grant EY07559 .

M-Pos392

ANTAGONISTS OF THE LIGHT-DEPENDENT CONDUCTANCE OF RODS BLOCK THE PHOTOCURRENT IN INVERTEBRATE CILIARY PHOTORECEPTORS. ((Enrico Nasi and **Maria del Pilar Gomez**)) Department of Physiology, Boston University School of Medicine and Marine Biological Laboratory, Woods Hole, MA.

Activation of the photocurrent in hyperpolarizing photoreceptors of the distal retina of the scallop is mediated by cGMP, the messenger substance that controls the light response in vertebrate photoreceptors. In order to ascertain whether the functional similarities between these two classes of sensory cells extend to the ion channels that underlie the receptor potential, we examined the effects of several antagonists of the light-dependent conductance of rods and cones. One of the few substances that have been found effective in rods is 3',4'-dichlorobenzamil (DCPA), an amiloride derivative. Extracellular DCPA dramatically suppressed the photocurrent in voltage-clamped ciliary photoreceptors. The effect had a sluggish onset and was rapidly reversible. Half-maximal inhibition was attained ≈5 μM. No change in photocurrent kinetics was induced by the drug, and no voltage- or use-dependence were detected. Amiloride was also inhibitory, but required ≈50-fold higher concentrations. L-*cis*-diltiazem, the best characterized blocker of cGMP-gated channels in rods, reversibly suppressed the light response in scallop ciliary photoreceptors, as well as the current elicited in the dark by direct administration of 8Br cGMP, bypassing the early steps of transduction; this suggests that its inhibitory effects are most likely at the level of the light-dependent membrane conductance. Like in vertebrate photoreceptors, the blockage by diltiazem increased with membrane depolarization regardless of whether it was applied extracellularly or intracellularly. Considering that olfactory neurons also utilize cyclic nucleotides for transduction and share a similar pharmacological profile, the present data support the notion that a kinship exists among different classes of sensory cells of ciliary origin. Supported by NIH grant EY07559.

OXIDATIVE PHOSPHORYLATION

M-Pos393

THE BINUCLEAR CHARACTER OF CUA IN CYTOCHROME *C* OXIDASE IS IMPORTANT FOR ELECTRON TRANSFER , NOT FOR PROTON PUMPING ((**Yuejun Zhen**[1], Kefei Wang[2], Denise Mills, Shelagh Ferguson-Miller[1] and Frank Millett[2])). [1]Dept. of Biochemistry, Michigan State University, East Lansing, MI. 48824; [2]Dept. of Chemistry and Biochemistry, University of Arkansas, Fayetteville, AR, 72701

CuA, located at subunit II of cytochrome *c* oxidase, is the initial electron acceptor from cytochrome *c*. Recently, its binuclear character, suggested by unusual EPR spectrum, was revealed by crystallography, but the functional significance of the binuclear center is still not clear; involvement in proton pumping had been previously suggested. Several mutants were made in the vicinity of CuA in subunit II of cytochrome *c* oxidase from *Rb.sphaeroides*. EPR spectra indicate that the CuA center was disrupted in H260N and M263L, two direct ligands, not in D214N and E157Q, two carboxyls close to CuA. Ruthenium rapid kinetic studies show that D214N and E157Q have much slower electron transfer (ET) rate from cytochrome *c* to CuA, indicating weaker binding and disruption of the cytochrome c binding site. The redox potential of CuA in H260N and M263L is about 50-80 mM more positive than that of heme *a*, contributing to inhibition of ET from CuA to heme *a*. The rate of ET from cytochrome *c* to CuA is also much slower than in wildtype.

Proton pumping assays show all the mutants still possess proton pumping activity. The mutagenesis study clear demonstrates that the binuclear character of CuA center is important in maintaining the correct redox potential for rapid electron transfer from cytochrome *c* to heme *a*, but not important for the proton pumping function.

M-Pos394

3-DIMENSIONAL STRUCTURE OF THE RAT LIVER F1-ATPASE. ((**M.A.Bianchet***, D.Medjamed*, Y.K.Ho‡, J. Hullihen‡., P. L.Pedersen‡ & L. M. Amzel*)). *Dept. of Biophysics & Biophysical Chemistry, ‡Dept. of Biological Chemistry. Johns Hopkins Medical School. Baltimore, MD 21205 (spon., L.M.A.)

F1-ATPase is the soluble part of the F1F0-ATP synthetase complex, the protein that carries out the synthesis of ATP in the mitochondria. The F1 portion by itself exhibits a Mg^{++} dependent ATP hydrolytic activity. Crystals of rat liver F1-ATPase were obtained using $(NH_4)_2SO_4$ as a precipitant in the presence of ATP, Pi and in the absence of Mg. Under the crystallization condition used, rat liver F1-ATPase is known to be active. F1 from redissolved crystals has all subunits and hydrolyzes ATP with full activity when Mg^{++} is added. The three dimensional structure of the rat liver F1-ATPase determined to 2.8 Å resolution is presented here. (A 3.6 Å map was previously reported[1]). In the rat liver F1-crystals the three α/β pairs are all in the same (or very similar) conformations as expected from the crystal symmetry. The crystal cell dimensions and symmetry indicate that its asymmetric unit contains a third of the F1 oligomer ($\alpha_3\beta_3\gamma\delta\varepsilon$)[1]. The small subunits are not observed, because they can not comply with such a symmetry requirement, suggesting that, they do not participate in crystal contacts and adopt different positions in each lattice point. (Similar disorder seem to occur in the bovine heart F1 crystals[2] in which δ, ε and part of γ are not observed either.) The nucleotides bound to both α and β subunits have been identified. The more symmetrical conformation of the α and β subunits observed in the rat liver F1 *vis-a-vis* bovine heart suggests that it may be in another stage of the proposed mechanism or perhaps suggest a different one. [Supported by NIH CA10951 + GM 25432]

1.- Bianchet et al. J. Biol. Chem. 266 , 21197-21201 (1991)
2. - Abrahams et al., Nature 370, 621-628 (1994)

M-Pos395

RAT LIVER F_0F_1-ATP SYNTHASE; OVEREXPRESSION, PURIFICATION AND RECONSTITUTION OF THE OSCP SUBUNIT ((**T. R. Golden** and P. L. Pedersen)) Johns Hopkins University School of Medicine, Department of Biological Chemistry, Baltimore, MD 21205

The F_0F_1-ATP synthase couples the energy of an electrochemical proton gradient to the synthesis of ATP. How the movement of protons through F_0 is communicated to the catalytic sites on F_1 remains the primary question in understanding the enzyme. The oligomycin sensitivity conferring protein (OSCP) is a subunit of the mitochondrial ATP synthase known to be essential for this process, making the role played by OSCP a promising starting point for investigating the coupling mechanism. To facilitate biochemical and biophysical studies of OSCP, an expression system was developed which provides pure, active OSCP in high yield. The cDNA encoding OSCP was obtained by RT-PCR from rat liver mRNA, and was cloned into the pET-25b expression vector. Upon induction, the expressed protein is found almost entirely in inclusion bodies. These are solubilized with GuHCl and the protein renatured by dialysis, resulting in 85% pure OSCP. The protein is then purified to homogeneity by ion-exchange chromatography. CD spectroscopy indicates that the pure OSCP has a highly α-helical structure. The protein is functional in reconstituting F_1 with F_1- and OSCP-depleted membranes, and forms a one-to-one complex with F_1. Current work is aimed at characterizing the interactions of OSCP with the F_1 and F_0 moieties. (Supported by NIH grant CA 10951 to PLP)

M-Pos396

TRANSIENT CHANGES OF MITOCHONDRIAL [NADH] IN CARDIAC TRABECULAE DURING PHYSIOLOGICAL CHANGES OF WORK. ((**Rolf Brandes** and Donald M. Bers)) Loyola University Chicago, IL 60153.

We have previously shown that, in intact trabeculae at ~27°C, increased average cytosolic [Ca^{2+}] and average force (~work or ATP consumption rate) caused mitochondrial [NADH] to decrease and recover (undershoot; see Fig). Upon reduction of work, an increase and relaxation (overshoot) was also seen. The magnitude of the fall (MIN) may be determined by the relation between a work-dependent decrease and a Ca^{2+}-dependent recovery mechanism. Here, we repeat our previous studies under more physiological conditions. At 37°C, Fig shows that when pacing frequency was stepwise increased from a baseline of 0.25 Hz to a higher frequency (max. 6 Hz) and back, $[NADH]_m$ under- and overshot (as seen at 27°C). However, at the same frequency, MIN was 2-3 times larger at 27°C vs. 37°C, possibly due to the lower average force at 37°C. By instead comparing MIN at the same average force, MIN was twice as large at 37°C vs. 27°C. This larger MIN at 37°C vs. 27°C may be explained by: A higher ATP consumption rate (driving a larger initial decrease) relative to a slower Ca^{2+}-dependent activation (resulting in less recovery at MIN). To summarize: $[NADH]_m$ transients also occur during physiological conditions although quantitatively different from those at 27°C.

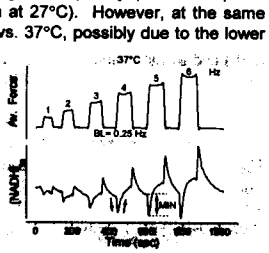

M-Pos397

MODELING HUMAN MITOCHONDRIAL DISEASE IN AN AEROBIC BACTERIUM. ((**Melyssa R. Bratton**, S. Craig Fairburn, Alicia G. Hamer, and Jonathan P. Hosler)) Dept. of Biochemistry, The University of Mississippi Medical Center, Jackson, MS 39216

Cytochrome *c* oxidase is the terminal member of the electron transport chain in mitochondria. It reduces oxygen to water while simultaneously creating a proton gradient across the inner mitochondrial membrane; the proton gradient drives the production of ATP by the ATP synthase. Four mutations in cytochrome *c* oxidase, all in conserved residues of subunit III, have been reported to cause three different mitochondrial diseases in humans. Point mutations G78S and A205T (*Rhodobacter* numbers) cause LHON, F256L causes MELAS while a short deletion of F94-F98 causes a skeletal muscle myopathy. We have introduced these mutations into the aa_3-type oxidase of *Rhodobacter sphaeroides* in order to investigate how they affect electron transfer and proton pumping. Using the *Rhodobacter* oxidase, a three subunit enzyme homologous in sequence and structure to the three-subunit core of the mammalian oxidase, we have expressed homogeneous populations of the mutant oxidases. All of the mutant enzymes can be overexpressed, appear structurally stable and retain some electron transfer activity. Studies are under way to determine the specific effects of the mutations. Since all of these disease mutations occur in subunit III, we also expect these studies to help determine the role of this subunit in oxidase function.

M-Pos398

FUNCTIONAL MYOGLOBIN ENHANCES THE AMPLITUDE OF CONTRACTIONS OF ISOLATED HEART CELLS. ((Roy L. White and Beatrice A. Wittenberg)) Temple University School of Medicine, Philadelphia, PA 19140 and Albert Einstein College of Medicine, Bronx, NY 10461.

Muscle contraction requires an adequate supply of ATP, which comes largely from oxidative phosphorylation with additional contribution from glycolysis. When glycolysis is inhibited, the rate of oxidative phosphorylation must increase to maintain ATP supply. We used a video motion edge detector to measure contraction of electrically stimulated, isolated heart cells. Heart cells can be stimulated electrically to contract at frequencies up to 5 Hz in medium equilibrated with (abundant) 50-95% O_2 and containing 3 mM Ca++, 5.4 mM glucose, 2 mM BOH butyrate, and 0.33 μM dobutamine. The magnitude of contraction of the cell is about 20% of its diastolic length and is not diminished by inhibition of glycolysis. When myoglobin (Mb) function is specifically inactivated, the contractile response is diminished reversibly in amplitude. The effect of Mb inhibition on contractile response at 4 Hz is further enhanced by inhibition of glycolysis (*See Fig.*). In the absence of functional Mb, mitochondrial NADH is increased significantly at 4 Hz, suggesting that O_2 supply to mitochondria is limited. These data show that in the absence of functional Mb, mitochondria are sufficiently O_2 limited to attenuate contractile function in cardiac myocytes. We conclude that Mb-enhanced O_2 delivery to cardiac mitochondria is essential to maintain vigorous contraction even in the presence of abundant extracellular O_2.

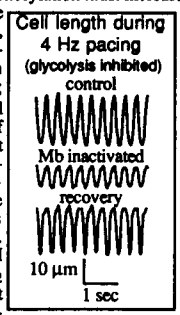

M-Pos399

OLIGOMYCIN SENSITIVITY CONFERRING PROTEIN (OSCP) OF MITOCHONDRIAL ATP SYNTHASE: OSCP-F_O INTERATIONS REQUIRE A LOCAL α-HELIX AT THE C-TERMINAL END OF THE SUBUNIT.
((**S. Joshi**, G-Jie Cao and C. Nath)) Boston Biomedical Research Institute, Boston, MA 02114 and Harvard Medical School, Boston, MA 02115.

We have reported previously that deletion mutant forms of OSCP lacking the last ten amino acid residues K181-L190 were unable to reconstitute energy linked reactions in OSCP-depleted F_1F_O complexes [Biochemistry 35, 12094, 1996]. According to the literature the sequence encompassing K181-L190 region is conserved among all mammalian species of OSCP, contains 4 charged residues and displays a high propensity to form a helix [Naturforsch Teil C. Biochem. Biophys. Biol. Virol. 46, 759, 1991]. The present studies were undertaken to clarify the role of individual amino acids in the K181-L190 region of OSCP in mitochondrial energy coupling using site-directed mutagenesis. The data show that the replacement of charged residues K181, R184, R187 and E188 by uncharged but polar glutamine, or of polar residues K181-R184 by apolar alanine, had no significant influence on the ability of mutant OSCPs to either couple energy-linked reactions, or fold into a helix. However, the substitution of residues K181-M186 by prolines led to a complete loss in the ability of resultant mutant form to complex with F_O, as well as in its potential to form a helix. Detailed analysis of the proline-mutant revealed that the altered subunit was indistinguishable from the WT form with respect to expression and gross secondary structure characteristics, immunological-properties, and most importantly in its ability to interact with the catalytic segment F_1, suggesting that the global protein structure was not destabilized. These results suggest that interactions between C-terminal end of OSCP and subunit(s) of the membrane segment have no specific requirement for basic or acidic residues, or residues with uncharged side chain, but do involve a local α-helix. Supported by NIH GM26420 and AHA 91014850.

M-Pos400

IN YEAST MITOCHONDRIA, POTASSIUM DEPLETES THE ΔΨ AND THE ΔpH WITHOUT INHIBITING THE SYNTHESIS OF ATP. ((**Vicente Castrejón**, Antonio Peña and Salvador Uribe)) Dept. of Microbiology, Institute of Cellular Physiology, Natl. University of Mexico (UNAM), Apdo Postal 70-242, 04510, México, D.F. México.

In yeast, potassium (K^+) is the most abundant cation. ATP stimulates a fast uptake of K^+ by yeast mitochondria. The permeability to protons in the presence of external ATP is inhibited by phosphate. We studied the effect of phosphate and potassium on the transmembrane potential (ΔΨ), the pH gradient (ΔpH) and the synthesis of ATP by yeast mitochondria. The additions of increasing concentrations of potassium in the presence of low concentrations of phosphate (0.4 mM) depleted the ΔΨ. An increment in the concentration of phosphate (4 mM) reversed the effects of potassium. The potential depleted by K^+ was recovered by the addition of phosphate. The addition of K^+ also provoked an decrease in the ΔpH. When the concentration of phosphate was increased (4 mM) K^+ increased the ΔpH. The synthesis of ATP with low (0.4 mM) an high (4 mM) concentration of phosphate was determined. With high concentration of phosphate, the presence of potassium incremented the synthesis of ATP, while at low phosphate the synthesis of ATP was not inhibited by the concentrations of K^+ by the concentrations of K^+ that deplete the protonmotive force. We propose the existence of a localize pool of protons which was not detected with our methods but was able to drive the synthesis of ATP.

M-Pos401

TYROSINE PHOSPHORYLATION IN INTACT CELLS STUDIED BY FT-IR SPECTROSCOPY.((M.Vivona, A.M.Villa, C.Lanzi*, R.A.Gambetta*,and **S.M.Doglia**)) Department of Physics, University of Milan, 20133 Milano (Italy), (*) Istituto Nazionale Tumori, 20133 Milano (Italy).

A new method to study tyrosine phosphorylation in intact cells by Fourier Transform Infrared Spectroscopy (FT-IR) will be presented. The FT-IR absorption spectra of tyrosine and phosphotyrosine have been studied in water solution by attenuated total reflection on an horizontal ZnSe window from 1350 to 850 cm^{-1}. Differences in the FT-IR spectra of the two aminoacids, due to the phosphates and ring vibrational modes, allowed to monitor dephosphorylation in water solution catalysed by alkaline phosphatases. This FT-IR study has been extended to the investigation of tyrosine phosphorylation and dephosphorylation in the human carcinoma cell line A431, exposed to epidermal growth factor (EGF) and to the inhibitor AG213 at different concentrations (20-200μM) High quality and well reproducible FT-IR absorption spectra from confluent cells have been obtained, with absorbance of 10^{-2} for the phosphates modes at 1150-1000 cm^{-1}. From the analysis of the FT-IR spectra it has been possible to evaluate the extent of tyrosine phosphorylation occurring in the cells in the presence of different effector molecules. A good agreement has been found in preliminary experiments between the FT-IR and the immunochemical Western blotting techniques, supporting the reliability of the new method. Although the sensitivity of Western blotting analysis is superior, the non destructive FT-IR method can be an alternative approach to study the *in situ* activity of tyrosine kinase.

M-Pos402

CARBON MONOXIDE INHIBITION IN MYOCARDIUM: IMPLICATIONS FOR A DIRECT MYOGLOBIN ROLE IN REGULATING RESPIRATION.
((Alan Glabe, Youngran Chung, Dejun Xu, and **Thomas Jue**)) Biol.Chem., UC Davis, Davis, CA 95616-8635

Observing the ^1H NMR myoglobin Val E11 signal in myocardium has presented a unique opportunity to investigate the cellular function of Mb as an oxygen storage protein, ready to compensate any oxygen deficit or as a facilitator of oxygen diffusion. Upon carbon monoxide infusion Mb function is completely inhibited. The Mb signal reflects the fractional CO saturation, since the MbO_2 Val E11 signal at -2.76 ppm gradually disappears and a new MbCO signal emerges at -2.26 ppm as pCO increases. Surprisingly, up to 80% MbCO saturation, neither the high energy phosphate level nor the oxygen consumption rate changes significantly. However contractile function has nevertheless decreased, while the lactate formation rate has increased. The CO/O_2 partition coefficient of 36 in myocardium matches closely the *in vitro* value and indicates no selective transport. The experimental observations raise provocative questions about the role of myoglobin in the cell and suggests a direct Mb role in mediating respiration.

M-Pos403

Effects of DNA Length and Coupled Conformational Changes on Binding of Cationic Oligopeptides to DNA. ((**Wentao Zhang**, Charles F. Anderson and M. Thomas Record, Jr.)) Departments of Chemistry and Biochemistry, University of Wisconsin-Madison, Madison, WI 53706.

Coulombic interactions and coupled folding affect stability and specificity of many protein-nucleic acid complexes. Previously we demonstrated the importance of the DNA polyelectrolyte character in ligand-DNA interactions by examining the large differences in the binding constant (K_{obs}) and the power dependence of K_{obs} on salt activity ($S_a K_{obs} \equiv d\ln K_{obs}/d\ln a_\pm$) for binding of an oligolysine octacation (L^{8+}) to poly dT and a short oligo dT. Here we report systematic studies of binding of L^{8+} to a series of dT-mers with different numbers of phosphate charges (Z_P) to investigate the onset of polyelectrolyte behavior with increasing DNA length. We find the magnitudes of both the site-binding free energy (ΔG°_{obs}) and $S_a K_{obs}$ increase monotonically with increasing Z_P, approaching their corresponding polymeric values as reciprocal functions of Z_P. Effects of coulombic interactions and coupled conformational changes on binding of 17-residue tetravalent (+4) alanine-lysine oligopeptides (± two central glycines) to DNA were studied by circular dichroism and fluorescence. We find the nonspecific DNA-binding of these ligands is determined primarily by the net positive charge on the oligopeptides, as indicated by the striking similarities (in [salt]-dependence and binding site size) to binding of other compact (+4) ligands. Coupled changes in the extended oligopeptide conformation (e.g. α-helix induction), which produce a compact bound state with a site size of 4 DNA phosphates, reduce K_{obs} to a small but significant extent, indicated by comparing the binding energetics of the compact and extended (+4) ligands.

M-Pos404

CONTRIBUTIONS OF NON-OPERATOR DNA TO THE STABILITY OF 1:1 and 2:1 *LAC* OPERATOR:*LAC* REPRESSOR COMPLEXES ((S. E. Melcher†, O. V. Tsodikov§, M. M. Levandoski†, D. E. Frank†, **R. M. Saecker**‡ and M. T. Record, Jr.‡†)) Program in Biophysics§ and Depts. of Biochemistry† and Chemistry‡ UW-Madison 53706

The interaction between *lac* repressor (LacI) and its specific DNA site (*lac* operator) serves as one of the key paradigms of gene regulation. To dissect the role of stoichiometry and DNA length in positioning this genetic switch, we have quantified the stability of LacI-operator complexes over a wide range of macromolecular and salt concentrations. We observe profound effects of DNA length; above 125 mM K^+ the stability of both 1:1 and 2:1 operator:LacI complexes increases with increasing DNA fragment length. However, for plasmid-length operator fragments, formation of the 2:1 complex becomes increasingly anticooperative relative to the 1:1 as [salt] decreases. We hypothesize that at low [salt], flanking non-operator sequences bind LacI by local wrapping and that distant regions of non-operator DNA occupy the second operator-binding site by looping. Here we present a semi-quantitative analysis of how the character of LacI-operator complexes changes with DNA length and [salt]. Wrapping and looping appear mainly driven by coulombic interactions but differ significantly in the number of cations displaced upon binding.

M-Pos405

ELECTROSTATIC CONTRIBUTIONS TO HEAT CAPACITY CHANGES UPON DNA BINDING. ((**K.R. Gallagher** and K.A. Sharp)) Johnson Research Foundation, Dept. of Biochemistry and Biophysics, University of Pennsylvania, Philadelphia, PA 19104.

Elucidation of the thermodynamic characteristics of binding processes is essential to understanding stability and specificity in biological complexes. Thus, it has become popular to employ calorimetric methods to determine the heat capacity change for binding events. Current interpretation of heat capacity measurements has relied on surface area models in which only nonpolar, or short-range, effects are taken into account. However, long-range electrostatic effects are known to make a large contribution to the free energy, enthalpy, and entropy of binding. The goal of this work has been to ascertain whether electrostatics play a role in heat capacity changes upon binding and to determine the magnitude of contributions arising from these effects (ΔC_p^{el}). Finite difference methods for solving the Poisson-Boltzmann equation provide a way to accurately calculate the electrostatic component of the free energy of binding (ΔG_{bind}^{el}), incorporating solvent shape, charge distribution, solvent and ionic atmosphere, from the atomic coordinates of the molecules involved. By calculating ΔG_{bind}^{el} over a range of temperatures, one can determine ΔC_p^{el} by means of a van't Hoff analysis of the free energy data. We have used this method to calculate ΔC_p^{el} for DNA binding to the drugs netropsin, lexitropsin, and dapi, as well as to the protein ligand λ repressor.

M-Pos406

INVESTIGATIONS OF DNA CONTEXT EFFECTS: INFLUENCES OF FLANKING SEQUENCE STABILITY ON SITE SPECIFIC BINDING OF *BAMHI* RESTRICTION ENZYME TO DUPLEX DNA OLIGOMERS. ((**P.V. Riccelli,** P.M. Vallone, M. J. Lane† and A.S. Benight)) Dept. of Chem. Univ. of Illinois, Chicago, IL 60607. †Dept. of Med.& Micro./Immunol.SUNY-Health Science Center at Syracuse, Syracuse, NY 13027.

Binding of BamHI restriction enzyme was investigated for short DNA duplex oligomer substrates containing the cognate site 5'-GGATCC-3' flanked on both sides by sequences of different A-T or G-C composition. Binding reactions were conducted in buffer containing 10 mM $CaCl_2$ and analyzed by gel-shift assays. While cleavage activity of the enzyme was eliminated under these conditions, site specific binding was retained. For each DNA substrate, binding isotherms were constructed and equilibrium binding constants evaluated. Binding constants greater than 10^9 M^{-1} were observed and found to vary at least 10-fold as a function of flanking sequence. Significantly higher binding of BamHI was observed for duplex substrates containing A-T flanking sequences. Optical melting curves of the DNAs were also measured in the binding buffer. From these results, the thermodynamic stabilities of the DNA substrates were evaluated. Comparisons of the results of the binding assays with those of the melting analysis revealed an inverse correlation between flanking sequence stability and binding affinity of BamHI suggesting stability of flanking DNA context may comprise a significant component of DNA recognition by site-specific binding agents.

M-Pos407

THERMODYNAMIC DISSECTION OF THE *BAMHI* ENDONUCLEASE-DNA INTERACTION. ((**L.E. Engler** and L. Jen-Jacobson)) Department of Biological Sciences, University of Pittsburgh, Pittsburgh, PA 15260, USA (Spons. by S. Gilbert)

We have measured the temperature dependence for the binding interaction of *Bam*HI endonuclease to DNA substrates containing a cognate, noncognate (one incorrect base-pair, *Bam*HI*), or nonspecific site. We find that the site-specific interaction is characterized by a large negative heat capacity change ($\Delta C^\circ_{p,obs}$), with the entropy ($T\Delta S^\circ$) and enthalpy (ΔH°) changing sign in the physiological temperature range. The nonspecific interaction is enthalpy driven (ΔH° = -7.4 kcal/mol) and shows no heat capacity change, while the *Bam*HI* site interaction is characterized by a $-\Delta C^\circ_{p,obs}$ that is smaller than the specific. Additionally, we have investigated the effects of DNA sequences flanking the cognate site, and find that flanking sequences which improve complex formation demonstrate more negative $\Delta C^\circ_{p,obs}$, more favorable ΔH°, and *less* favorable ΔS°. Isothermal titration calorimetry was used to verify the predicted heats of complex formation.

These data allow us to begin to estimate the contributions of water release and conformational factors to the overall energetics of the *Bam*HI endonuclease-DNA interaction. By comparison of ethylation interference data, and the effects of osmotic stress and salt on the binding interaction, we can begin to assess the origins of the large $\Delta C^\circ_{p,obs}$, and assign possible sources of the observed entropy changes.

M-Pos408

DNA BINDING MECHANISM OF *O6*-ALKYLGUANINE-DNA ALKYLTRANSFERASE: STOICHIOMETRY AND EFFECTS OF DNA BASE COMPOSITION AND SECONDARY STRUCTURE ON COMPLEX STABILITY. ((**M.G. Fried**, S. Kanugula, J.L. Bromberg & A.E. Pegg)) Department of Biochemistry and Molecular Biology, Penn. State University College of Medicine, Hershey, PA 17033.

O6-Alkylguanine-DNA alkyltransferase (AGT) is an important cellular defense against the mutagenic effects of DNA alkylating agents. In humans this defense can contribute to the ability of some tumors to resist the effects of chemotherapeutic agents that act through DNA alkylation. We report here studies that characterize the interaction of AGT with DNA. We show that although AGT sediments as a monomer in the absence of DNA, it binds cooperatively to single stranded deoxyribonucleotides. The stoichiometries of complexes formed with 16-, 30- and 80-base oligodeoxyribonucleotides are 3.8 ± 0.3, 5.3 ± 0.2 and 8.9 ± 0.2, respectively; the binding density decreasing from ~4nt/monomer to ~9nt/monomer as DNA length increases over this range. Binding competition assays show that DNA-affinities depend only weakly on base composition or secondary structure, although in general G+C-rich sequences are bound with greater affinity than are A+T-rich ones and single-stranded DNA is bound with greater affinity than duplex forms. These results suggest mechanisms by which AGT may search for alkylated sites and interact with them to effect DNA repair. Supported by NSF grant DMB 91-48816.

M-Pos409

INTERACTION OF SINGLE AND DOUBLE STRANDED DNA WITH BOVINE LENS ALPHA-CRYSTALLIN. ((**K. Singh**[1], B. Groth-Vasselli[1] and P. Farnsworth[1,2])) [1]Ophthalmology and [2]Pharmacology and Physiology, UMD-NJ Medical School., Newark, NJ 07103.

α-Crystallin, a major lens structural protein, is also known to have a chaperone-like function. Recently, identification of a conserved (R/K-R-X-R/K) sequence in a helix-turn-helix motif, a putative DNA binding site and ATP binding to α-crystallin suggest the possibility of additional function. The present study was designed to characterize α-crystallin/DNA binding by UV-mediated photocrosslinking. The crosslinking conditions were optimized by varying the concentration from 10-100 μM for α-crystallin, 10-80 mM KCl and 0.5-100 μM of DNA. A 37-mer self annealing template-primer and a dA_{36} polynucleotide were selected as double (ds) and single stranded (ss) DNA, respectively For crosslinking 10, 25 and 50 μM of α-crystallin and the desired concentration of DNA (1000 cpm/pM) were incubated on ice in a reaction mixture containing 10 mM phosphate buffer pH 7.3 and 10-80 mM KCl, followed by exposure to UV radiation at a dose rate of 375 mJ/cm^2. The UV-exposure at this dose results in the formation of tetramers of its subunits. The major crosslinking of dA_{36} and 37-mer with α-crystallin occurs with these tetramers. Since such crosslinking occurs only if protein binds DNA, these data show that α-crystallin binds both ss and ds DNA. Evidence for the binding of α-crystallin to both ATP and DNA suggests that α-crystallin and its subunits αA and αB have both cytoplasmic and nuclear functions which is in accord with the observation that αB translocates to the nucleus under stress.

M-Pos410

CHROMATIN DYNAMICS IN INTERPHASE NUCLEI AND ITS IMPLICATIONS FOR NUCLEAR STRUCTURE. ((Bryan Cutler[1], Misty L. Fillbach[1], **Daniel Axelrod**[2], James R. Abney[1] and Bethe A. Scalettar[1])) [1]Dept. of Physics, Lewis & Clark College, Portland, OR 97219; [2]Biophysics Research Division and Dept. of Physics, University of Michigan, Ann Arbor, MI 48109.

Chromatin dynamics in interphase nuclei of living Swiss 3T3 and HeLa cells was studied using fluorescence microscopy and fluorescence recovery after photobleaching. Chromatin was fluorescently labeled using dihydroethidium, a membrane-permeant derivative of ethidium bromide. Following labeling, a laser was used to bleach small (~ 0.8 μm diameter) spots in the euchromatin of cells of both types. These spots were observed to persist for more than one hour, implying that interphase chromatin is substantially immobile over distance scales ≥0.4 μm. Over very short times (less than one second), a partial fluorescence recovery within the spots was observed. This partial recovery is attributed to independent dye motion, based on comparison with results obtained using ethidium homodimer-1, which binds essentially irreversibly to chromatin. The immobility of interphase chromatin observed here is consistent with the idea that chromatin is bound to a nuclear matrix; these results thus provide some of the first support for the matrix model of nuclear structure obtained from studies of chromatin dynamics in living interphase cells. Supported by grants #CC3819 from Research Corporation and #BIR-9510226 (to B.A.S.) and NSF MCB-9405298 (to D.A.)

M-Pos411

CHARACTERIZATION OF BINDING OF HISTONE H1° TO DNA. ((**S.E. Wellman** and N.M. Mamoon)) Dept. of Pharmacology, Univ. MS Med. Center, Jackson, MS 39216-4505.

The interactions between the H1 histones and DNA are not well-described. Because of their role in packaging of DNA, H1 histones have been expected to bind to DNA with no sequence specificity. However, there is accumulating evidence that H1 histones do show DNA sequence preference. For example, we showed that two individual H1 variants, H1-4 and H1°, preferentially bound to one region of a 214-base-pair fragment of DNA. We have synthesized the two halves of the 214-base-pair fragment and have examined the binding of H1° to them, using thermal denaturation. We used the model of McGhee and von Hippel and the method of McGhee to simulate thermal denaturation curves. While the simulated DNA-only curve is very similar to the observed curve, thermal denaturation curves of the DNA in the presence of H1° cannot be simulated by this method. The DNA sequences are heterogeneous; however, were the binding of H1° totally non-sequence-selective, the heterogenous DNA should, as in the McGhee-von Hippel model, behave as an extended homogenous lattice with overlapping binding sites for the protein ligand. In contrast, thermal denaturation curves of a homogeneous DNA sequence, poly(dAT), in the presence of H1° are reasonably similar to simulated curves. These observations are further evidence that H1°, and most likely H1 histones in general, exhibit DNA sequence preference.

M-Pos412

PREDICTING THE FREE ENERGY OF NONSPECIFIC ASSOCIATION OF CRO REPRESSOR PROTEIN WITH B-DNA ((**Kathryn A. Thomasson**[1], Tamara Baumgartner[1], Jennifer Czlapinski[1], Thea Kaldor[1], Scott H. Northrup[2])) [1]Department of Chemistry, University of North Dakota, Grand Forks, ND 58203-9024 [2] Department of Chemistry, Tennessee Technological University, Cookeville, TN 38505

The Brownian dynamics (BD) simulation method has been employed to study the energetics of nonspecific binding of λ Cro repressor protein (Cro) to model B-DNA. BD simulates the diffusional dynamics as Cro repressor protein encounters the DNA surface and describes: (i) the steric effects of encounter between the irregular surfaces of the protein and DNA molecules based on crystallographic coordinates, and (ii) the electrostatic effects based on a finite difference numerical solution of the Poisson-Boltzmann (PB) equation. A direct calculation of the free energy and entropy of the encounter is performed by computing the potential of mean force versus the radial distance from the protein center to the DNA helix. The PB equation is solved by several different approximations: (i) the linearized form, (ii) the full nonlinear form, and (iii) the full form with periodic boundary conditions implemented. The effect of the solution to the PB equation on the predicted free energy curve shows that all three methods give qualitatively similar results, but different values for the minima. For example, using the full PB with periodic boundary conditions results in a minimum free energy of -5 kcal/mol; whereas, using the linearized PB results in a minimum at -7 kcal/mol. Using the free energy profile of nonspecific docking and assuming free one-dimensional lateral diffusion (sliding) of docked pairs, we can estimate the lifetime of a nonspecifically docked state to be 5 μsec. Thus, the protein should be able to slide laterally about 100 base pairs before becoming detached.

M-Pos413

EVIDENCE FOR ELECTROSTATIC CONTRIBUTIONS TO THE INTERACTION BETWEEN DNA, WILD TYPE TRP REPRESSOR PROTEIN, AND TWO SUPER-REPRESSOR MUTANTS

((**Martha P. Brown**, Adeola Grillo, and Catherine A. Royer))
University of Wisconsin at Madison, School of Pharmacy, Madison, WI 53706

In *Escherichia coli* aromatic amino acid synthesis is regulated by the thermodynamic linkage of multiple equilibria involving the trp repressor protein (protein-protein, protein-corepressor, and protein-specific and non-specific DNA interactions). Several single site mutants of the tryptophan repressor protein (TR), among them the super-repressor mutants AV77 and EK18, have proven useful in dissecting out the structural basis of the energetics of this complicated system. The electrostatic contribution to the coupled protein-DNA and protein-protein equilibria are investigated here by determining the effect of salt on the specific interaction between wild type TR, the two super-repressor mutants, and two oligonucleotides containing the 5'-GNACTNNNNNNNNTCATG-3' sequence proposed to confer sequence specificity in the TR-DNA binding event. The shorter target is a 20mer which carries a 5'-fluorescein covalently linked to the terminal phosphate through a thiol bond. The second target is a 36mer bearing a 5'-rhodamine label linked through a 6-carbon tether for which the sequences flanking the target site were designed to disfavor tandem binding of two or more repressor dimers. The fluorescence intensity and anisotropy of these two fluorophores were monitored. Titrations were performed at salt concentrations ranging from 0 to 500mM, and revealed a strong salt dependence of wild type TR binding to both DNA sequences, whereas the binding of the mutants showed a strong salt dependence for the 20mer, but not the 36mer.

M-Pos414

A FLUORESCENCE STUDY OF THE *Escherichia coli* GALACTOSE REPRESSOR-DNA INTERACTION

((**K. Wang**[1], M.E. Rodgers[2], V. Munsen[2], D. Toptygin[2] and L. Brand[2])) Department of Chemistry[1] and Department of Biology[2], Johns Hopkins University, Baltimore, MD 21218.

The interaction between a fluorescently labeled 33 bp oligonucleotide containing the O_E site of *E. coli* galactose operon and the galactose repressor (galR) as well as the effect of D-galactose on the DNA-protein complex have been studied by steady state fluorescence anisotropy and intensity measurements. An amino-modified C6 dT nucleotide replaced a thymidine residue at an internal position of the O_E site and was labeled with fluorescein-5-isothiocyanate (FITC). The labeled single strand was hybridized with unlabeled complimentary strand to form FITC-labeled 33 bp O_E DNA. Fluorescence measurements were used to characterize the equilibrium binding of FITC-labeled 33 bp O_E DNA with galR and to examine the effect of D-galactose on the DNA-galR complex. The program SPECTRABIND was used to fit all anisotropy and intensity data simultaneously. Assuming a model of two equal and independent binding sites for D-galactose to galR, the equilibrium dissociation constant for galactose binding was 8.6 μM and the K_d of galR to FITC-33 bp O_E DNA was 83 nM. Other models were also analyzed. Experiments were performed in a buffer containing 300 mM KCl, 25 mM KH_2PO_4-K_2HPO_4 (pH 7.4), 1mM $MgCl_2$, 0.02% (w/v) NaN_3. (Supported by NIH grant GM-11632)

M-Pos415

THIOL REACTIVITY AND FLUORESCENCE CHARACTERIZATION OF SITE-DIRECTED MUTANTS OF THE *E. coli* GALACTOSE REPRESSOR

((**M.E. Rodgers**, F. Moshiri, V. Munsen, K. Wang and L. Brand)) Department of Biology, Johns Hopkins University, Baltimore, MD 21218

Cysteine residues are prime targets for attachment of spectroscopic labels in proteins. The proposed galactose repressor (galR) structure (Hsieh, *et al.*(1994) J. Biol. Chem. 269, 13825-35) shows C116 is close to the DNA binding domain and the most solvent exposed; C155 is near the galactose binding site and less exposed; the remaining two cysteines are essentially buried. Specific labeling at one or the other of these sites should provide spectroscopic signals that are sensitive to either galactose binding or DNA binding. To this end, site directed mutants were constructed wherein cysteine is replaced by serine at positions 116, 155 or both.

DTNB titrations of native galR show that several thiols react at various rates. Similar titration of C116S and C155S were performed and their reaction curves sum to equal that of the wild type. The reaction of C155S can be described by the sum of two first order rate processes of nearly equal amplitude with rate constants differing by a factor of about 5. Results also show C116S reacts substantially slower than C155S. The reactivity of both of these mutants is sensitive to galactose. Galactose binding to the mutants has been characterized by tryptophan fluorescence and compared to wild type. In each case, cooperative binding is observed with K_d's = 24.9, 26.7 and 11.2 μM and Hill coefs. = 1.7, 1.5 and 1.4 for wild type, C116S and C155S respectively. (Supported by NIH grant GM-11632)

M-Pos416

OPERATOR AND COREPRESSOR BINDING ACTIVITES OF PURINE REPRESSOR BY THERMODYNAMIC AND KINETIC STUDIES

((**Han Xu and Kathleen Matthews**))Department of Biochemistry and Cell Biology, Rice University, Houston TX, 77251.

Lac repressor (LacI) and purine repressor (PurR) are both members of the lacI family of genetic regulatory proteins and share significant amino acid sequence similarity and tertiary structure. However, these two proteins regulate expression of genes involved in metabolic pathways with divergent aims, one catabolic and the other anabolic. LacI binding to *lac* operator to repress the transcription of genes encoding the enzymes involved in the transport and catabolism of lactose is diminished by the binding of inducer, *e.g.*, allolactose or IPTG. In contrast, PurR, which serves as a master regulator of purine and pyrimidine biosynthesis, requires the binding of a corepressor (*e.g.*, guanine or hypoxanthine) to acquire the proper conformation for DNA binding. The divergent metabolic functions of the regulated gene products as well as the distinct effects of ligand binding on DNA affinity suggest that LacI and PurR may differ in both DNA and ligand binding parameters. Thermodynamic and kinetic studies are performed to characterize these properties of PurR. *In vitro* analysis of PurR-guanine binding in the presence or absence of operator suggests that operator DNA has a significant effect on PurR-guanine binding. Similarly, guanine affects PurR-operator binding. These results can be rationalized in terms of the metabolic function of the regulated enzymes.

M-Pos417

FLUORESCENCE STUDIES OF INTERACTIONS OF WHEAT GERM INITIATION FACTORS WITH POLY(A)-BINDING PROTEIN.

((**C.-C. Wei**[1], **M.L. Balasta**[1], H. Le[3], R.L. Tanguay[3], K.S. Browning[2], D.R. Gallie[3], **D.J. Goss***[1])) [1]Department of Chemistry, Hunter College of the City University of New York, New York, NY 10021, [2]Department of Chemistry and Biochemistry, University of Texas-Austin, Austin, TX 78712, [3]Department of Biochemistry, University of California, Riverside, CA 92521.

Most eukaryotic mRNAs contain a 5' m^7GpppG cap structure and a 3' poly(A) tail, which synergistically increase protein translational efficiency. The communication between both ends of mRNA, in conjugation with their associated proteins, may plays an important role during translation although no direct interaction has been demonstrated. A cap-associated initiation factor (eIF), eIF-4B, and cap-binding proteins, eIF-4F and eIF-(iso)4F, were found to interact with poly(A)-binding protein (PABP) in the presence and absence of poly(A) by Western blotting. The binding of wheat germ PABP to the eIFs was measured by direct fluorescence titration techniques. An analysis of the equilibrium constants (K_{eq}) also demonstrates that eIF-4B, eIF-4F, and eIF-(iso)4F have high binding affinities to PABP. The K_{eq} of eIF-4B to PABP is on the order of 10^8, which is 10-fold stronger than that of eIF-(iso)4F or eIF-4F. To investigate the interaction of these protein complexes with the cap and poly(A), a cap analog, anthraniloyl-m^7GTP (Ant-m^7GTP), and a fluorescently labeled poly(A) were utilized to investigate this system using steady-state, anisotropy, and lifetime fluorescence measurements.

M-Pos418

CHARACTERIZATION OF MAX AND OLIGONUCLEOTIDE INTERACTION BY FLUORESCENCE SPECTROSCOPY.

((**M. Huang, M.L. Balasta**, S.K. Burley[#] and **D.J. Goss**)) Chem. Dept., Hunter College, CUNY, NY, NY 10021; [#]Laboratories of Molecular Biophysics & Howard Hughes Medical Institute, The Rockefeller University, 1230 York Avenue, NY, NY 10016

Max is a b/HLH/Z (basic-helix-loop-helix-leucine zipper) protein that hetero-oligomerizes with two other b/HLH/Z proteins, Myc and Mad, enabling them to bind DNA under physiological conditions. Max also readily homodimerizes and binds DNA with high affinity. These proteins specifically recognize and bind to a DNA sequence 5'CACGTG 3', termed an E-box. The Myc-Max heterodimer is an activator and triggers cell malignant transformation. Max homodimer and Mad-Max heterodimer function as repressors. Direct fluorescence anisotropy titration measurements were used to characterize the binding of Max to oligonucleotides and Max dimer/tetramer formation. Utilizing fluorescently labeled oligonucleotides as well as fluorescently labeled protein allowed determination of the protein dimer-tetramer equilibrium and the dimer-oligonucleotide equilibrium. An equilibrium constant K_{eq} of ~200 nm was obtained for the dimer-tetramer equilibrium. The Max homodimer bound to the E-box containing oligonucleotides with a K_{eq} of ~4.26 nM. Further data analysis reveals that Max binds oligonucleotides as a tetramer as well.

M-Pos419

E.coli UvrD (HELICASE II) UNWINDS DUPLEX DNA WITH A STEP-SIZE OF ~ FIVE BASE PAIRS

((**Janid A. Ali** and Timothy M. Lohman)) Department of Biochemistry and Molecular Biophysics, Washington University School of Medicine, 660 S.Euclid Ave., Box 8231, St. Louis, MO 63110

The E. coli UvrD helicase (Helicase II) functions to unwind DNA during nucleotide excision repair and methyl-directed mismatch repair. Using rapid chemical quenched-flow techniques we have examined the unwinding kinetics of a series of short oligodeoxynucleotides with duplex regions ranging from 10-40 base pairs and possessing a flanking 3'-single stranded DNA (dT_{40}). Under single turnover conditions, a distinct lag phase precedes the unwinding of each DNA substrate reflecting the presence of partially unwound DNA intermediates along the pathway to fully unwound DNA. The lag phase increases with increasing duplex length reflecting an increase in the number of "steps" required by UvrD to unwind duplexes of increasing length. Analysis of these unwinding kinetics indicates that the UvrD helicase unwinds duplex DNA in steps of 4-5 bp (~one-half turn of B-form DNA). These results suggest that the dimeric UvrD helicase unwinds DNA by an active, rolling mechanism through direct interactions of alternating subunits with the duplex DNA.

M-Pos420

ATP HYDROLYSIS STIMULATES BINDING AND RELEASE OF SINGLE STRANDED DNA FROM ALTERNATING SUBUNITS OF THE DIMERIC *E. COLI* REP HELICASE.

((**Keith P. Bjornson**, Isaac Wong and Timothy M. Lohman)) Department of Biochemistry and Molecular Biophysics, Box 8231 Washington University School of Medicine 660 S. Euclid Ave. St. Louis, MO 63110

In the process of unwinding duplex DNA processively, DNA helicases must also translocate along the DNA filament. To probe the mechanism of ATP-driven translocation by the dimeric *E. coli* Rep helicase along single stranded (ss) DNA, we examined the effects of ATP on the dissociation kinetics of ss DNA from the Rep dimer. Stopped-flow experiments show that the dissociation rate of a fluorescent ss-oligodeoxynucleotide bound to one subunit of the dimeric Rep helicase is stimulated by ss-DNA binding to the other subunit, and that the rate of this ss-DNA exchange reaction is further stimulated ~60-fold on hydrolysis of ATP. This ss-DNA exchange process occurs via an intermediate in which both subunits of the Rep dimer are transiently bound to ss-DNA. These results suggest a subunit switching mechanism for processive translocation of the Rep helicase along ss-DNA where the role of ATP hydrolysis is to interconvert the tight and weak DNA binding sites on the Rep dimer. Such a mechanism requires the extreme negative cooperativity for DNA binding to the second subunit of the Rep dimer, which insures that the doubly DNA-ligated Rep (P_2S_2) dimer is formed only transiently and relaxes back to the singly-ligated Rep (P_2S) dimer. The fact that other oligomeric DNA helicases share many functional features with the dimeric Rep helicase suggests that similar mechanisms for translocation and DNA unwinding may apply to dimeric and hexameric DNA helicases.

M-Pos421

A TWP-SITE MECHANISM FOR ATP HYDROLYSIS BY THE ASYMMETRIC REP DIMER AS REVEALED BY SITE-SPECIFIC INHIBITION WITH ADP-ALF$_4$. ((**I. Wong** and T. M. Lohman)) Washington University School of Medicine, St. Louis, MO 63110. (Spon. By P. S. Ho)

The *E. coli* Rep Helicase, a dimeric motor protein, catalyzes the transient unwinding of duplex DNA to form ss-DNA using energy from the binding and hydrolysis of ATP. We have used pre-steady state methods to study the kinetics of ATP binding and hydrolysis by the asymmetric Rep dimer state, P_2S, an important intermediate in the unwinding reaction, to understand this mechanism of energy transduction. In order to differentiate between the two ATPase active sites in the dimer, we constructed dimers with one subunit covalently crosslinked to ss-DNA and where one or the other of the ATPase sites was selectively complexed to the tightly bound transition state analog ADP-AlF$_4$. When ADP-AlF$_4$ is bound to the Rep subunit in *trans* from the subunit bound to ss-DNA, native steady-state ATPase activity of 18 s^{-1} per dimer was recovered. However, when the ADP-AlF$_4$ and ss-DNA are both bound to the same subunit (*cis*), then a titratable burst of ATP hydrolysis is observed corresponding to a single-turnover of ATP. Using rapid chemical quenched-flow techniques we resolved the a minimal mechanism for ATP hydrolysis by the unligated Rep subunit of the *cis* dimer which quantitatively accounted for all the data. A salient feature of this mechanism is the presence of a kinetically trapped long-lived tight nucleotide binding conformation, E', in which ATP and ADP-P$_i$ are in rapid equilibrium, K_{int} =4. In the context of our "subunit switching" model for Rep dimer translocation during processive DNA unwinding [Bjornson, K. B., Wong, I. & Lohman, T. M. (1996) *J. Mol. Biol.* in press], this state may serve an energy storage function, allowing the energy from the binding and hydrolysis of ATP to be harnessed and held in reserve for DNA unwinding.

M-Pos422

ACTIVATION OF RIBONUCLEASE L.

((**James L. Cole**, Steven S. Carroll, Elaine S. Blue, Tracy E. Viscount and Lawrence C. Kuo)) Department of Antiviral Research, Merck Research Laboratories, West Point, PA 19486.

Ribonuclease L (RNase L) is an enzyme involved in the interferon pathway. The enzyme is activated upon binding of adenosine oligomers linked 2' to 5' to hydrolyze viral and cellular RNAs. Our model for activation of RNase L is depicted below. Each RNase L monomer (**E**) binds one activator (**A**) and **EA** dimerizes to form the active **E$_2$A$_2$** species; however, **E** is not able to dimerize. Activation is thus governed by two equilibrium constants: K_A and K_D. These equilibria were characterized using sedimentation equilibrium and fluorescence anisotropy measurements. Sedimentation equilibrium data obtained at several activator concentrations were analyzed using a global fitting algorithm. For the activator 5'-HO-2'-5'-A$_3$ K_A =1.7 μM and K_D = 18 nM. Activators containing a free 2'-NH$_2$ moiety were conjugated to reactive fluorophores and were found to activate RNAse L. For the conjugate of 5'-HO-2'-5'-A$_3$-2'-NH$_2$ and 7-hydroxycoumarin-3-carboxylic acid the anisotropy increased from 0.05 for the free probe to 0.32 upon binding to RNAse L. RNase L titrations were performed at several activator concentrations and were fit to obtain K_A = 1.3 μM and K_D = 1.1 nM.

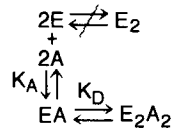

M-Pos423

A NOVEL KINETIC MECHANISM FOR THE CLEAVAGE OF PLASMID DNA BY THE RESTRICTION ENZYME EcoRV ACCOUNTS FOR NONSPECIFIC BINDING. ((J.R. Wenner and V.A. Bloomfield)) Dept. of Biochemistry, University of Minnesota, St. Paul, MN 55108 (Spon. by M. Gulotta)

The cleavage of pBR322 by the restriction enzyme EcoRV was assayed by quantifying DNA bands on agarose gels. The nonlinear reaction kinetics were fit by the mechanism:

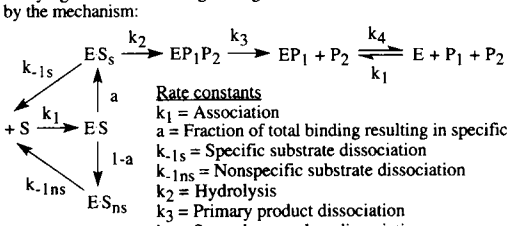

Rate constants
k_1 = Association
a = Fraction of total binding resulting in specific binding
k_{-1s} = Specific substrate dissociation
k_{-1ns} = Nonspecific substrate dissociation
k_2 = Hydrolysis
k_3 = Primary product dissociation
k_4 = Secondary product dissociation

Good fits were obtained only if nonspecific binding and slow product release were included. A key parameter is the fraction of total binding that results in specific binding. EcoRV must cycle through the nonspecific binding process a number of times before the specific site is located. This kinetic picture will be used to measure how macromolecular crowding with inert agents affects the rate at which EcoRV finds its specific cleavage site.

M-Pos424

THE CONFORMATION OF (CG) DNA SEGMENTS REGULATES RNA POLYMERASE ACTIVITY. (V. Ramsauer, L. Aguilar, M. Ballester, R. D. Sheardy & S. A. Winkle) Departments of Chemistry, Florida International University, Miami, FL 33199 and Seton Hall University, South Orange, NJ 07079.

Restriction enzyme inhibition assays in our laboratory have suggested that restriction enzymes, drugs such as 1,4-bis(((di(aminoethyl)amino)ethyl)amino)anthracene-9,10-dione (Spider) and actinomycin as well as RNA polymerases bind at or near junctions between (CG)$_n$ DNA segments and flanking sequences. The presence of such (CG) segments alters the activity of enzymes working near these segments. In this paper we present the results of RNA polymerase activity assays on DNA molecules possessing (CG)$_8$ downstream of both T7 and SP6 promoter sites. When the(CG)$_8$ is in a right handed conformation, both T7 and SP6 RNA polymerase activities are *enhanced* relative to control DNA not containing the (CG)$_8$ segment. When the (CG)$_8$ segment is left-handed, both T7 and SP6 polymerases *are completely shut off* relative to control sequences. These results suggest that the conformational switching ability of (CG) segments serves as a regulatory function for DNA. Actinomycin D and Spider, which bind at or near (CG) segments, alter the observed activities of T7 and SP6 polymerases on DNA possessing the (CG)$_8$. Molecules such as (phenanthroline) Ruthenium(II) and ametantrone, which do not show such binding selectivity, do not effect alterations in RNA polymerase activity. (This work supported by PHS MBRS 08205 (SAW))

M-Pos425

DISTINGUISHING DIFFERENT MODES OF DNA:PROTEIN BINDING BY RAMAN SPECTROSCOPY: SIGNATURES OF SPECIFIC AND NONSPECIFIC RECOGNITION. ((**J.M. Benevides** and G.J. Thomas, Jr.)) School of Biological Sciences, University of Missouri, Kansas City, MO 64110.

The repertoire of structural motifs utilized by proteins in nucleic acid recognition and binding has expanded greatly in recent years. Although high-resolution crystal and solution structures of specific protein:DNA complexes reveal complex networks of hydrogen bonding, hydrophobic and electrostatic interactions, the general principles underlying binding specificity and affinity remain largely unresolved. Nonspecific DNA recognition is also poorly understood, and insights into relevant mechanisms are hindered further by the unavailability of high-resolution structural information. To address these issues we have undertaken a comparative analysis of the Raman spectra of several classes of DNA-binding proteins in complexes with DNA. The Raman signature of the DNA ligand has also been examined in the complexes. Included in this analysis are specific major-groove binding proteins (phage λ and phage D108 repressors), a specific minor-groove binding protein (hSRY), a telomere binding protein, and a nonspecific single-stranded DNA binding protein (phage Ff gene-V protein). We find that nonspecific binding is accomplished with minimal perturbation to secondary structures of the protein subunit and DNA binding site. This contrasts sharply with major- and minor-groove binding proteins, which undergo substantial and different secondary structural changes upon DNA binding and strongly perturb the conformation of the DNA ligand. Implications for use of Raman spectroscopy as a discriminant of specific and nonspecific protein:DNA recognition will be considered. [NIH Grant GM54378.]

M-Pos426

HIV-1 NUCLEOCAPSID (NC) PROTEIN p7 EXHIBITS SPECIFIC NUCLEIC ACID BINDING. ((M.A. Urbaneja, **J.R. Casas-Finet**, R.J. Fisher, A. Rein, S. Bladen, M. Fivash, R.J. Gorelick, B.P. Kane, L.O. Arthur, and L.E. Henderson)) AVP and PCL, SAIC Frederick; DMS; and ABL-BRP, NCI-FCRDC, Frederick, MD 21702. (Spon. by J.R. Casas-Finet)

Retroviral NC proteins have conserved sequences (zinc fingers) of 14 amino acids with 4 invariant residues (CCHC) that coordinate Zn(II), and are encoded as part of a polyprotein Gag precursor that binds and packages genomic RNA during viral assembly. The stoichiometry and binding affinity of NC proteins for homo- and hetero-polymeric DNA lattices was measured by fluorescence and surface plasmon resonance spectroscopy. Earlier, a 9-base region (GACTTGTGG) with high affinity for p7 was identified in a 28-mer DNA oligonucleotide. 9-mer oligos required TGTG for tight binding, and exceeded the affinity of p7 for d(G)$_8$ or d(T)$_8$. This result strongly suggests a sequence recognition component in the binding process. p7 binding to d(TG)$_n$ (n = 2, 3, 4, 5) was characterized thermodynamically. p7 bound 2 d(TG)$_2$ oligos with μM K_d, whereas d(TG)$_3$ or d(TG)$_4$ bound with 1:1 stoichiometry and 30-fold higher affinity (p7 occluded binding site size is *ca.* 7 bases). Two p7 molecules bound to d(TG)$_5$, suggesting an interactive site size of at least 5 bases. Thus, d(GTGTG) or d(TGTGT) showed a 1 oligo:p7 stoichiometry and enhanced affinity, relative to d(TG)$_5$. The alternating-base octanucleotides d(GA)$_4$ and d(TT)$_4$ were compared with d(TG)$_4$ in their p7 binding properties. d(TT)$_4$ and d(TG)$_4$, but not d(GA)$_4$, showed an increase (10- and 145-fold, resp.) in binding affinity in the standard state (1 M NaCl), compared to the mean value for their constituent homopolymeric octanucleotides. The dominant hydrophobic character of complex formation and the near-total Trp fluorescence quenching of bound p7 stem from a stacked conformation of the indole ring with nucleobases. We attribute the difference in ΔG° between d(TT)$_4$ and d(TG)$_4$ to the presence in G of an H-bonding amino group. Aromatic intercalation and hydrogen bonding can impart p7 with sequence discrimination toward nucleic acids. The ionic dependence of ΔG was similar for all alternating-base oligos, as expected from the mild dependence of DNA counterion density on sequence. p7 mutants carrying swapped or duplicated zinc fingers (p7(2.1), p7(1.1), p7(2.2)) or modified metal cluster sequences (CCHH or CCCC) bound d(TG)$_4$ with 1:1 stoichiometry but affinity reduced by 1-3 orders of magnitude at near-physiological conditions (150 mM NaCl, pH 7.0); the affinity for the homopolymer poly(εA), however, was similar to that of wt p7 or showed only a modest reduction. In conclusion, p7 exhibits a clear preference among related nucleic acid sequences. p7 mutations severely impair binding to a specific sequence, but do not greatly affect non-specific binding. These results support the requirement for sequence and context conservation of retroviral zinc fingers, and can be compared with earlier findings showing loss of viral infectivity and RNA packaging for mutations altering the zinc fingers.

M-Pos427

A GENERAL METHOD OF ANALYSIS OF LIGAND BINDING TO COMPETING MACROMOLECULES USING THE SPECTROSCOPIC SIGNAL ORIGINATING FROM A REFERENCE MACROMOLECULE. APPLICATION TO PROTEIN - NUCLEIC ACID INTERACTIONS. ((Maria J. Jezewska & Wlodzimierz Bujalowski)) Department of Human Biological Chemistry & Genetics, The University of Texas Medical Branch at Galveston, Galveston, Texas, 77555-1053.

Quantitative analyses of protein-nucleic acid interactions in solution are greatly facilitated if the formation of the complex is accompanied by a large spectroscopic signal change. However, there are many instances when protein-nucleic acid interactions do not induce adequate changes in their spectroscopic properties. We describe the theoretical and experimental aspects of a general method to analyze such interactions. The method is based on quantitative titrations of a reference nucleic acid, with the protein in the presence of a competing nucleic acid, whose interaction parameters with the protein are to be determined. The Macromolecule Competition Titration (MCT) method allows for the determination of the absolute average binding density and the free ligand concentration over a large binding density range, unavailable by other methods, and construction of a model-independent true binding isotherm; this determination is independent of *a priori* knowledge of the binding characteristics of the protein to the reference nucleic acid. As a reference, the polymer nucleic acid, as well as short oligomers, can be used. To analyze simultaneous binding of a ligand to different competing nucleic acid lattices, we introduced the combined application of the McGhee-von Hippel and the Epstein theories for the binding of a large ligand to a homogeneous nucleic acid. Our approach allows one to perform a direct fit of the entire experimental isotherm for the protein binding to two competing nucleic acids, without resorting to complex numerical calculations.

M-Pos428

CORRELATING DNA-PROTEIN BINDING ENERGIES AND WATER RELEASE. ((**N.Yu. Sidorova*** and D.C. Rau)) LSB/DCRT* and ODIR/NIDDK, NIH, Bethesda, MD 20892

Crystal structures of many specific DNA-protein complexes show that direct DNA-protein contacts mostly replace DNA-water and protein-water interactions with little or no water left at the interface. Nonspecific complexes seem to retain a full hydration layer on the DNA and protein surfaces. Differences in the number of water molecules between different complexes can be detemined from the dependence of comparative binding constants on bulk water activity, controlled by the concentration of added solutes such as betaine, sucrose or glycerol. Two different systems, restriction enzyme EcoRI and λ *cro* protein are chosen for measuring the dependence of the binding energy to DNA on water activity. EcoRI-DNA is incredibly specific system. Changing a single base pair of the recognition sequence ('star' site) essentially destroys specific binding. At low osmotic pressures both nonspecific and the 'star' complexes retain about the same number of waters. At high osmotic pressures these waters are seen removed in the 'star', but not in the nonspecific complex. *cro* protein system shows smooth variation of binding constants to different sequences from specific to nonspecific. Water release accompanying *cro* protein binding to different operator sequences are measured at low osmotic stress and correlated directly with binding energies. The link between energy and water release is important for understanding the physics of molecular recognition.

M-Pos429

DIFFERENTIAL WATER RELEASE IN DNA BINDING BY ULTRABITHORAX AND DEFORMED HOMEODOMAINS OF *Drosophila melanogaster*. ((**Likun Li**, Doris von Kessler, Philip A. Beachy, and Kathleen S. Matthews)) Department of Biochemistry & Cell Biology, Rice University, Houston, Texas 77251, and Department of Molecular Biology and Genetics, Howard Hughes Medical Institute, The Johns Hopkins University School of Medicine, Baltimore, Maryland 21205

The amino acid sequences of the homeodomains (HD) within the Ultrabithorax (Ubx) and Deformed (Dfd) proteins from *Drosophila melanogaster* are highly conserved despite distinct genetic regulatory functions for these proteins in embryonic development. We reported recently that Ubx-HD binding to a single target site displayed significantly increased affinity and greater salt concentration dependence at lower pH; in contrast, Dfd-HD did not show pH dependence in its DNA binding properties (Li *et al.* (1996) *Biochem. 35*, 9832-9839). We demonstrate in the present study that water activity differentially affects Ubx-HD and Dfd-HD DNA binding affinity. The sensitivity of the protein-DNA binding constant to osmotic pressures generated by neutral solutes was measured, and the formation of Ubx-HD-DNA complex is associated with significantly greater water release than that of Dfd-HD-DNA complex. No influence of pH on water release was detected for either HD. Experiments with chimeric Ubx-Dfd homeodomains demonstrated that the C-terminal region of the Ubx-HD is the primary determinant for the greater water release associated with DNA binding for this protein. The magnitude of water release associated with protein-DNA binding for Ubx-HD and the chimeric HD, UDU, is also influenced to a minor extent by DNA sequence.

M-Pos430

CHARACTERIZATION OF WATER AT THE WATER–MEDIATED INVARIANT ASPARAGINE 51 DNA CONTACT OF THE vnd/NK–2 HOMEODOMAIN BY NMR

((**J. M. Gruschus**,[1] D. H. H. Tsao,[1] L.–H. Wang,[2] M. Nirenberg[2] & J. A. Ferretti[1])) [1]Lab. of Biophys. Chem., [2]Lab of Biochem. Genetics, NHLBI, NIH, Bethesda MD 20892

The homedomain is a highly conserved DNA–binding doman of approximately 60 amino acids residues that is found in many proteins known to specify positional information and segmental identity in the commitment of embryonic cells to specific developmental pathways. While different homeodomains have different DNA sequence binding specificities, the interaction of the invariant N51 homeodomain residue with an adenine always present in the consensus DNA binding sites constitutes the most highly specific contact in their sequence specific binding. X–ray structures of homeodomain/DNA crystals have shown a well–ordered interaction between N51 and adenine involving two hydrogen bonds. In contrast, NMR studies of the Antennapedia and vnd/NK–2 homeodomain/DNA complexes in solution have shown that the environment of N51 is disordered on the NMR timescale. Bound water plays a central role in this disorder, and in a series of multi–dimensional NMR experiments, the behavior of the bound water is characterized.

M-Pos431

INHIBITION OF ZINC FINGERS BY TRANSITION METAL COMPLEXES: MECHANISMS AND SPECIFICITY ((**A.Y. Louie**, T.J. Meade)) Department of Biology, Beckman Institute, California Institute of Technology, Pasadena CA 91125.

It has been shown that transition metal chelates are effective and irreversible enzyme inhibitors. These complexes have strong affinity for nitrogen donors and are believed to act by irreversibly binding to histidine residues in the active site of enzymes. These complexes should also interact with histidines in zinc fingers and we have previously evaluated the effects of these cobalt chelate complexes on human transcription factor Sp1 (which contains three CCHH zinc finger sequences) and a synthetic retroviral zinc finger peptide (CCHC type). Cobalt complex effectively inhibited DNA binding by Sp1 and disrupted the structure of the synthetic zinc finger peptide as shown by gel shift, circular dichroism and NMR[1].

Disruption of DNA-binding represents a new approach for therapeutics. Zinc finger proteins have been implicated in a number of types of cancer[2,3] In HIV, binding of the zinc finger nucleocapsid protein to a specific RNA sequence (psi) has been shown to be essential for viral packaging. Nucleocapsid protein contains a "non classical" CCHC sequence which is highly conserved among different strains of HIV but is rare in eukaryotic proteins, and thus, is an attractive target for therapeutics.

Inhibition by the cobalt complexes, however, is nondiscriminatory--any accessible histidine can be bound. Because zinc fingers manifest strong affinities for particular consensus sequences, we sought to specifically inhibit particular zinc finger proteins by conjugating the cobalt complexes to such oligonucleotides. We here show that these conjugates can inhibit specifically. In addition, we delve further into the mechanism of the inhibition to demonstrate that cobalt complexes bind covalently to zinc fingers and that binding results in ejection of zinc from the zinc finger proteins.

1. A.Y. Louie, T.J. Meade (1995) American Society for Cell Biology #.H112, Washington D.C..
2. N. Tommerup, H. Vissing: (1995) Genomics 27(2):259-264.
3. G.F. Barnard, R.J. Staniunas, M. Puder, G.D. Steele, L.B. Chen: (1994) Biochim. Biophys. ACTA:Gene Struc. and Expr. 1218(3):425-428.

M-Pos432

MOLECULAR DYNAMICS SIMULATIONS OF A CONSENSUS SEQUENCE BASED ZINC FINGER ((**T.B. Woolf** and J. M. Berg)) Depts of Physiol & of Biophysics & Biophys Chem., Johns Hopkins Univ, Baltimore, MD 21205 (Spon. by B. Agnew)

The Berg lab recently determined a 2.2 Å resolution x-ray structure of a consensus sequence based three domain zinc finger DNA complex (Nature Struc. Biol., in press). Molecular dynamics computer calculations of the complex, the oligonucleotide, and the zinc-finger are described based on the new structure. The solvation environment consists of water and counterions for each simulation to a total of 25,000 atoms in a spherical droplet of 40 Å radius. Minimization and equilibration was performed for the full droplet model in each case. After equilibration was finished, the model was divided into three zones. The central reaction zone was 12 Å in radius, a buffer zone was from 12-16 Å in radius, and the remaining atoms were fixed. All three simulations were stable with RMS deviations from the initial structure under 1 Å. The results are analyzed in terms of hydrogen bond lifetimes, water and cation behavior, and the average interactions between amino acids, nucleic acids and the surroundings. The trajectories are used as the basis for linear response calculations to predict the relative ΔΔG changes in binding for sixteen small changes in amino acid and/or nucleic acid sequence. The results represent the first steps in a combined experimental and computational attempt to understand the binding affinity of zinc-finger proteins and DNA.

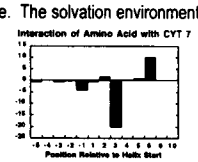

M-Pos433

One nanosecond molecular dynamics simulation of the N-terminal domain of the λ repressor and its cognate DNA operator OL_1.

David C. Kombo, Matthew A. Young, G. Ravishanker & David L. Beveridge

Department of Chemistry and Molecular Biophysics Program, Hall-Atwater laboratory, Wesleyan University, Middletown, CT 06457.

We have carried out molecular dynamics simulation of the N-terminal domain of the λ repressor protein and its cognate OL1 DNA operator using both the canonical form and its crystallographic protein-bound conformations. In the three simulations, the surrounding environment included explicit waters and ions as to mimic an ionic strength of 138 mM NaCl. The Amber 4.1 macromolecular computer package was used for energy minimization and dynamics simulation. We find that two dynamics substates exit in the 1 ns protein simulation, the transition occuring around 500 ps. A significant change in the interhelical distance between the recognition helices follows the transition. Many amino-acid residues, including those involved in DNA-recognition, undergo a simultaneous transition in their side-chain conformations, consistent with the relationship between side-chain conformation and secondary structural elements. The computed B-factors of the flexible N-terminal arms are higher in the non-consensus monomer compared to the consensus monomer, in agreement with experimental findings. The 1 ns simulation of the canonical form of the OL1 operator reveals that the unusually large helical twist (49°) observed in the protein-bound form at a TG base-step in the non-consensus monomer, is probably inherent to sequence-dependent DNA structure deformability.

M-Pos434

MICROGRAVITY CRYSTALLIZATION OF NUCLEOSOME CORE PARTICLES. ((**J.M. Harp**, D.E. Timm, S.A. Plichta and G.J. Bunick)) The University of Tennessee Graduate School of Biomedical Sciences and Biology Division, Oak Ridge National Laboratory, Oak Ridge TN 37831. (Supported by NIH Grant GM29818 and DOE Contract DE-AC05-96OR22464.)

Nucleosome core particles reconstituted using a 146-bp DNA palindrome and purified chicken histone octamer were grown aboard the Second United States Microgravity Laboratory (STS-73 USML-2). The DNA palindrome, developed in this laboratory prior to 1993, is based on one-half of a nucleosome phasing sequence found in the alpha satellite DNA of the human X chromosome. A relatively small crystal obtained from USML-2 provided excellent diffraction data to 2.5 Å using synchrotron radiation at the National Synchrotron Light Source at Brookhaven National Laboratory. The nucleosome diffraction images do not show the strong diffuse scatter characteristic of diffraction from crystals of the histone octamer. This observation suggests that the interaction of histone tail domains with the DNA in the nucleosome is highly ordered. Large and well-formed nucleosome core particle crystals have now been grown in the microgravity environment of the Mir space station (Mir-3). Results of the Mir-3 experiments will be presented and evaluated with respect to ground-based crystallization.

MECHANISMS OF GENE REPLICATION AND TRANSCRIPTION

M-Pos435

EFFECTS OF ANIONS AND pH ON THE NONSPECIFIC DNA BINDING OF *E.COLI* LEXA REPRESSOR. ((E.S. Jenuwine, N.K. Relan, and **S.L.Shaner**)) Department of Chemistry, Wayne State University, Detroit, MI 48202.

Binding of *E. coli* LexA repressor to random sequence DNA was examined as a function of concentration of NaCl, KCl, NaF, and $MgCl_2$ at pH 7.5, 21°C using zonal DNA affinity chromatography. The effects of NaCl and NaF were also examined at pH 6.0 and 8.9. Anion identity and pH significantly affected the nonspecific DNA binding. Decreased pH resulted in tighter nonspecific binding and steeper dependences of the binding affinity on NaCl concentration. NaCl and KCl yielded identical results at pH 7.5, indicating that monovalent cation identity is unimportant. Binding affinities in NaF were tighter than in NaCl and the dependence of the affinity on salt concentration was weaker in NaF at each pH examined. Gel mobility shift experiments were performed to characterize these nonspecific complexes further. Several intermediate ligation states were detected on 5% polyacrylamide gels using a 160 bp DNA fragment at 31 pM. The distribution of these ligation states varied with salt concentration. These results indicate that anion and proton binding, previously observed to be coupled to the specific binding of LexA repressor to the *recA* operator, also affect nonspecific binding modes. The observed pH effects are consistent with the possibility that *in vivo* derepression of SOS genes by acidic pH could be mediated by loss of selectivity of DNA binding by LexA repressor.

M-Pos436

THERMODYNAMIC AND KINETIC MEASUREMENTS OF PROMOTER BINDING BY T7 RNA POLYMERASE ((Andrea Újvári & Craig T. Martin)) Department of Chemistry, University of Massachusetts, Amherst, MA 01003-4510

The fluorescent nucleotide analog, 2-aminopurine, placed at unique positions within the promoter of T7 RNA polymerase, is used to monitor DNA conformational changes associated with enzyme binding. Results support a model which includes melting, in the statically bound complex, of the region of the promoter near the start site. Equilibrium titrations at 25 °C provide a thermodynamic measure of binding (K_d = 4.8 nM), while stopped flow kinetic assays measure the apparent association ($k_1 = 5.6 \times 10^7\ M^{-1}\ s^{-1}$) and dissociation ($k_{-1} = 0.20\ s^{-1}$) rates. These results indicate that binding is close to the diffusion limit and that helix melting is extremely rapid, in agreement with previous steady state kinetic studies in this system which have shown that melting of the DNA is not rate limiting in initiation. In studies of structurally altered promoters, a base functional group change at position -10 in the upstream duplex recognition region is shown to significantly decrease k_1, with little effect on k_{-1}. In contrast, removal of the nontemplate strand from position +1 downstream results in a large decrease in k_{-1}, with no significant effect on k_1, suggesting an important role for the nontemplate strand in the dissociation of the bound complex.

M-Pos437

LINKAGE BETWEEN SITE-SPECIFIC DNA BINDING AND PROTEIN ASSEMBLY IN THE BIOTIN REPRESSOR SYSTEM, ((**Dorothy Beckett*** and Emily Streaker)), Department of Chemistry and Biochemistry, University of Maryland Baltimore County, 1000 Hilltop Circle, Baltimore, MD 21250

The *Escherichia coli* repressor of biotin biosynthesis (BirA) is a site-specific allosteric DNA binding protein. Binding of the small ligand, bio-5'-AMP, to the repressor is positively linked to site-specific binding of the protein to the forty base pair biotin operator (bioO) sequence. Thermodynamic linkage functions at multiple levels in this system. Results of equilibrum binding measurements of the holorepressor to the wild type biotin operator performed using the quantitative DNase footprint titration technique indicate that two protein monomers bind cooperatively to the adjacent two bioO half-sites. The footprint titration measurements have been extended to mutant operator templates in which one of the half-sites contains either two point mutations or is replaced by nonspecific sequence. Results of these measurements indicate that although the total Gibbs free energy for interaction of holoBirA with any mutant template is considerably less favorable than that measured for binding to the wild type biotin operator, the repressor binds with the same apparent cooperativity to the mutant templates. These results support a model in which the biotin repressor dimerization free energy contributes significantly to the total free energy of site-specific association with the biotin operator. Because of this significant energetic contribution, site-specific DNA binding is obligatorily linked to protein assembly in the system.

M-Pos438

DYNAMIC MODELING OF POSITIVE CONTROL FROM λ cI MUTANT DATA . ((**Peter D. Munro** & Gary K. Ackers)) Dept. of Biochemistry & Molecular Biophysics, Washington University School of Medicine, St. Louis, MO 63110

The λ and *lac* repressor systems are paradigms for understanding the effects of coupled positive and negative control of gene transcription. Plasmid constructs combining these two systems have been used recently by Kolkhof and Müller-Hill (1994, *J. Mol. Biol.* **242**, 23-36) to characterize positive-control mutants of the λ cI repressor. In this study, we have analyzed their results to equations based on the transcriptional control model of Shea and Ackers (1985, *J. Mol. Biol.* **181**, 211-230) for the λ right operator. The analysis yielded equilibrium parameters for polymerase binding to the repressor maintenance promoter P_{RM}, as well as the rate constants for gene transcription from that promoter. These values, in conjunction with the dynamic model equations, provide a quantitative description for the characteristic behavior of these cI transcriptional mutants.

Supported by NIH R37-GM24486 and R01-GM39343.

M-Pos439

RELATIVE MOVEMENT OF LARGE ENZYME COMPLEXES WITH RESPECT TO THEIR THREAD-LIKE SUBSTRATES.
((**Eugene Hamori**)) Tulane University, School of Medicine, Department of Biochemistry, New Orleans, LA 70112.

The interaction of long quasi-linear biological macromolecules (e.g., the polynucleotides DNA and RNA) with certain enzyme complexes can generate a mechanochemical action resulting in a relative displacement between the thread-like substrates and their massive enzymes. Considering the large disparities between the actual molecular masses involved, the Newtonian action-reaction principle of physics would seem to contradict the commonly envisioned concept of the enzyme complex "moving" along its long thin substrate (as, for example, in the schematic mechanisms of transcription, DNA replication, protein synthesis, etc.).

Among the cricial factors to be considered in this "what-really-moves" debate are the molecular masses involved, the effectiveness of anchoring and attachments (if any) of the reacting components to fixed points in the cell, the viscosity of the medium, the flexibility of the linear substrate, and the linear diffusion rate of the polymer segments involved.

BIOTECHNOLOGY AND BIOENGINEERING

M-Pos440

DNA FRAGMENT SIZING BY FLOW CYTOMETRY: AN ALTERNATIVE METHOD TO ELECTROPHORESIS.
((Z. Huang, J.T. Petty, R. Habbersett, J.H. Jett and R.A. Keller)) Chemical Science and Technology Division and Life Sciences Division, Los Alamos National Laboratory, Los Alamos, NM 87545.

A flow cytometry-based, ultrasensitive fluorescence detection technique is used to size individual DNA fragments ranging from 200 base pairs to 167 kilobase pairs. Fluorescence bursts are recorded as individual, dye stained DNA fragments pass through a low power, focused, continuous laser beam at a rate of ~40 fragments per second. The size of the burst emitted by each stained DNA fragment is measured in 1-2 ms. The magnitudes of the fluorescence bursts are linearly proportional to the length of the DNA fragments. The histograms of the burst sizes are generated in <3 minutes with <1 picogram of DNA. Application of this technology to the sizing of P1 artificial chromosomes (PACs) in both linear and supercoiled forms is described. This method is well suited to characterizing PAC/BAC clones and will be very useful for the analysis of large insert libraries. Restriction fingerprinting and mapping the clones will also be demonstrated.

We have also constructed a simple, inexpensive apparatus to perform these measurements. Excitation is accomplished with a 30 mw diode pumped Nd:YAG laser that emits at 532 nm. Photon detection is with a solid state avalanche photodiode which provides a logic signal to a multichannel scaler board that resides in a PC. The whole apparatus can be contained in a cubic foot plus the personal computer. This work is supported by Los Alamos National Laboratory LDRD funds and the DOE/OHER Human Genome Program.

M-Pos441

DESIGNING PUSHING, PULLING, HYBRID PUSH-PULL AGENTS FOR PROTEIN PRECIPITATION.
Daumantas Matulis, Charles Wu, and Rex Lovrien. Biochemistry Department, University of Minnesota, St. Paul, MN 55108

Protein molecules can be thermodynamically and mechanically pushed out of solution with appropriate agents, and pulled out by others. Crowding, exclusion, osmolytic agents do not bind (much) and are nearly purely pushing. Matrix and entanglement ligands purely pull. Pushing agents operate by dint of large (0.5-4 M) concentrations. Pulling agents that rely on binding work in 10^{-4}-10^{-5} M concentrations to coprecipitate and sometimes cocrystallize proteins. Some agents including the sulfate anion are hybrid agents, both push, and pull depending on binding levels (Chakrabarti, J. Mol. Biol. 234, 1993). Protein molecules start out dissolved in water because they are penetrated by water. Getting them to precipitate or coprecipitate first requires squeezedown (or tightening) their conformation in solution, necessary for the next main step, precipitation. Protein hydrate water and how it is handled by the various agents is the third, important reactant in both pushing and pulling precipitative reactions. There exist about ten common means for precipitating proteins, and enabling them to assemble. In the end-product, precipitated or aggregated proteins, protein-protein interactive forces dominate if the mechanism is pushing. If pulling dominates, ligand-ligand interactions – which can be tailored and adjusted – dominate. Before the end product, coprecipitate, or homogeneous aggregate is obtained however, selection of agents now can be tailored to influence proteins in solution to get ready to precipitate, coprecipitate, cocrystallize.

M-Pos442

EXPRESSION OF RECOMBINANT α-BUNGAROTOXIN FROM *PICHIA PASTORIS*
((**Mark M. Levandoski** and Edward Hawrot)) Department of Molecular Pharmacology, Physiology & Biotechnology, Brown University, Providence, RI 02912 (Spon. by A. Zimmerman)

The α-neurotoxins from the venom of elapid and hydrophid snakes are a large family of proteins with conserved structure, some of which bind with high affinity and specificity to the nicotinic acetylcholine receptor (nAChR) of muscle or neuronal tissue. One of these, α-bungarotoxin (BGTX) has proved to be invaluable in biochemical, pharmacological and structural studies of the muscle type nAChR. We have introduced a synthetic gene coding for BGTX into the methylotrophic yeast *Pichia pastoris*. Secretion of BGTX into the culture medium is directed from the *AOX1* promoter, inducible by growth in methanol. By directly assaying spent culture medium for solid-phase competition binding with radiolabelled native BGTX using purified nAChR from *Torpedo* electroplax as the source of receptor, we have obtained levels of expression of 2-3 mg BGTX activity per L of shake-flask or fermentor culture. This level of expression is comparable to the final yields of BGTX obtained from an intracellular, fusion-protein expression system in the bacterium *E. coli* in which considerable loss occurs due to incorrect pairing of the five disulfide bonds of BGTX. Using standard ion-exchange and size-exclusion chromatographic steps, an active fraction has been partially purified from the *Pichia* expression system that co-migrates with native BGTX in SDS-PAGE analysis. Thus, production of BGTX from *Pichia pastoris*, which may circumvent the problematic *in vitro* refolding of disulfides in the *E. coli* system, is highly suited to site-directed mutational analysis to probe structure-function relationships between toxins and muscle or neuronal nAChRs, and may provide a more practically useful system for the production of metabolically labelled (^{15}N and ^{13}C) BGTX for NMR-based structural studies. Supported by NIH NS34348 and the American Heart Association (RI Affiliate) 9604510S.

M-Pos443

EXPERIMENTAL EVIDENCE OF A NON-DIFFUSIONAL NATURE OF BAND SPREADING IN GEL ELECTROPHORESIS. CORROBORATION OF AN ALTERNATIVE MODEL OF BAND SPREADING
((**E.Yarmola***,**, P.P.Calabrese***, A.Chrambach* and G.H.Weiss***)) *SMA, LTPB, NICHD, NIH, Bethesda, MD 20892 **LBP, IMB RAS, Moscow, 117984 Russia, ***PSL, DCRT, NIH, Bethesda, MD 20892. (Spon. by M.Garner)

The conventional theory of electrophoretic processes is based on a model which implies diffusional band spreading and predicts linear dependence of the peak position and of the square of the band width on time. This model implies that any degree of resolution is attainable provided that the experiment is run for a long enough period of time. The use of the automatic instrumentation, the HPGE-1000, permitted us to collect data otherwise unavailable from standard electrophoretic experiments".The kinetic behaviour of phycoerythrin in an agarose gel shows significant deviation from predictions of the the conventional electrophoretic theory and is in much better agreement with a non-Markovian theory based on an alternative phenomenological two-state model of the electrophoretic process. A practical implication of this finding is that the resolution of two peaks, after an initial transient period, need not increase with time.

M-Pos444

MICROLITHOGRAPHIC PATTERNING OF FLUID BILAYER MEMBRANES

((Nick Ulman*, Jay T. Groves†, and Steven G. Boxer†)) *Edward L. Ginzton Laboratory and †Department of Chemistry, Stanford University, Stanford, CA 94305-4085.

Fluid lipid bilayer membranes are assembled on planar, solid supports by vesicle fusion. A ~10Å water layer separating the membrane from the substrate surface preserves the natural lateral fluidity of the bilayer. Membranes are assembled on patterned surfaces for the purpose of subdividing the lipid bilayer into micron scale arrays of fluid membrane patches. We have made box patterns with as many as ~10^6 elements where each box in the array contains a fluid membrane. Patterned membrane patches as small as 5 microns square have been observed and we believe that much smaller scale patterns are possible. The arrays are created using microlithography and planar silicon processing techniques. Surfaces are made with spatially varying properties which selectively permit or inhibit fluid membrane formation. Further lithographic steps on the patterned membrane are possible. We demonstrate that the membrane array elements may be selectively modified by a photochemical transformation. As an example, fluorescently labeled lipids are selectively bleached on an element by element basis in the array. Because the membrane is fluid, a mask with variable size openings will deliver different exposures to each box, yet the composition within each element quickly becomes homogeneous by diffusive mixing. This work opens up the possibility of light directed, parallel chemical synthesis on fluid membrane substrates.

M-Pos445

FUNCTIONAL AND MORPHOMETRIC STUDY OF *DROSOPHILA* INDIRECT FLIGHT MUSCLE USING ATOMIC FORCE MICROSCOPY.

((Lori Nyland, Jon Peterson, David Maughan)) Department of Molecular Physiology and Biophysics, University of Vermont, Burlington, VT 05405

Atomic Force Microscopy was used to investigate the topology and transverse static stiffness (K⊥) of *Drosophila* indirect flight muscle myofibrils in physiologic buffer. Myofibrils were secured to a positively charged glass slide with a cytospin centrifuge. Subsequently, the surface of an isolated myofibril was imaged in contact mode by rastering a silicon nitride tip, attached to a cantilever (mfgr's stiffness, 0.38 N/m). Images were acquired in activating (pCa 4.5, MgATP 5 mM), rigor (4.5, 0), and relaxing (8, 5) buffers (ionic strength 175 mM). Banding patterns representing the A-band, I-band, and M-line of the sarcomere were clearly observed. Over 4 consecutive sarcomeres, the average sarcomere length was 2.90±0.03(m±sd) μm in rigor, 2.46±0.04 μm in activating, and 2.74±0.03 μm in relaxing buffer. Cross sectional height did not vary significantly among myofibrils in the three different buffers, although it did vary with the sarcomeric banding pattern. Cross sectional height at the A-band was 939±91 nm. Electron micrographs show 30-35 thick filaments across one myofibrillar diameter. K⊥ of the myofibril was determined from the relationship between cantilever deflection and specimen indentation. Glass, assumed infinitely stiff, was used to calibrate the system. In each buffer, the A-band was indented 50 nm (at 8 locations along 4 sarcomeres). K⊥ in rigor was 0.11 N/m, decreasing 9% in activating buffer and 28% in relaxing buffer. These molecular-scale transverse stiffness measurements, carried out in the intact filament lattice under physiological conditions, are in qualitative agreement with measurements of longitudinal stiffness at the whole fiber level.

M-Pos446

IMPROVING THE EFFICIENCY OF ELECTROTRANSFECTION AND ELECTROLOADING BY CENTRIFUGATION.

((L.H. Li*, P. Ross and S.W. Hui)) Biophysics Department, Roswell Park Cancer Institute, Buffalo, NY 14263.*on leave from Biomedical Engineering Department, Hunan Medical University, Changsha, China.

By forming centrifugation pellets during or immediately after the application of electric pulses in electrofusion and electroporation processes, post-pulse colloidal-osmotic swelling of cells is inhibited, and the viability of cells is significantly improved. We apply this method to improve the electrotransfection and electroloading efficiencies of CHO cells and NK-L cells; the latter cells are very difficult to transfection by other physical methods. CHO cells are grown as adherent cultures but pulsed in suspension, whereas NK-L cells are grown and pulsed in suspension. For forming CHO cell pellets, centrifugation force (300g-13000g) and duration are not crucial; 5-10 cell layers in the pellet are optimal for cell viability. NK-L cell pellets must be formed immediately after pulsing, by centrifugation at 13000g for 3 sec in an Eppendorf desktop centrifuge. The number of cell layers is not important. This method is applied to load CHO cells with FITC-Dextran (41000 MW), with close to 100% success rate. CHO and NK-L cells are transfected with pSV-βgal plasmid.. More than 20% of CHO cells, and about 10% of NK-L cells are transfected. The improved post-pulse cell viability using the pellet method enables the application of higher pulse field strengths, thereby increasing the electrotransfection and electroloading efficiencies considerably above those by conventional electroporation techniques, and enabling transfection of cells which are not previously possible.

M-Pos447

DIELECTROPHORETIC CHARACTERISATION AND SEPARATION OF HERPES SIMPLEX VIRUS PARTICLES

((M.P. Hughes[1], H. Morgan[1], F.J. Rixon[2])) [1] Bioelectronics Research Centre, Department of Electronics and Electrical Engineering, University of Glasgow, Glasgow G12 8QQ UK. [2] MRC Virology Unit, University of Glasgow, Glasgow G12 8QQ UK

Dielectrophoresis (DEP) is the phenomenon of motion induced in particles suspended in non-uniform AC electric fields. The direction of motion acts with or against the field gradient, as governed by the relative properties of the particle and medium, and by the frequency of the field. By studying particle behaviour as a function of applied frequency is is possible to probe the biophysical properties of the particle.

Recent advances in electrode fabrication have led to the development of devices small enough to manipulate sub-micron particles such as viruses and proteins. We have performed such studies on the human virus Herpes Simplex Virus type 1 (HSV-1). Using fluorescence microscopy the dielectrophoretic properties of the HSV-1 virion and capsid have been analysed independently. Using the techniques described above, it has been possible to determine some of the biophysical properties of the key components of the intact HSV-1 virion, and to determine the mechanisms of charge movement.

Furthermore, it is shown that virion and capsid particles can be selectively manipulated using a combination of dielectrophoretic and thermal-convective forces. Examples of this include the specific isolation of a single capsid or virion particle, and the separation of a mixture of both particle types into homogeneous groups.

This work is supported by the Biotechnology and Biological Sciences Research Council (UK), Grant No. 17/T03515.

M-Pos448

DIELECTROPHORESIS OF TOBACCO MOSAIC VIRUS

((N.G. Green[Y], H. Morgan[Y] and J.J. Milner [f])) Y- Bioelectronics Research Centre, Department of Electronics and Electrical Engineering, *f*- Division of Biochemistry and Molecular Biology,
University of Glasgow, Glasgow G12 8QQ, Scotland, UK.

Dielectrophoresis is the motion of polarisable particles induced by non-uniform electric fields. This movement depends on the dielectric properties of both particle and suspending medium, together with the frequency of the applied AC field. It has been used to characterise and separate a variety of biological particles. The movement of small particles (<0.5microns) is governed by Brownian motion and in order to generate an electrokinetic force of sufficient magnitude to control such particles, field strengths of the order of 10^5 -10^6 V/m are required. Suitable electric fields are generated using devices consisting of micron and sub-micron sized electrode arrays. The dielectrophoretic response of Tobacco Mosaic Virus (TMV) to AC fields over the frequency range 1kHz to 500MHz in electrolytic media of varying composition and conductivity is presented. A protein modification technique has been used to fluorescently label the coat protein, allowing fluorescence microscopy to be used to observe the behaviour of individual viruses. Numerical simulation of the movement of TMV in non-uniform fields taking into account both electrokinetic and thermal forces is also presented.

M-Pos449

CHANGES IN MEMBRANE ELECTRICAL PROPERTIES OF HUMAN T-LYMPHOCYTES INDUCED BY MITOGENIC STIMULATION

((Y. Huang, X.-B. Wang, F. F. Becker and P. R. C. Gascoyne)) Box 89, UT M. D. Anderson Cancer Center, 1515 Holcombe Blvd., Houston TX 77030

Recent dielectrophoresis and electrorotation measurements on biological cells have led to the development of the concept of cell dielectric phenotype wherein cells of different types possess unique frequency-dependent dielectric properties. To determine the biological basis of cell dielectric phenotype, we investigated the relationship between dielectric properties and phases of the cell division cycle. Human T-lymphocytes purified from peripheral blood were utilized as the model. T-lymphocytes, normally resting at the G0 phase, were stimulated with phytohemagglutinin. Cells were studied at 24 hr intervals up to 96 hrs by flow cytometry to determine size and phase distributions in the division cycle (G1, S, and G2/M) and by electrorotation to determine membrane dielectric properties. While the percentage of cells in S and G2/M increased from 0 to about 40% at 72 hrs following activation, the average membrane specific capacitance increased from 9.2 (± 0.8) to 16 (± 0.5) mF/m^2, total cell capacitance increased from 10 (± 1.0) to 35 (± 12) pF. Based on scanning electron microscope studies, it was concluded that the change in the specific capacitance reflected the increased complexity in cell membrane morphology following activation. A correlation between specific capacitance and membrane lipid synthesis during cell division cycle was analyzed.

M-Pos450

DIELECTRIC PROPERTIES OF HUMAN BREAST CANCER CELL LINES CORRELATE WITH CELL SURFACE MORPHOLOGY AND METASTASIS. ((J. Yang, X.J. Wang, Y. Huang, X-B. Wang, P.R.C. Gascoyne and F.F. Becker)) Dept. of Experimental Pathology, Box 89, U.T. MD Anderson Cancer Center, 1515 Holcombe Blvd. Houston, TX 77030.

The dielectric properties of three human breast cancer cell lines from pleural effusion (MDA-MB-435, MDA-MB-231, MDA-MB-468) were studied by electrorotation (cell rotational motion induced by a rotating electric field). Mean values of specific membrane capacitance were found to fall in the order: MDA-MB-435 < MDA-MB-231 < MDA-MB-468, the exactly opposite of the order of their metastatic potential. A correlation between cell specific membrane capacitance and cell metastatic potential was also found in experiments on several other tumor cell lines. An analysis of the dielectric properties of cellular membrane components was carried out, and taken together with our simulations of the effects of changes in surface structure, revealed that the differences in specific membrane capacitance observed are largely determined by differences in the cell surface morphology, rather than membrane composition. This suggests that correlation between oncogene expression and cell surface structure should be stressed in further investigations of metastasis. Our findings potentiate new ways of separating and manipulating cancer cells of different metastasis potential and is significant in understanding underlying mechanisms of metastasis.

M-Pos451

OPTICAL PROPERTIES OF CELLS: RELEVANCE TO NONINVASVE TISSUE DIAGNOSTICS

((J. R. Mourant, J. P. Freyer, A. H. Hielscher, and T. M. Johnson))
Bioscience and Biotechnology Group, Los Alamos Nat. Lab, Los Alamos, NM 87545

Optical techniques for tissue diagnosis without removal of tissue are being developed. These techniques offer significant advantages over standard biopsy techniques, such as tissue biopsy because they are faster, sedatives are not needed and complications associated with tissue removal are eliminated. The potential for elastic-scatter and fluorescence spectroscopy has been demonstrated in clinical trials *in vivo* in which sensitivities and specificities in the upper 90th percentile were obtained. At this time, however, there is no fundamental understanding of the relationship between the optical signals and the morphology and biochemical features of the tissue. Differences in tissue optical signatures may arise from biochemical and morphological features of the cells themselves, differences in tissue organization or changes vascularity. We have investigated the first possibility. Optical properties of pairs of cancerous and noncancerous cells have been measured. We find that the particles primarily responsible for scattering are on average about 0.3 microns in diameter. The amount of light scatter was found to correlate with cell volume (when the cell number was kept constant). Consistent with this, the amount of scattering was found to depend on the growth stage of the cells (exponential vs plateau). A difference in the scattering properties of cancerous and noncancerous cell lines both derived from rat embryo fibreoblasts was also measured.

M-Pos452

SITE-SPECIFIC IMMOBILIZATION OF BIOMOLECULES ON MICRO- AND NANOFABRICATED GOLD AND SILICON SURFACES. ((P. Wagner, A. Spudich, N. Ulman*, C.E.D. Chidsey#, and J.A. Spudich)) Dept. of Biochemistry, Stanford University, Stanford, CA 94305,*Ginzton Laboratory, Stanford University, Stanford, CA 94305, #Dept. of Chemistry, Stanford University, Stanford, CA 94305.

Immobilization of biomolecules on solid surfaces has been widely used for solid-phase analytical techniques and affinity chromatography. However, applications such as surface-dependent in vitro assays, biosensor devices, supramolecular systems, scanning probe microscopy, and nanostructure technologies require more sophisticated approaches with well-defined molecular architecture on a nm-scale.

Here, we present the immobilization of biomolecules, such as molecular motors, on micro- and nanostructured self-assembled monolayers chemisorbed on gold and silicon. Feature sizes in the sub-100 nm range allow the control of the spatial distribution of the immobilized protein and therefore the construction of protein assemblies for biophysical analyses.

In addition, we have worked out strategies to bind histidine tagged fusion proteins on monolayers with Ni^{2+}/NTA functionalities to achieve oriented binding on the surface and to maximize interaction with other proteins or ligands at the liquid-solid interface. As model proteins we use single-headed his-tagged myosin species and show their functionality on these surfaces by the sliding actin filament assay.

M-Pos453

A COMPUTATIONAL ENVIRONMENT FOR THE STUDY OF CIRCULATING CELL MECHANICS AND CELL ADHESION

((Grenmarie Agresar, Jennifer J. Linderman, Kenneth G. Powell))
Depts. of Biomedical Engineering, Chemical Engineering, and Aerospace Engineering, University of Michigan, Ann Arbor, Michigan, 48109 USA

Specific cell adhesion is important in cell-mediated immunity, embryogenesis and wound healing. Previous research has demonstrated that cell adhesion is governed by several forces which act on drastically different length scales. On the scale of the cell diameter are cellular deformation and the flow of external fluid. At the gap near the area of contact are specific molecular bonds and colloidal interactions. The complex coupling of these events and the different length scales at which they occur have complicated both experimental and mathematical studies of cell adhesion.

Further difficulties arise from the fact that the mechanical behavior of most cells is not clearly defined. Cell mechanics has been studied extensively due to its relevance to whole blood dynamics and capillary occlusion. However, the constitutive relationship between stress and deformation for most cells is still elusive. The common procedure for testing hypotheses for such a relationship requires that the relationship be declared a priori and that a new analytical set-up be established.

In this work, a modular computational framework has been developed to study cell deformation and adhesion. As a tool to study cell mechanics, the program allows the incorporation of different mechanical models without significant changes in the set-up. As a tool to study cell adhesion, the program provides the coupling of the relevant forces and resolution of the different length-scales involved. Simulations of various test cases are in agreement with experimental data and analytical solutions. Simulations of cell-entry micropipet experiments showed that alternate models for the cell mechanics affect both the shape and the rate of entry of the cell entering the pipet. Finally, simulations of cells adhering under flow demonstrated that the cell mechanics affect the size, shape and temporal evolution of the contact area, as well as the number of molecular bonds existing at a given time.

MACROMOLECULAR THEORY

M-Pos454

MOLECULAR DYNAMICS SIMULATIONS OF CROSSLINKED AND NORMAL HEMOGLOBINS. ((L. Zhao and K. W. Olsen)) Department of Chemistry, Loyola University, 6525 N. Sheridan Rd., Chicago, IL 60626

Molecular dynamics simulations have been calculated for 200 ps on deoxy hemoglobin (HbA) and crosslinked hemoglobin (α99XLHbA). Bis (3,5-dibromo-salicyl) fumarate crosslinks deoxy hemoglobin between the Lys α99's, producing a potential blood substitute. The simulations produced stable trajectories in which HbA and α99XLHbA did not deviate greatly from the X-ray structures. The average rms deviations of 100 transient structures were calculated relative to the average dynamics structure. The RMSD patterns for HbA and α99XLHbA were similar. The α subunits were less flexible that the β subunits. The fumarate crosslink pulls the α chains closer and greatly decreases movement close to the crosslink. The $\alpha_1\beta_1$ contacts have smaller RMSD values that the average, while the terminal and loop regions, including the CD and EF corners, show quite large values. Thus, the mobility of the exposed areas is higher than that of the internal regions, as would be expected. There were no significant changes in the $\alpha_1\beta_1$ contacts of either molecule. The RMSD values for the $\alpha_1\beta_2$ contacts of α99XLHbA are about 10-15% smaller than those of HbA. Thus, the crosslink stabilizes the molecule by tightening the $\alpha_1\beta_2$ contacts. Since the $\alpha_1\beta_2$ contacts move during the allosteric transition, these results suggest that T-state α99XLHbA would be less able to shift to the R-state than T-state HbA. The decreased oxygen affinity of α99XLHbA may result from decreased mobility in the $\alpha_1\beta_2$ contacts of the deoxy crosslinked protein.

M-Pos455

MATHEMATICAL ANALYSIS OF LYSOZYME FOLDING: NUCLEATION OR HYDROPHOBIC COLLAPSE?

((C. Wagner, G. Wildegger, A. Bachmann and T. Kiefhaber))
Biozentrum, University of Basel, CH-4056 Basel, Switzerland.

The folding of Lysozyme from hen egg white is one of the best studied system for protein folding. A triangular scheme (Unfolded, Intermediate and Native) was suggested representing the direct folding pathway (U-N) and the pathway via an intermediate (U-I-N). The scheme provides two macroscopic rate constants (phases), a slow and a fast one, depending on the concentration of Guanidinhydrochlorid (GdmCl). The bending of the fast phase at high GdmCl concentration and the observation of an ultrafast phase gave rise to extend the model by a further state.

We investigated the following candidates: the hydrophobic collapse and a second intermediate which might be due to nucleation at zero GdmCl concentration. By mathematical analysis we were able to exclude several schemes. We performed simulations of the remaining models and checked the predictions in experiments.

M-Pos456

WHAT MAKES PROTEIN MODELS FOLD COOPERATIVELY?
((*S. Bromberg, **K. A. Dill, *W. E. Hart, *S. C. Istrail)) *Sandia National Laboratories, Albuquerque, NM 87185; **Dept. of Pharm. Chem., Univ. of California, San Francisco, CA 94118.

The signature of thermodynamic cooperativity in protein folding is an energy gap between the native and denatured states. Such a gap is created by repulsions that do not allow low energy denatured states to be populated. Many interactions may contribute repulsively. We present exhaustive simulations that show that -- even in the simplest 2-dimensional models with only two types of monomers, hydrophobics (H) and hydrophilics (P), and with only attractive interactions between H's -- specific HP sequences, excluded volume and chain connectivity give rise to cooperativity. We explore additional contributions to cooperativity from the repulsions between hydrophobic monomers and solvent or polar monomers, and from the additional steric hindrance introduced by sidechains. We show how the ratio of van't Hoff to calorimetric enthalpies relate to such rigorous statistical mechanical models in identifying the cooperativity of protein folding transitions.

M-Pos457

REVISION OF THE THERMODYNAMIC ROLE OF THE IMINO ACIDS IN COLLAGEN. RESOLUTION OF THERMODYNAMIC PARADOX.

((**N.G.Esipova**, L.E.Tiktopulo, Yu.A.Lazarev, V.G.Tumanyan)) Engelhardt Institute of Molecular Biology, Russian Academy of Sciences, Vavilova 32 B-334, Moscow, Russia (Spon. By S.Korolev)

On the basis of theoretical and experimental data included the dependence of the thermodynamic parameters of the denaturation transition in taxonomically remote collagens the conclusion have been drawn on the independence of hydration of the native collagen molecule from the content and position of the imino acids in the protein. Lack of amid protons at the sites of proline incorporation interrupts continuous network of water molecules around polypeptide in the polyproline II type conformation. As a consequence with increase in the imino acid content in the molecule, the entropy of the denatured collagen-water system increases and as a result this supply increasing of entropy of the denaturation transition in the collagens. On the other hand increase in the enthalpy of the transition with increase in the number of imino acids is determined by the van der Waals interactions of pyrrolidine rings in the native triplehelical collagen molecule. Thus, the proline decreases the hydration of single polypeptide chain in the polyproline II conformation, which leads to increasing of the entropy of the polypeptide-water system. The initiation of structure formation in the collagens by the imino acids occurs for two reasons: because of the disadvantage of proline being in aqueous surroundings in the single chain and because of the enthalpic stabilization of the triple helix. Method of IR-spectroscopy demonstrates increasing of halfwidth of Amid A in the denatured protein band hand by hand with increasing of imino acid content in collagens from different sources. Microcalorimetry experiments performed confirms the increasing entropy of denatured polypeptide with increasing of imino acid content as well.

M-Pos458

NEW METHODS TO ENUMERATE CONFORMATIONS OF COMPACT PROTEINS

((**A. Kloczkowski**, R.L. Jernigan)) Lab. Math. Biol. NCI, NIH, Bethesda, MD 20892 (Spon. by R.L. Jernigan)

A new method has been developed to generate and enumerate all possible conformations within a specified volume and shape for compact proteins on simple lattices. This transfer matrix method is far superior to traditional methods of computer generations of self-avoiding walks, because it is attrition-free, i.e. each computation leads to successful comformations, with no failures. The method has been developed for simple, regular shapes - rectangles on the square lattice and parallelepipeds on the cubic lattice and generalized to irregular shapes and generalizable to other types of lattices. Exact counts of the number of conformations routinely are performed for more than 10^{20} conformations. For example the number of conformations of a chain with ends within a rectangle of the size 8x15 on a square lattice is 404,654,754,079,984,324 and the number of conformations within a parallelepiped of the size 2x3x12 is 6,254,157,199,388,224.

M-Pos459

FAST ADAPTIVE MULTIGRID BOUNDARY ELEMENT METHOD FOR BIOMOLECULAR ELECTROSTATICS

((**Y.N.Vorobjev** and Jan Hermans)) UNC, Chapel Hill, NC 27599-7260, vorobjev@femto.med.unc.edu

A Fast Adaptive Multigrid Boundary Element (FAMBE) method has been developed for the numerical solution of the Poisson equation and calculation of solvent polarization density, **solvation free energy, potentials of mean force** between charged groups and **forces** exerted by the solvent reaction field on atoms of the macromolecule. The **computational complexity** of the FAMBE scales as $O(N_{MEF_{source}})[lg(N_{at})]^2$) ($\sim$ 80s of CPU time for a 50-70 residue protein, one processor of the SGI Power Onyx supercomputer). In conjunction with FAMBE, a **fast, stable and rotationally** invariant mehtod SMIS of calculation of a boundary elements of a molecular surface has been developed. The FAMBE method solves a set of uncoupled matrix equations and is ideally suitable for **parallel implementation.**

The FAMBE method has been implemented for simulations of the folding of a short peptides, taking into account **the conformational - ionizational coupling** and free energy of the ionization of an ionizable groups at a given pH. Other applications of the FAMBE method is in progress: i)simulation of **essential dynamics** of a protein in aqueous solution; ii) free energy of **water molecules in proteins** and assignment of buried and surface waters to cavities and crevices; iii) free energy of **loop conformations** in proteins for rational protein design. iv) free energy of **binding of drugs** with proteins for rational drug design.

M-Pos460

A STATISTICAL MECHANICAL DESCRIPTION OF BIOMOLECULAR HYDRATION.

((A. E. García[1], G. Hummer[1] and D.M. Soumpasis[2])) [1]Theoretical Biology and Biophysics Group T-10, MS K710, Los Alamos National Laboratory, Los Alamos, NM 87545, U.S.A. and [2]Biocomputation Group, Department of Molecular Biology, Max Planck Institute for Biophysical Chemistry, D-37077 Göttingen, Germany.

We present a statistical mechanical theory for the biomolecular hydration that accurately describes the hydrophobic and hydrophilic hydration. The water density distribution is approximated in terms of two- and three-particle correlation functions of solute atoms with water using a potential of mean force expansion. To test the accuracy of the method we perform molecular dynamics simulations of a model α - helix in solution. The PMF approach quantitatively reproduces all features of the peptide hydration determined from the molecular dynamics simulation. In the α-helix, regions of hydrophobic hydration near the C_α and C_β atoms along the helix are well reproduced. The hydration of exposed polar groups at the N- and C-termini of the helix are also well described by the theory. A detailed comparison of the local hydration by means of site-site radial distribution functions evaluated with the PMF theory shows agreement with the molecular dynamics simulations. The formulation of this theory is general and can be applied to any biomolecular system. The accuracy, speed of computation, and the local character of this theory make it specially suitable for studying large biomolecular systems.

M-Pos461

HOW TO ANALYZE DATA WHEN THE MEAN AND VARIANCE ARE NOT DEFINED

((L. S. Liebovitch[1], A. T. Todorov[1], M. A. Wood[2], J. M. Herre[2], R. C. Bernstein[2], K. A. Ellenbogen[2]))
[1]Center for Complex Systems, Florida Atlantic University, FL
[2]Dept. Internal Medicine, Medical College of Virginia, Richmond VA

Most data analysis has assumed that the mean and variance exist and therefore are good measures of central tendency and dispersion. This is not true for fractals where such moments depend on the resolution at which they are measured. For example, we found that there is no average time between events of ventricular tachyarrhythmia recorded by implanted cardioverter defibrillators in 30 patients. The distribution of interevent times t was a power law $t^{-\alpha}$. Even though the moments do not exist, this distribution can be characterized by its slope α.

Supported by NIH EY6234.

M-Pos462

Theoretical Studies of Gel and Steady State Electrophoresis of DNA, ((U. Mohanty)), Eugene F. Merkert Chemistry Center, Boston College, Chestnut Hill, MA 02167

We propose new theoretical techniques to describe (i) the electrophoretic mobility and diffusion of polymer chains through agarose gel. The lifetime of the conformations of the gel as well as the entropic interactions between the matrix and the probe are taken into account by a generalization of the Zimm-Lumpkin model; (ii) the effective charge of DNA oligonucleotide obtained recently by Lau and coworkers using steady-state electrophoresis at various salt concentrations and electric field strengths.

M-Pos463

OSMOTIC BALANCE AND TURGOR PRESSURE IN *ESCHERICHIA COLI* K-12 AS A FUNCTION OF EXTERNAL OSMOLARITY ((**Harry J. Guttman**§, D. Scott Cayley§, Mike W. Capp§, and M. Thomas Record, Jr.§‡)) Departments of Chemistry§ and Biochemistry‡University of Wisconsin-Madison, 53706

We have measured water accessible cellular ($\overline{V}_{cell}$) and cytoplasmic ($\overline{V}_{cyto}$) volumes of *E. coli* grown at low osmolarity (0.03 OsM), and of *E. coli* grown at 0.03 OsM and subsequently plasmolyzed with NaCl up to 2.0 OsM. $\overline{V}_{cell}$ initially decreases with increasing external osmolarity and eventually reaches an osmolarity-independent plateau value ($\overline{V}_{cell}$ = 1.8 μL/mg). Using an interpolated functional form for the combined $\overline{V}_{cell}$ data and the volumetric elastic modulus to relate V_{cell} (the total cellular volume) to turgor pressure, we globally fitted the new $\overline{V}_{cyto}$ plasmolysis data (for cells grown at 0.03 OsM) together with extant $\overline{V}_{cyto}$ plasmolysis data of cells grown at 0.1, 0.28 OsM, and 1.0 OsM + 1 mM betaine (an osmoprotectant). From this global fitting we predict that the turgor pressure decreases from ~2.0 atm at 0.03 OsM to ~0.3 atm. at 1.0 OsM, and that the volumetric elastic modulus is constant as a function of external osmolarity. We find that the turgor pressure predicted from the best-fittings of the plasmolysis data has the same trend and similar values as the turgor pressure predicted from the concentrations of periplasmic MDO's using an ideal Donnan distribution with monovalent MDO counterions.

M-Pos464

IMPROVED FITS TO OSMOTIC PRESSURE DATA. ((**Joel A. Cohen** and Stefan Highsmith)) University of the Pacific, San Francisco, CA 94115.

Osmotic pressure has become a useful perturbant of biophysical and biochemical systems. The method requires accurate knowledge of the osmotic pressure of a bulk-phase osmolyte in equilibrium with the system of interest. Osmotic pressures (Π) for a number of useful osmolytes have been measured at various concentrations, tabulated, and are available on the World Wide Web. For interpolation, much of this data is fitted by the function $\log \Pi = a + b\,(C_{wt\%})^c$, where a,b,c are fitted parameters, and $C_{wt\%}$ is [osmolyte] in wt% (g/dl). These fits are adequate within the data range, but they are inapplicable outside this range, do not extrapolate correctly to $\Pi = 0$, so cannot be used for extrapolation to low values of Π. Here we demonstrate significant advantages of *polynomial* fits to Π vs. $C_{wt\%}$ data in place of the above expression. The polynomial (1) has a physical basis (virial expansion), (2) gives the correct limiting behavior at low Π (van't Hoff's law), (3) permits use of the osmolyte molecular weight (if known) to improve the fit, *ensuring* accurate extrapolation to low Π, (4) permits determination of an unknown osmolyte molecular weight, (5) yields information on osmolyte excluded volumes and intermolecular interactions, (6) permits ready identification of bad data points, especially at low Π. For various polyethylene glycols ranging up to 67 wt%, 2-parameter constrained polynomials give better fits to the measured data than the above 3-parameter log Π fits. A comparison of the 2 fitting methods will be shown.

M-Pos465

CALCULATION OF SOLVENT DENSITY AROUND COMPLEX BIOMOLECULAR SOLUTES

((D. Beglov and B. Roux)) Départements de Physique et de Chimie, Université de Montréal, Montréal, Québec, Canada H3C 3J7.

The average solvent site distribution near complex biomolecular solutes of arbitrary geometry is calculated by solving a statistical mechanical liquid state integral equation on a three-dimensional discrete cubic grid. A numerical fast Fourier transform in three dimensions is used to calculate the spatial convolutions appearing in the equation. The present theory is a generalization of the reference interaction site model (RISM) in three dimensions. The approach is illustrated by calculating the average density of water oxygen and hydrogen centers in the neighborhood of N-methylacetamide, alanine dipeptide and other biomolecules. Molecular dynamics simulations are performed to test the results obtained from integral equation. It is observed that the average solvent density is described accurately by the integral equation. The present calculations demonstrate the feasibility of a numerical solution of liquid state integral equation for arbitrarily complex solutes using a three-dimensional discrete grid.

M-Pos466

ELECTROSTATIC INTERACTION FORCE DUE TO HETEROGENEOUS 3-D POTENTIAL DISTRIBUTION

((**A. O. Wistrom**, C. A. Aurell and A. W. M. Khachatourian)) College of Engineering, University of California, Riverside, CA 92521.

Deviations from DLVO theory have been shown to be related to a non-homogeneous sources of surface charge (potential). Depending on the details of the source distribution the interaction force between two such surfaces can be either smaller or larger than for the case having a uniform distribution of sources of charge (potential). In the present study we have extended the analysis of the interaction force between two parallel plates by evaluating the consequences of having sources of charge (potential) randomly distributed on the surface as well as having sources of charge (potential) protruding away from the surface. This development permits us to explicitly evaluate the interaction force due to the three dimensional microstructure of the surface. The analysis consists of first formalizing the use of the Lorentz force and then combining the results with the tangential and normal components of the electric field on and between the two surfaces. By invoking the Debye-Hückel approximation i.e. $e\psi(r)/K_BT<1$, a closed form solution is obtained. Here we have considered the electrostatic interaction force between two planar surfaces, 100 nm by 100 nm, each having a polymer-chain, 10 nm by 10 nm grafted to the surface. The electrostatic interaction force was calculated for the two configurations having the lowest and highest interaction force, respectively.

M-Pos467

HIV PROTEASE SOLVATION. ((**T. J. Marrone** [1], H. Resat [2], C. N. Hodge[3], and J. A. McCammon[1])) [1]Department of Chemistry & Biochemistry, University of California, San Diego, 9500 Gilman Drive, La Jolla, CA, 92093-0365. [2]Koç University, Istinye, Instanbul 80860, Turkey. [3] Dupont Merck Pharmaceutical Company, Wilmington, DE, 19880-0500.

We examine the water solvation of the inhibitors DMP323 and A76928 bound to the HIV protease using Grand Canonical Monte Carlo (GCMC) simulations. This simulation method is used to identify structurally important waters which may not be resolved in the crystal structures. The starting structures for the simulations are taken from the protein-inhibitor crystal coordinates. Within the GCMC simulation framework, protein and inhibitor remain fixed while water molecules are allowed to move. We identify favorable water occupancy sites in both complexes and compare the results for the two systems.

M-Pos468

DYNAMICS OF MYOGLOBIN IN SOLUTION SIMULATED AT MULTIPLE TEMPERATURES ((**Peter J. Steinbach** and Bernard R. Brooks)) DCRT, NIH, Bethesda, MD 20892

Molecular dynamics simulations of myoglobin in solution have been performed at temperatures above and below the dynamical transition temperature near 220 K. Solution conditions were modeled using a cubic unit cell with sides of length 54 Å and periodic boundary conditions. The unit cell contained one carboxymyoglobin (MbCO) molecule and 4985 water molecules. Simulations were performed at constant temperature and pressure. Electrostatic forces were calculated using Ewald summation.

The current simulations will be compared to previous simulations of MbCO hydrated by 350 or 3830 waters (1). Preliminary results for the solution environment indicate little change in the amplitudes of harmonic motion at 100 K and an enhancement of motion at 300 K. The dynamics of MbCO in solution therefore appears to be more anharmonic than the dynamics simulated for an MbCO molecule hydrated in vacuum.

1. P.J. Steinbach and B.R. Brooks, *Proc. Natl. Acad. Sci. USA 93* (1996), 55-59.

M-Pos469

ANALYSIS OF PEPTIDE:PROTEIN INTERACTIONS -- MODELING A BAND 3 PEPTIDE AND ALDOLASE.

((**A.P.R. Zabell** and C.B. Post)) Dept. of Medicinal Chemistry and Molecular Pharmacology, Purdue University, West Lafayette, IN 47907-1333.

Our work focuses on how tyrosine phosphorylation controls the formation of protein complexes involved in signal transduction. In the case of band 3, phosphorylation mediates *against* association with glycolytic enzymes, an association that ultimately leads to an increase in glycolysis in the cell. Previous studies [Low *et.al.*, *Journal of Biological Chemistry*, **1993**, *268*, 14627-14631] have shown that the N-terminal fifteen residues of band 3 (B3P) can bind and inhibit some glycolytic enzymes. Exchange Transfer Nuclear Overhause Effect Spectroscopy (ET-NOESY) generated 68 NOE distance restraints for B3P bound to aldolase, resulting in a novel structural motif which we have termed a PSI-loop [Post and Schneider, *Biochemistry*, **1995**, *34* 16574-16584]. This loop folds around Tyr8, with Leu4 and Met12 interacting with the aromatic ring. Kinetic assays indicate that this peptide binds the active site, but there is no experimental evidence to provide us with an orientation of the two molecules. We describe here exaustive modeling of the B3P:aldolase interaction; cluster analysis of the initial 200 simulations was performed, followed by an explicit grid search of the active site to provide a starting point for further simulations. Monte Carlo searching with energy minimization (MCM) was then performed, as was a more conventional Simulated Annealing (SA) method. Eleven complexes were obtained, and thoroughly analyzed to determine the best agreement with experiment. This work shows B3P capable of binding to the active site in either of two conformations rotated 180 degrees about an axis perpendicular to the active site --- a duplicity of binding which is at least partially supported by the inability of any one structure to satisfy all 68 distance restraints.

M-Pos470

Molecular Dynamics Studies of Protein-Ligand Adhesion in the Avidin-Biotin Complex.

(S. Izrailev, S. Stepaniants, M. Balsera, Y. Oono and K. Schulten)
Beckman Institute and Department of Physics, UIUC Urbana, IL 61801.

Molecular dynamics simulations have been carried out to study protein/ligand adhesion forces and the dissociation mechanism for the avidin-biotin complex. The unbinding of biotin over time scales of 40 ps to 500 ps was induced by means of harmonic forces similar to those in atomic force microscopy (AFM) experiments. The simulations revealed key roles of hydrogen bonding and of the 3-4 biotin-lid polypeptide loop of avidin during rupture. This loop constitutes a major obstacle in nanosecond simulations which, however, is likely to clear biotin's path in millisecond AFM experiments due to thermal fluctuations. The simulations showed that rupture is initiated when hydrogen bonds and contacts between the ureido ring of biotin and polar residues are broken. The motion of biotin then proceeds in slips, where each slip is accompanied by maximum force values and can be identified with the breakage and formation of hydrogen bonds and contacts with further residues. Rupture is also modeled by means of a one-dimensional Langevin equation and a linear ramp binding potential, the associated Smoluchowski equation, and the theory of first passage times. The model demonstrates that picosecond to nanosecond simulations of rupture proceed far from the thermally activated regime of millisecond AFM experiments.

M-Pos471

CYSTEINE CONTRIBUTIONS TO BINDING SITE PREFERENCE FOR Zn/Cd IN METALLOTHIONEIN - A SEMIEMPIRICAL SIMULATION (**Chia-Ching Chang** and P.C.Huang) Department of Life Sciences, National Tsing Hua University, Hsin-Chu 300 Taiwan, ROC and Department of Biochemistry, Johns Hopkins University, Baltimore, MD 21205, USA

Metallothionein, a two-domain protein, naturally binds seven gram atoms of divalent ions such as Zn and Cd, through tetrahedral coordination via thiolate bonds with its 20 cysteines. Four of the metals [M1, M5, M6, M7] are found in the alpha-domain and three [M2, M3, M4] in the beta-domain. Previous studies show that metals in the beta-domain are more readily exchangeable, and the level of avidity is site specific. This is reflected by energy differences computed with a series of simulated structures derived from either X-ray crystallography or NMR coordinates. By semiempirical MNDO calculations combined with FEP methods, we find the tendency of binding energy for Cd to be M4 > M2 > M3 in the beta-cluster and M5> M7> M1, M6 in the alpha-cluster. Thus, replacement of Zn by Cd can be expected to follow the order: M4 -> M2 -> M3 in the beta-domain and M5-> M7 -> M1 or M6 in the alpha-domain. For the nine cysteines in the beta-domain, the relative average binding strength was the strongest for Cys 21 to Cd[M4] and for Cys 15 and Cys 26 to Zn[M3]. These results support the notion that binding site preference for Zn/Cd is determined by binding strength between specific cysteines and metal ion species.
[Supported in part by grants 85-2113-M007-032 from NSC]

M-Pos472

MOTIONS OF CRYSTALLINE CALMODULIN STUDIED BY MULTIPLE-CONFORMER REFINEMENT AND DIFFUSE X-RAY SCATTERING.

((**M.E. Wall**, G.N. Phillips, Jr.)) Department of Biochemistry and Cell Biology, Rice University, Houston TX 77005-1892. (Spon. by M.E. Wall).

Calmodulin is a calcium-activated regulatory protein which bends as it binds. Meador *et al.* [Science **262** (1993) 1718] have previously reported a structure of Bovine Brain calmodulin complexed with calmodulin-dependent protein kinase (CaMKII) which is missing electron density in the flexible linker domain. Such crystals are well suited for studies of the motions of calmodulin.

Streaks of diffuse intensity are observed in images of x-ray diffraction from these crystals. The direction of streaks indicates that there are protein motions which are coupled along the end-to-end packing direction in the crystal. In addition, atomic displacements in structures from a four-conformer refinement are primarily transverse to this packing direction. The electron-density maps show a few more residues resolved than in the published data, but we do observe a loss of connectivity in the density associated with the linker domain, causing great differences among the four structures in the model of this domain. Further characterization of these motions will help reveal how motions in calmodulin influence its regulatory activity.

We gratefully acknowledge W. Meador and F. Quiocho for initial crystals and CaMKII peptide. This work was supported by the Robert A. Welch Foundation, the Keck Center for Computational Biology (NSF Research Training Group), and NSF grant MCB-9315840.

M-Pos473

STRUCTURAL EFFECTS OF SMALL MOLECULES IN SIMULATIONS OF DIFFUSION WITHIN MYOGLOBIN. ((**M.L. Carlson**)) Physics Department, Benedictine University, 5700 College Rd., Lisle, IL 60532. (Sponsored by M. Carlson)

Structural fluctuations play a role in protein function. Since a passageway to the heme is absent in hemoglobin and myoglobin, deviation from the crystal structures is necessary for oxygen to penetrate and bind. In simulations, a small molecule diffusing inside myoglobin did not merely sample the transient internal passageways within the protein. It also influenced the average structure and fluctuations of the protein. To illustrate this point, volumes near the heme binding site in the presence of none, one, or multiple diffusing small molecules (CO and H_2O) were calculated from numerous molecular dynamics simulations. Expansion of the protein was estimated by volume changes in a pyramid where the vertices are the locations of the 3 helices and 1 inter-helical segment that surround the distal binding site. The volumes and connectivity of ligand-accessible cavities were also calculated to assess the opportunity for ligand movement. Introducing a single diffusing ligand near the heme site had a noticeable effect upon structure. The distal portion of the protein expanded and had more extreme fluctuations. The ligand-accessible cavities in that region became considerably larger and more frequently inter-connected. The effect of an additional small molecule was not necessarily cumulative. When a water molecule was included near the heme iron (close to its location in the deoxy crystal structure), the volume occupied by the distal portion of the protein and its fluctuations did not further increase substantially. Locating that water molecule elsewhere within the distal cavities has led to similar results thus far. (This work was supported by HHMI grant #71191-528601.)

M-Pos474

STRUCTURE OF THE COMPLEX OF HMG-D PROTEIN WITH DNA AS PREDICTED BY MEANS OF MOLECULAR MODELLING. ((**A. Balaeff**, M. Churchill and K. Schulten)) Beckman Institute and Departments of Biophysics, Cell & Structural Biology and Physics, UIUC, Urbana, IL 61801.

The NMR model of the DNA binding domain of HMG-D protein [Jones et al., Structure 2:609 (1994)] was docked to several DNA segments with experimentally solved structures. The docking was guided by suggestions that, similarly to a homologous protein [Haqq et al., Science 266:1494 (1994)], the positively charged protein binds the DNA minor groove, and that the residue Met13 partially intercalates between DNA bases. Molecular dynamics simulations were conducted for three of the resulting structures for 160 ps. One of the simulated structures was selected as the most stable and best conserving the pre-set intercalation. It was simulated for an additional 60 ps; the simulation confirmed the stability of the complex and provided data for an extensive analysis of protein-DNA contacts. In addition to the partial intercalation of Met13, two more partial intercalations were observed: at an adjacent base pair (Leu9) and two basepairs downstream (Val32). Many residues of the protein established hydrogen bonds with the DNA backbone, whereas only two direct hydrogen bond contacts to the nucleotide bases were determined. Comparisons with the observed structures of two complexes of HMG-D homologues with DNA [Werner et al., Cell 81:705 (1995); Love et al., Nature 376:791 (1995)] allowed us to explain the sequence-non-specificity of HMG-D binding to DNA.

M-Pos475

DNA BINDING SPECIFICITY OF THE ESTROGEN RECEPTOR - A MOLECULAR DYNAMICS STUDY.
((D. Kosztin, T. Bishop, and K. Schulten)) Beckman Institute, UIUC, Urbana, IL 61801.

We have investigated, by means of molecular dynamics simulations, the role of waters in the DNA binding specificity of the estrogen receptor. Two separate structures (I, II) have been simulated based on the available crystallographic structure of the DNA binding domain dimer of the estrogen receptor in complex with DNA: structure I includes the dimer and a consensus segment of DNA, ds(ccAGGTCACAGTGACCTgg); structure II includes the dimer and a non-consensus segment of DNA, ds(ccAGAACACAGTGACCTgg). The 100 ps simulations employed a full atomic model including counterions, a 45 A radius sphere of explicit water, accounted for complete long-range electrostatic interactions and used the molecular dynamics package NAMD on a cluster of eight workstations. Analysis of the simulations revealed differences at the protein-DNA interface of consensus and non-consensus sequences, a bending and unwinding of the DNA, a rearrangement of several amino-acid side-chains and inclusion of water molecules at the protein-DNA interface region. Specificity is conferred by a network of direct and water mediated protein-DNA hydrogen bonds. The network of hydrogen bonds involves, for the consensus sequence, three water molecules, residues Glu25, Lys28, Lys32, Arg33 and the bases of DNA; such tight binding is not achieved for the non-consensus sequence in which case the network involves five water molecules. Water is therefore demonstrated to influence and play a role in the binding specificity.

M-Pos476

BACKBONE DYNAMICS OF THE RAT INTESTINAL FATTY ACID BINDING PROTEIN BY ^{15}N NMR
((L. Zhu, **M. D. Kemple**, E. Kurian†, and F. G. Prendergast†)) Dept. of Physics, Indiana University-Purdue University Indianapolis, Indianapolis, IN 46202, †Depts. of Biochemistry and Molecular Biology, and Pharmacology, Mayo Foundation, Rochester, MN 55905

Recombinant rat intestinal fatty acid binding protein (I-FABP) is a 15 kDa protein which tightly binds a number of long chain fatty acids with a stoichiometry of 1:1. The dynamics of I-FABP, uniformly enriched with ^{15}N, were investigated in the absence and presence of palmitic acid or 1,8-anilinonaphthalenesulfonic acid (ANS) at pH 5.5 and 22°C by ^{15}N NMR relaxation measurements (T_1 and the steady-state NOE at two different resonance frequencies, 50.6 MHz and 30.4 MHz). The data were analyzed using the model-free approach of Lipari and Szabo. An overall rotational correlation time, τ_m, of ~ 6 ns was found for I-FABP in both forms of the protein. This value was approximately the same as that obtained from ^{13}C relaxation measurements of bound palmitic acid in I-FABP(1). Overall, relatively rigid motion was found in both the apo- and holoproteins. However, there are some regions where distinct differences in internal dynamics between the two forms were found.

Supported in part by PHS Grant GM34847(FGP).

(1) L. Zhu, M. D. Kemple, E. Kurian, and F. G. Prendergast, ^{13}C NMR dynamics studies of palmitic acid in rat intestinal fatty acid-binding protein, *Biophys. J.* 70, A99 (1996).

M-Pos477

INTESTINAL FATTY ACID BINDING PROTEIN: CONFORMATIONAL STATISTICS OF MYRISTATE LIGAND AND BINDING POCKET SIDE CHAINS ((**Christopher Haydock** and Franklyn G. Prendergast)) Department of Biochemistry and Molecular Biology, Mayo Foundation, Rochester, MN 55905.

Intestinal fatty acid binding protein (I-FABP) folds into a β-clam shell structure that binds a fatty acid in the interior. Numerous high resolution crystallographic structures of I-FABP and other homologous lipid binding proteins are now available. The large temperature factors and discrete disorder of apoprotein interior side chains suggest that these side chains are involved in the process of noncovalent binding of fatty acid. Because the protein interior including side chains, ligand and solvent contains of the order of about a thousand atoms, molecular dynamics simulations long enough to obtain a statistically accurate picture of the interior side chain and ligand conformational dynamics on the nanosecond time scale are feasible. We are currently in the process of computing several 100 nanosecond simulations of the I-FABP interior in the apoprotein form and with bound myristate. We have developed new statistical techniques for analyzing these long simulations based on Markov chain models. This analysis gives not only the side chain and ligand backbone rotational isomer probabilities and cross-correlations, but also provides estimates of the statistical significance of these rotational isomer probabilities and cross-correlations. This work is supported in part by GM 34847.

M-Pos478

MOLECULAR DYNAMICS OF THE HAMMERHEAD RIBOZYME.
((**V. Gandhi** and K. W. Olsen)) Department of Chemistry, Loyola University, 6525 N. Sheridan Rd., Chicago, IL 60626

This study investigates and characterizes the dynamics, structure, and thermodynamics of a catalytic ribonucleic acid, the hammerhead ribozyme, during the initial stages of its thermal unfolding pathway. Molecular dynamics techniques were used to analyze the internal motions and thermodynamic properties of structural and energetic intermediates. Four simulations were conducted at different temperatures (300K and 500K) using different dynamics methodologies (Newtonian and Langevin). A distance-dependent dielectric constant was used in order to reduce the computational time required. The 600 pico-second dynamics trajectories were analyzed to probe molecular changes. The structural and energetic properties examined, including radius of gyration, dipole moment, hydrogen bonding and potential energy, equilibrated quickly and remained relatively constant during the simulations. No major conformational changes were observed; however, detailed structural analysis showed variation in flexibility for different part of the molecule.

M-Pos479

SIMULATION OF TRANSLATIONAL AND ROTATIONAL DIFFUSION OF ANTHRACENE IN SOLUTION: INFLUENCE OF TEMPERATURE, AND VISCOSITY. ((Gouri S. Jas, Yan Wang, and Krzysztof Kuczera)) Department of Chemistry and Biochemistry, The University of Kansas, Lawrence, KS 66045. gouri@tedybr.chem.ukans.edu

Molecular dynamics (MD) simulations of 1 ns length were performed for anthracene in cyclohexane (at 284 K, 300 K, 314 K) and in 2-propanol (at 300 K). Rotational and translational diffusion parameters were calculated and compared with the hydrodynamic theory predictions, and with fluorescent anisotropy decay measurements. The computed translational diffusion coefficient of anthracene in cyclohexane and in 2-propanol agree more closely with the hydrodynamic theory of *slip* boundary than *stick* conditions. Translational diffusion coefficients along each molecular axis (X,Y,Z) are also computed. Computed rotational diffusion coefficients for anthracene in both solvents fall between stick and slip conditions. The time constant found in the second order correlation function along the direction of transition dipole moment (17 ps and 25 ps) agrees very closely with the measured decay time (16 ps and 25 ps). Influence of viscosity and temperature on translational and rotational diffusion coefficients are in good agreement with the hydrodynamic theory. The solvent structure around anthracene was analyzed to generate a microscopic picture of solvation.

M-Pos480

THE SIMULATION OF SUPERCOILED DNA DYNAMICS USING AN ELASTIC CONTINUUM MODEL. ((T.P. Westcott, J.A. McCammon)) Department of Chemistry & Biochemistry, University of California, San Diego, 9500 Gilman Drive, La Jolla, CA, 92093-0365

The main objective of this research is to understand and visualize the dynamics of supercoiled DNA. Since supercoiled DNA is hundreds, thousands, tens of thousands of base pairs or longer, traditional molecular dynamics cannot be used to simulate such DNA because it is not fast enough to treat such large DNA for long time scales. Thus, developing methods which can treat long DNA for long time scales is important. Classical continuum elasticity theory provides a good, yet simple model of DNA. Elastic rod theory is used to develop equations for DNA dynamics using arguments based upon the balance of forces and the balance of momentum at each cross section of the rod. The dynamical equations can include external forces such as electrostatic interactions, energy dissipation terms to account for viscous drag, and a random force to account for thermal fluctuations. It is also possible to study chains containing regions of intrinsic curvature, altered twist, differences in intrinsic bending and twisting stiffness, or bound drugs and/or proteins.

(Supported by Sloan-DOE Joint Postdoctoral Fellowship in Computational Molecular Biology).

CHANNELS (OTHER)

Tu-AM-A1

PERMEATION THROUGH THE CALCIUM RELEASE CHANNEL (*CRC*) OF CARDIAC MUSCLE ((D. Chen*, Le Xu†, A. Tripathy†, G. Meissner†, R. Eisenberg*)) Dept's of Biophysics, *Rush Medical College, Chicago IL 60612 and †Univ. of North Carolina, Chapel Hill NC 27599.

Current voltage (*IV*) relations were measured from single open *CRC* channels in twelve KCl solutions, symmetrical and asymmetrical, from 25mM to 2M. *IV* curves are surprisingly linear, even at the extremes of voltage (±150mV≈6*kT/e*), even in asymmetrical solutions, e.g., 2M‖100mM. It is awkward to describe straight lines as sums of exponentials in a wide range of solutions and potentials and so traditional barrier models have difficulty fitting this data.

We have fit the data with the Poisson and Nernst Planck equations (PNP: J. Membrane Biology, *150:* 1-25, 1996) using adjustable parameters for the diffusion constant of each ion and for the effective density of fixed, i.e., permanent charge $P(x)$ along the channel's 'filter' (7Å diameter, 10Å long). If $P(x)$ is described by just one parameter (i.e., $P(x) = -4.2$M independent of x), the fits are satisfactory (*RMS* error/*RMS* current = 6.4/67, pA/pA). If $P(x)$ is described by 4 parameters, the fit is significantly better (5.8/67), and the parameter values are reasonable, $P(x) = -4.8 + 8.1J_0(\pi x) - 4.1J_0(2\pi x) - 9.9J_0(3\pi x)$ (in Molar, where x is the (normalized) location in the channel; J_0 is a Bessel function of order zero) and diffusion constants in the pore, $D_K = 1.5 \times 10^{-6}$, $D_{Cl} = 4.1 \times 10^{-6}$ cm²/sec.

Because the fixed charge density of *CRC* is so high, and the filter so small (in PNP's view of the channel's pore), the concentration of ions in and near the filter have a large effect on the potential profile and permeation. The change in the shape of the potential profile from solution to solution predicted by PNP is thus large, often more than *kT/e*.

This work was supported by NSF and NIH grants.

Tu-AM-A2

PERMEATION THROUGH PORIN AND ITS MUTANT G119D. ((J. Tang*, D. Chen*, N. Saint†, J. Rosenbusch†, R. Eisenberg*)) *Dept of Biophysics, Rush Medical College, Chicago IL 60612 and †Biozentrum, Basel, Switzerland.

Current voltage (*IV*) relations were recorded from single open channels of *OmpF* (wild type) porin and its mutant *G119D* that has one additional negative charge (aspartate) in its constriction site. Measurements have been made so far in eight KCl solutions, symmetrical and asymmetrical, from 3M to 10 mM in the voltage range ±200mV ≈ 8*kT/e*.

IV curves were fit with the Poisson and Nernst Planck equations (PNP) using adjustable parameters to describe the diffusion constant of each ion and the effective density of fixed, i.e., permanent charge $P(x)$ lining the channel's pore. Pore dimensions are taken from the known structure of the channel proteins. Fits to data are satisfactory if $P(x)$ is described by three parameters. PNP is able to fit a wide range of *IV* relations because the shape of the potential profile along the channel changes with solution, as it must in any self-consistent theory.

PNP is an approximate theory that ignores almost all the complexity of porin structures seen by crystallography, and describes the protein by effective, not real parameters. Thus, it is surprising that even our first fits of PNP to the *IV* data give nearly the ideal result, within ±15%, *net charge* $= \int [P(x;OmpF) - P(x;G119d)]dx = -1e$. (Fits to data from *OmpF* and *G119D* were done independently and parameter values were not adjusted in any way.)

Evidently, changes in the actual charge of the protein can be well described by changes in the effective profile $P(x)$. It is important to see how well PNP predicts *IV* relations of other mutants, and how well the charge distribution $P(x)$ describes the spatial average of the real (three-dimensional) charge distributions of those mutants, as determined by crystallography.

Tu-AM-A3

CURRENTS THROUGH SINGLE CHANNELS OF MALTOPORIN. ((J. Tang*, N. Saint†, J. Rosenbusch†, *R. Eisenberg**)) *Dept of Biophysics, Rush Medical College, Chicago IL 60612 and †Biozentrum, Basel, Switzerland.

Maltoporin is a trimeric channel protein, whose structure is known at 2.7Å resolution, containing three adjacent narrow pores, 4.5Å in diameter. Each pore has a 'greasy slide' and 'ionic track' that allow rapid diffusion with considerable selectivity.

Single trimers insert into azolectin bilayers and their pores show cooperative gating, as expected from the structure. The voltage dependence of gating is qualitatively similar to, but quantitatively different from *OmpF* porin: more voltage (and time) is needed to start maltoporin's much slower 'open/then close' behavior. Fig. 1 shows current in 1M KCl solutions after a 280mV step. Fig. 2 shows the finely curved current-voltage relation of a trimer with 3 open channels. The chord conductance is ~400 pS, compared to ~4 nS for *OmpF* under the same conditions.

Fig. 1

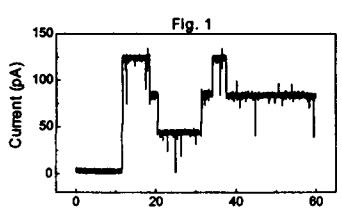

Fig. 2

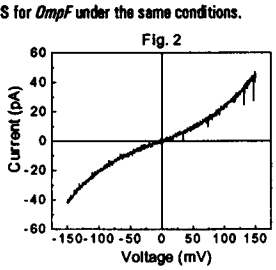

Tu-AM-A4

WHERE IS THE RATE-LIMITING STEP IN PERMEATION THROUGH VOLTAGE-GATED PROTON CHANNELS? ((T.E. DeCoursey and V.V. Cherny)) Dept. Mol. Biophys. & Physiology, Rush Medical Center, Chicago, IL

The proton conductance (g_H) of voltage-gated H^+ channels is 10-100 fS near physiological pH (Byerly & Suen, 1989, *J.Physiol.* 413:75; D&C, 1993, *Biophys.J.* 65:1590). Between pH_i 7.5-5.5 g_H increases only ~1.8/Unit (D&C, 1995, *J.Physiol.* 489:299-307). In contrast, g_H of gramicidin and other channels increases 10-fold/Unit decrease in pH, between pH 4-0, consistent with diffusion being rate-limiting. The effects of substituting deuterium, D_2O, for water, H_2O, on the voltage-activated H^+ conductance of rat alveolar epithelial cells were studied. D^+ carried current through proton channels, but g_H was ~twice as large in H_2O as in D_2O. D_2O reduced g_H more than could be accounted for by bulk solvent properties- the mobility of H^+ is only 41% greater than D^+ (Lewis & Doody, 1933, *J.Am.Chem.Soc.* 55:3504). This result suggests that the rate-limiting step in permeation occurs in the channel rather than in the diffusional approach and that D^+ interacts specifically with the voltage-gated H^+ channel during permeation. The g_H is evidently near saturation at neutral pH, seven orders of magnitude lower [H^+] than where saturation occurs in gramicidin (Akeson & Deamer, 1991, *Biophys.J.* 60:101). This result also strengthens the hypothesis that H^+ (D^+) and not OH^- (OD^-) is the ionic species carrying current.

Support: NIH grant HL52671, American Heart Association Grant-in-Aid.